Yeast as a Model for the Study of *Fusarium graminearum* Resistance

Amanda Bernice Gunter

Thesis submitted to the Faculty of Graduate and Postdoctoral Studies
in partial fulfillment of the requirements for the degree of Master of Science
Ottawa-Carleton Institute of Biology
University of Ottawa

Thèse soumise à la Faculté des Études Supérieures et Postdoctorales
en vue de l'obtention du diplôme de Maîtrise ès Sciences
Institut de Biologie d'Ottawa-Carleton
Université d'Ottawa

ABSTRACT

Fusarium graminearum trichothecene mycotoxins, notably deoxynivalenol (DON), contaminate cereal grains and threaten food and feed safety. This study identified the ATP-binding cassette (ABC) transporter Pdr5p as the main exporter of DON in the model system *Saccharomyces cerevisiae*. Toxin export by Pdr5p from living cells was, however, blocked by an unidentified inhibitory compound produced by *F. graminearum*. The main objective of this study was to create Pdr5p mutants demonstrating insensitivity to inhibition while maintaining the ability to export DON. A total of 38 Pdr5p mutants, each containing a single amino acid substitution at two important sites of the transporter, were generated and expressed in yeast harboring a deletion of wild-type Pdr5p. This study demonstrated that while most of these mutants maintained DON export, some were more resistant than the wild-type to inhibition by the Pdr5p-specific inhibitors FK506 and enniatin B. Results suggest that Pdr5p mutants S1360D and S1360E are resistant to *F. avenaceum* culture filtrate while none of the 38 mutants analyzed are resistant to *F. graminearum* culture filtrate. This study has shown that knowledge gained though the study of Pdr5p mutants in yeast could be extended to plants in an attempt to improve their ability to confer resistance to *Fusarium* species.

RÉSUMÉ

Les mycotoxines trichothécènes telles que le déoxynivalénol (DON) produites par *Fusarium graminearum* contaminent les grains céréaliers et menacent la sécurité alimentaire. Le transporteur Pdr5p est un transporteur ABC (ATP-binding cassette) retrouvé chez le système modèle de levure *Saccharomyces cerevisiae*. Dans cette étude, Pdr5p a été identifié comme l'exportateur principal du DON. Son activité d'export a cependant été bloquée par un composé inhibiteur non-identifié produit par *F. graminearum*. L'objectif principal de cette étude était de créer des mutants de Pdr5p qui étaient résistants à l'inhibition tout en maintenant la capacité à exporter le DON. Un total de 38 mutants de Pdr5p, chacun ayant une substitution unique d'un acide aminé à deux sites importants du transporteur, ont été générés et exprimés dans une souche de levure qui n'exprimait pas le transporteur Pdr5p de type sauvage. Cette étude a démontré qu'alors que la plupart de ces mutants maintenaient l'export du DON, certains étaient plus résistants que le type sauvage contre l'inhibition causée par FK506 et l'énniatine B, deux inhibiteurs spécifiques au Pdr5p. Les résultats suggèrent que les mutants S1360D et S1360E de Pdr5p sont résistants au filtrat de culture produit par *F. avenaceum* alors qu'aucun des 38 mutants analysés ne sont résistants au filtrat de culture produit par *F. graminearum*. Cette étude a démontré que les connaissances acquises par l'étude des mutants de Pdr5p dans la levure pourraient être utilisées chez les plantes pour tenter d'améliorer leur habileté à conférer la résistance contre des espèces du genre *Fusarium*.

ACKNOWLEDGEMENTS

I would like to express my sincerest gratitude to my supervisors Dr. Steve Gleddie and Dr. Doug Johnson for having provided me the opportunity to undertake this project. This has truly been a great learning experience and I thank you for your continued patience, guidance, and insight. I extend my thanks to my committee members Dr. Christiane Charest and Dr. John Vierula for your time and support.

During my time working at the Central Experimental Farm, I have had the chance to meet and work with some exceptional people. I would especially like to recognize Anne Hermans, Christine Gagnon, Frances Tran, and Whynn Bosnich for the time you dedicated to helping me in the lab. Your knowledge and technical expertise have been invaluable to me. Thank you for all the help and advice you gave me during my course work, lab work, and thesis writing, and most importantly, thank you for your friendship.

I would also like to send a big thank you to my friends and family for having been there for me outside of the lab. To Kathryn Aubin, Michelle Thomas and my sisters Ashley and Annie: in times of frustration you kept me motivated to reach the light at the end of the tunnel. I knew I could count on you to brighten my day and for that, I am thankful.

Finally, thank you Mom and Dad for your constant encouragement and emotional support. You have been there for me through thick and thin. I can't thank you enough for everything you have done to help me accomplish my goals.

TABLE OF CONTENTS

LIST OF FIGURES

LIST OF TABLES

LIST OF ABBREVIATIONS

ABC	ATP-binding cassette
ANOVA	Analysis of variance
AUC	Area under the curve
bp	Base pair
Da	Dalton
DAS	4,15-diacetoxyscirpenol
DON	Deoxynivalenol
ECL	Enhanced chemiluminescence
ER	Endoplasmic reticulum
ERM	Endoplasmic reticulum membrane
FHB	Fusarium head blight
gDNA	Genomic DNA
GFP	Green fluorescent protein
G418	Geneticin
HA	Hemagglutinin
HCl	Hydrochloride
HPLC	High-performance liquid chromatography
HSD	Honestly significant difference
kDa	Kilodalton
MDR	Multidrug resistance, referred to as pleiotropic drug resistance (PDR) in fungi
MON	Moniliformin
MQ-H_2O	Milli-Q-H_2O
MRP2	Multidrug resistance-associated protein 2
NBD	Nucleotide binding domain, found in ABC transporters
OD_{600}	Optical density at 600 nm
ORF	Open reading frame

PCR	Polymerase chain reaction
PDR	Pleiotropic drug resistance
PDRE	Pleiotropic drug resistance elements (PDREs), regulatory element located in promoters of the target genes of transcriptional regulators *PDR1* and *PDR3*
P-gp	P-glycoprotein
PM	Plasma membrane
PVDF	Polyvinylidene difluoride
RBB	(Roche) Blocking buffer
R6G	Rhodamine 6G
SD-ura	Synthetic dropout agar lacking uracil
SDS-PAGE	SDS-polyacrylamide gel electrophoresis
S1360	Pdr5p amino acid residue S1360
TAE	Tris-acetate-EDTA (buffer)
TBS	Tris-buffered saline (buffer)
TE	Tris-EDTA (buffer)
TMD	Transmembrane domain, found in ABC transporters
TMH	Transmembrane helix, found in the TMDs of ABC transporters
T1364	Pdr5p amino acid residue T1364
UV	Ultraviolet
WT	Wild-type
YKO	Yeast knockout (strain)
YPD	Yeast peptone dextrose
3A-DON	3-acetyl-deoxynivalenol
15A-DON	15-acetyl-deoxynivalenol
3,15A-DON	3,15-acetyldeoxynivalenol
3' UTR	Three prime untranslated region
±SEM	Plus or minus the standard error of the mean

CHAPTER 1 – INTRODUCTION

Fusarium graminearum Schwabe [telomorph *Gibberella zeae* (Schwein.) Petch] is an economically important fungal pathogen of cereal crops. In North America, it is the predominant causal agent of Gibberella ear and stalk rot in maize (*Zea mays* L.) and Fusarium head blight (FHB) in wheat (*Triticum aestivum* L.) and barley (*Hordeum vulgare* L.) (Harris, 1999; Goswami & Kistler, 2004). Notable epidemics caused by FHB in winter wheat, spring wheat, and barley date back to the 1990s. In 1993, 10 million acres of spring wheat and barley crops were infected in Manitoba and the tri-state area of Minnesota, North Dakota, and South Dakota, causing massive declines in grain yield and quality with losses amounting to $1 billion (McMullen et al. 1997). In 1996, Ontario wheat producers lost over $100 million following a 30% FHB-attributed yield loss in winter wheat crops (Schaafsma, 1999).

In addition to reducing crop yield and quality, infection of cereal grains by *F. graminearum* often leads to their contamination by trichothecene mycotoxins. The trichothecene deoxynivalenol (DON) is commonly found in infected grains and causes health problems in human and animal consumers (Schaafsma et al., 2002; Gilbert et al., 2010). Regulatory guidelines have been implemented by many countries, including Canada, in an effort to limit the levels of DON and other mycotoxins permitted in grain used for food and feed. Unfortunately, current approaches used for preventing *F. graminearum* infection and mycotoxin contamination of grains are, for the most part, ineffective or impractical (Pestka & Smolinski, 2005; Gilbert & Haber, 2013). Plant breeding, for example, has not yet been successful in producing crop varieties that are resistant to *F. graminearum*. Currently, the majority of maize inbreds and hybrids are susceptible to ear rot and wheat cultivars are, at most, moderately resistant to FHB (Mesterházy et al., 2012; Gilbert & Haber, 2013).

With important economic repercussions and serious health risks associated with grain contamination by *F. graminearum* trichothecene mycotoxins, notably DON and its acetylated derivatives 3-acetyl-deoxynivalenol (3A-DON) and 15-acetyl-deoxynivalenol (15A-DON) (Figure 1.1), there is a need to identify resistance mechanisms against these contaminants with the aim of preventing their entry into the food and feed supply chains. A promising approach to achieve this involves the use of yeast, which has been identified as an ideal model system to study the effects of trichothecenes on eukaryotic cells (Doyle et al., 2009; Suzuki & Iwahashi, 2012). In the yeast *Saccharomyces cerevisiae*, the following resistance mechanisms have been identified against DON: detoxification of the toxin by the acetyltransferase ScAyt1p; modification of its ribosomal target by amino acid substitutions in ribosomal protein L3 (ScRpl3p); and reduced uptake of the toxin by the ATP-binding cassette (ABC) transporter ScPdr5p (simply referred to as Pdr5p in this thesis) (Mitterbauer & Adam, 2002). By further evaluating the resistance mechanisms of *S. cerevisiae* against *F. graminearum* mycotoxins, it could then be possible to select those that are the most promising and analyze them *in planta*.

1.1 *F. graminearum* trichothecenes

1.1.1 Crop infection by *F. graminearum*

The infection of cereal crops by *F. graminearum* is promoted when warm temperatures and high levels of humidity coincide with silk emergence in maize or anthesis in wheat and barley (McMullen et al., 1997; Reid & Sinha, 1998). The progression of infection caused by this fungal pathogen is characterized by the development of a red or pink mold on maize ears or by the discoloration of wheat and barley florets (McMullen, 1997; Munkvold, 2003). The main source of *F. graminearum* comes from infected plant debris on which the pathogen grows saprophytically (Goswami & Kistler, 2004). For the dispersal of inoculum, *F. graminearum*

DON **3A-DON** **15A-DON**

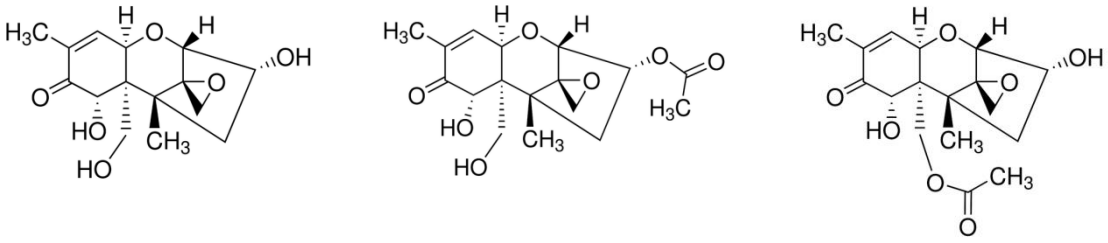

296.32 Da 338.35 Da 338.35 Da

Figure 1.1 Molecular structure and weight of DON and its acetylated derivatives 3A-DON and 15A-DON.

produces macroconidia (asexual spores) and ascospores (sexual spores) (Beyer et al., 2005; Trail, 2009). While macroconidia rely on splash dispersal by raindrops to reach host plants, ascospores, which are the main source of inoculum, are contained within perithecia, which forcibly release them into the air, allowing for widespread ascospore dispersal by wind, rain, insects, or birds (Reid et al., 1996; Trail, 2009). Beyer et al. (2005) demonstrated that the level of DON in wheat grain is influenced by spore type and humidity. In comparison to macroconidia, ascospores require a lower humidity level to germinate and their inoculum produces more DON.

1.1.2 Trichothecene biosynthesis

In North America, most *F. graminearum* isolates produce either 3A-DON or 15A-DON, which are deacetylated into DON, presumably by fungal or plant deacetylase enzymes (Gilbert et al., 2010; Alexander et al., 2011). Genes responsible for the biosynthesis of trichothecenes are located at three loci: a twelve-gene cluster (*TRI3* through *TRI14*); a small two-gene cluster (*TRI1* and *TRI16*); and a single gene (*TRI101*) (reviewed in Alexander et al., 2009). The genes located within the twelve-gene cluster are collectively known as the *TRI5* gene cluster. The core of this cluster contains the genes that initiate the biosynthesis of the basic trichothecene precursor molecule, while the genes flanking the core are involved in strain-specific trichothecene differentiation (Brown et al., 2004; Goswami & Kistler, 2004; Kimura et al., 2007).

The first step in the synthesis of all trichothecenes involves the conversion of farnesyl pyrophosphate by the trichodiene synthase Tri5p, encoded by *TRI5*, to form the trichothecene precursor molecule trichodiene. A series of oxygenation and acetylation reactions catalyzed by enzymes encoded by the *TRI* genes lead to the formation of the molecule 3,15-

acetyldeoxynivalenol (3,15A-DON). In 3A-DON-producing *F. graminearum* strains, Tri8p deacetylates 3,15A-DON at the C-15 position to form 3A-DON; while in 15A-DON-producing strains, it deacetylates 3,15A-DON at the C-3 position to form 15A-DON. Finally, 3A-DON or 15A-DON is converted to DON by an unknown gene product (Alexander et al., 2011). In infected grain, the acetylated derivative corresponding to the *F. graminearum* isolate can be found along with DON. All have toxic effects on consumers of contaminated food and feed (Gilbert et al., 2010).

1.1.3 Host contamination by DON

DON is unlikely involved in the initial stage of host infection by *F. graminearum,* as its production seems to be induced following this stage. Harris (1999) and Jansen et al. (2005) demonstrated that in maize and wheat respectively, DON appears to act as a virulence factor that promotes the spread of fungal colonization following the initial point of infection. They showed that *F. graminearum* mutants lacking the ability to produce DON are not as effective at causing disease compared to their wild-type (WT) counterparts. Ilgen et al. (2009) used a *F. graminearum* strain transformed with a *TRI5* promoter-green fluorescent protein (GFP) construct to follow the localization of DON production over time in a wheat head. Despite visible growth of mycelium on the wheat anthers, which corresponds to the landing site of fungal spores, no GFP fluorescence was visible, indicating an absence of DON production on the anthers. The fluorescence of GFP became noticeable during the early stages of fungal infection, following the hyphae as they colonized a spikelet of the wheat head.

The rachis node at the base of the spikelets serves as a barrier against the colonization of uninfected spikelets. Ilgen et al. (2009) showed that GFP fluorescence became elevated at the rachis node as the fungal hyphae spread across to the following spikelet. Supporting the role of

DON as a virulence factor in the spread of infection, Jansen et al. (2005) demonstrated that when *F. graminearum* is incapable of producing trichothecenes, it becomes unable to cross the rachis node of a wheat spikelet. Surprisingly in barley, fungal hyphae of both trichothecene-producing and non-producing *F. graminearum* strains are inhibited at the rachis node, suggesting that wheat and barley have different resistance mechanisms against infection by *F. graminearum* (Jansen et al., 2005). In maize, Harris (1999) determined that trichothecene-producing strains of *F. graminearum* are significantly more virulent than non-producing strains. Additionally, Reid & Sinha (1998) demonstrated that ear rot symptoms of maize are correlated with DON concentrations and that disease symptoms stabilize concurrently with the stabilization of DON levels in infected maize. Taken together, these results show that DON has a key role in the infection cycle of wheat and maize by *F. graminearum*.

1.1.4 Impact of DON on consumers

Although DON contamination occurs primarily in the field, it can also arise from inadequate grain storage conditions. Furthermore, once DON is present in grains, it is nearly impossible to eliminate. Several treatment options have been employed in an attempt to remove DON from grains; however, none are completely effective. DON is very heat stable; therefore, baking or heating has little to no effect on its stability. Sorting, cleaning, and milling can help reduce toxin concentrations, but they are incapable of destroying DON. Finally, treatments involving the use of chemicals such as ammonia, calcium hydroxide, hydrochloric acid, sodium bisulfite, or sodium hydroxide have been useful in eliminating DON; however, they interfere with grain processing and can pose additional health risks to consumers (Bullerman & Bianchini, 2007; Pestka & Smolinski, 2005; Sobrova et al., 2010). The lack of suitable DON treatment options increases the threat of mycotoxicoses in consumers of

commodities produced with contaminated ingredients. These ingredients include cereals and processed grains derived from DON-contaminated plants as well as meat, milk, and eggs produced from animals fed DON-contaminated feed (Mitterbauer & Adam, 2002; Pronk et al., 2002; Coppock & Jacobsen, 2009).

Once they cross the plasma membrane, trichothecenes exert multiple inhibitory effects on eukaryotic cells, impacting numerous cellular processes in animals and plants. Their main toxic effect involves protein synthesis inhibition. By targeting and binding to the 60S ribosomal subunit, trichothecenes impede peptidyl transferase activity by inhibiting the initiation, elongation, or termination step during protein synthesis (reviewed in Arunachalam & Doohan, 2013).

The intestine acts as the first barrier against exposure to ingested trichothecenes. Through the use of human intestinal epithelial cells, Videmann et al. (2007) demonstrated that *ex vivo*, DON is a substrate for the plasma membrane ABC transporters P-glycoprotein (P-gp) and multidrug resistance-associated protein 2 (MRP2), which are expressed apically in epithelial tissues (Leslie et al., 2005). Videmann et al. (2007) also showed that inhibition of P-gp or MRP2 prevents DON transport which led them to suggest that *in vivo*, other substrates and inhibitors of either of these transporters could be involved in blocking the efflux of DON from intestinal epithelial cells. This would therefore enable DON to begin exerting its cytotoxicity within contaminated cells.

In summary, the trichothecene mycotoxin DON commonly occurs in grain infected by *F. graminearum*. It acts as a virulence factor that contributes to the propagation of fungal infection in host plants. Additionally, DON interferes with numerous processes, notably protein biosynthesis, in eukaryotic cells. ABC transporters have a role in DON export in

animals and yeast, with a putative role in plants. Further analysis of these transporters using the yeast *S. cerevisiae* as a model organism could provide important details of their interaction with DON.

1.2 ATP-binding cassette (ABC) transporters

1.2.1 Overview of ABC systems

ATP-binding cassette (ABC) systems form one of the largest protein superfamilies. They are present in essentially every prokaryotic and eukaryotic cell and have a fundamental role in the maintenance of normal cell function (Higgins, 2001; Vasiliou et al., 2009). ABC systems are categorized either as cytosolic non-transport proteins involved in mRNA translation and DNA repair (reviewed in Licht & Schneider, 2011) or as integral membrane proteins. The latter category includes the majority of ABC systems, most of which couple the binding of ATP to the transport of a wide range of chemically and functionally distinct compounds (Higgins, 1992; Rees et al., 2009).

ABC transport proteins are located in the plasma membrane of prokaryotes and eukaryotes as well as in the organellar membranes of higher organisms, and are involved in various cellular processes such as osmoregulation, cholesterol and lipid trafficking, energy supply, detoxification, and virulence (Davidson et al., 2008; Rees et al., 2009; Licht & Schneider, 2011). Transporters that move compounds from the extracellular space to the cytosol are known as importers, while those that move compounds from the cytosol or the inner leaflet of the plasma membrane to the extracellular space or intracellular organelles are known as exporters (Taglicht & Michaelis, 1998; Hollenstein et al., 2007). Importers enable the accumulation of essential nutrients including carbohydrates, vitamins, ions, and amino acids within the cell (Eitinger et al., 2011). They are found exclusively in prokaryotes, although

potential eukaryotic importers have recently been identified in the model plant *Arabidopsis thaliana* (reviewed in Knöller & Murphy, 2011). Exporters, which will be the focus of this review, are found in both prokaryotes and eukaryotes, and are responsible for the transport of compounds such as polysaccharides, cholesterol, lipids, peptides, hormones, hydrophobic drugs and natural toxins from the cell (Higgins, 1992; Rees et al., 2009).

Regardless of the species of origin, eukaryotic ABC systems can be grouped into nine subfamilies, designated ABCA to ABCI (Verrier et al., 2008). With a remarkable broad range of substrate specificity for over one hundred compounds (Kolaczkowski et al., 1998), Pdr5p from the ABCG subfamily has become one of the best-studied ABC transporters. Additionally, in the model plant *Arabidopsis thaliana* and in *Z. mays,* putative Pdr5p-like transporters grouped within the ABCG subfamily have been identified (van den Brûle & Smart, 2002; Pang et al., 2013). Suzuki & Iwahashi (2012) analyzed the growth inhibitory effects of trichothecenes against a mutant strain of *S. cerevisiae* incapable of expressing Pdr5p and demonstrated that this transporter has an essential role in the resistance to trichothecene mycotoxins, including DON and 15A-DON. Furthermore, Muhitch et al. (2000) successfully transformed tobacco plants with the *S. cerevisiae PDR5* gene, which increased the plants' resistance to 4,15-diacetoxyscirpenol (DAS), a trichothecene mycotoxin generally produced by *F. poaea* and *F. equiseti.* Additional investigation of the interactions between Pdr5p and *F. graminearum* trichothecenes could provide valuable information about how this transporter could be manipulated to be used as a first line of defense against DON and other trichothecenes in crop plants.

1.2.2 Structure, function, and mechanism of ABC transporters

Ongoing studies in the fields of structural and functional biology, biochemistry, biophysics, and genetics continue to unveil important details about the structure and function of

ABC transporters. Although individual transporters have a distinct specificity for the type and range of transportable substrates, they all share a common architecture consisting of two cytosolic nucleotide binding domains (NBDs) and two transmembrane domains (TMDs). The NBDs bind and hydrolyze ATP, thereby creating energy for substrate transport, and the TMDs form the pathway for unidirectional substrate transport (Hyde et al., 1990).

In ABC exporters, the four structural domains are typically fused in one of two ways: all four domains fused together in a single polypeptide chain to form a "full-sized transporter", or one NBD fused with one TMD to form a "half-sized transporter" (Figure 1.2). Full-sized transporters are found exclusively in eukaryotes, while half-sized transporters are found in both prokaryotes and eukaryotes and necessitate the formation of homodimers or heterodimers to become functional (Biemans-Oldehinkel et al., 2006). In ABC exporters, the domains are often encoded as individual polypeptides or are fused together in various permutations (Biemans-Oldehinkel et al., 2006). These four domains are joined together in a modular pattern: the NBDs are typically C-terminal to the TMDs in a "forward order" [N-(TMD1-NBD1)-(TMD2-NBD2)-C], but they can also be N-terminal in a "reverse order" [N-(NBD1-TMD1)-(NBD2-TMD2)-C] (Taglicht & Michaelis, 1998).

The NBDs consist of two components: a catalytic subdomain and an α-helical signalling domain. The NBDs of all ABC transporters share conserved motifs, which are involved in ATP binding and hydrolysis. Among these motifs, the catalytic subdomain contains the hydrophobic Walker A and Walker B motifs, and the α-helical signalling domain contains the signature LSGGQ motif, which is the signature feature of every ABC transporter identified as of yet. In an intact transporter, the NBDs face each other, forming a head-to tail dimer with two ATP-binding sites at the dimer interface. Each ATP-binding site comprises the Walker A

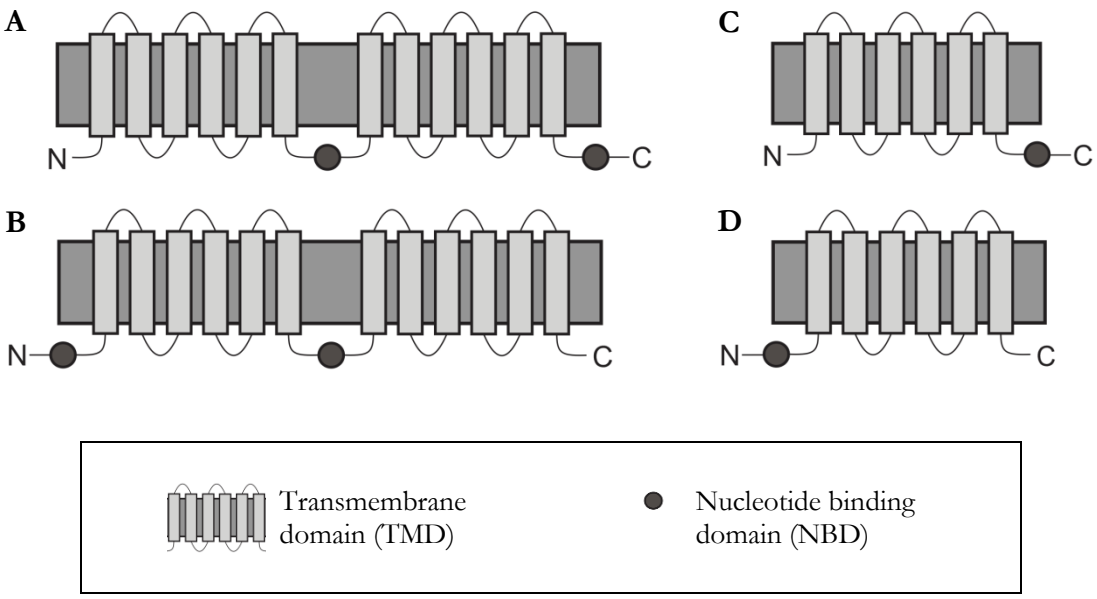

Figure 1.2 Arrangement of ABC transporter domains. (**A**) Full-sized transporter arranged in a forward order [N-(TMD1-NBD1)-(TMD2-NBD2)-C]. (**B**) Full-sized transporter arranged in a reverse order [N-(NBD1-TMD1)-(NBD2-TMD2)-C]. (**C**) Half-sized transporter arranged in a forward order [N-(TMD1-NBD1)-C]. (**D**) Half-sized transporter arranged in a reverse order [N-(NBD1-TMD1)-C] (modified from Yazaki et al., 2009).

motif of one NBD and the LSGGQ motif of the other NBD (Loo et al., 2002; Schmitt & Tampé, 2002; Smith et al., 2002).

Unlike the NBDs, which have conserved motifs among all ABC transporters, the TMDs have no sequence homologies, reflecting the ability of transporters to recognize and transport unrelated compounds. Each TMD consists of α-helix bundles known as transmembrane helices (TMHs), which span the membrane. The TMDs of most ABC exporters follow the "two-times-six" α-helix paradigm for a total of twelve TMHs (Higgins, 1992), while ABC importers have a total of ten to twenty TMHs (Biemans-Oldehinkel et al., 2006). Adjacent TMDs are interlinked in an alternating pattern by intracellular loops on the cytosolic side of the membrane and extracellular loops on the extracellular side (Dawson & Locher, 2006).

Elucidation of the complete mechanism of action of ABC transporters has been hindered by a lack of high-resolution crystal structures. To date, crystal structures of only four plasma membrane ABC exporters [murine multidrug transporter P-gp; *Staphylococcus aureus* multidrug transporter Sav1866; *Escherichia coli* lipid flippase MsbA; and *Thermotoga maritima* TM287/288 (Dawson & Locher, 2006; Ward et al., 2007; Aller et al., 2009; Hohl et al., 2012)], have been resolved at medium to low resolution, none of which have been captured at all stages of the transport cycle (George & Jones, 2012). Despite this limitation, many models building onto the "alternating access and release mechanism" (Jardetzky, 1966) have been proposed to explain the mechanism of action of ABC transporters.

The NBDs and TMDs are physically linked together through a transmission interface that ensures cross-talk between the domains (Sauna et al., 2008; Ananthaswamy et al., 2010; Downes et al., 2013). It has been proposed that the ATP-binding sites of the NBD dimer are always saturated with ATP (Licht & Schneider, 2011). When the ABC exporter is in its resting

state, the NBD dimer is in an "open" position, with low affinity for ATP, and the TMDs are in an "inward-facing" conformation, with the substrate-binding pocket, which has high substrate affinity, facing the cytosol (Figure 1.3A). Following substrate binding within the substrate-binding pocket, the NBD dimer gains high affinity for ATP and adopts its "closed" position, allowing for binding and hydrolysis of ATP (Figure 1.3B). This simultaneously causes the TMDs to adopt their "outward-facing" conformation, which has lower substrate affinity, and the substrate is released from the substrate-binding site (Figure 1.3C). Due to the lower substrate affinity of the outward-facing conformation, this prevents substrate re-entry into the cell, thereby creating a transmembrane substrate concentration gradient. Following substrate release, the NBD dimer returns to its open position, releasing ADP/Pi, and causes the TMDs to return to their inward-facing conformation (Figure 1.3D) (George & Jones, 2012; 2013). A comprehensive analysis of the structure and function of ABC exporters is essential for understanding their role in substrate transport; however, much is yet to be fully understood.

1.2.3 ABC transporters and drug resistance

ABC transporters have significant clinical implications in human health and disease. Mutations in ABC genes lead to functional deficiencies in respective ABC transporters, causing severe genetic disorders such as cystic fibrosis (respiratory and digestive systems), adrenoleukodystrophy (nervous and endocrine systems), Stargardt disease (visual system), and Tangier disease (cardiovascular system) (Knazek et al., 1983; Marcil et al., 1999; Quinton, 1999; Sun et al., 1999; Dean et al., 2001). The clinical importance of ABC transporters is, however, not limited to the manifestation of genetic disorders. The phenomenon of multidrug resistance (MDR) has contributed to drug therapy failure in over 90% of patients with metastatic cancer (Longley & Johnston, 2005). Additionally, it is often the cause of drug failure during the

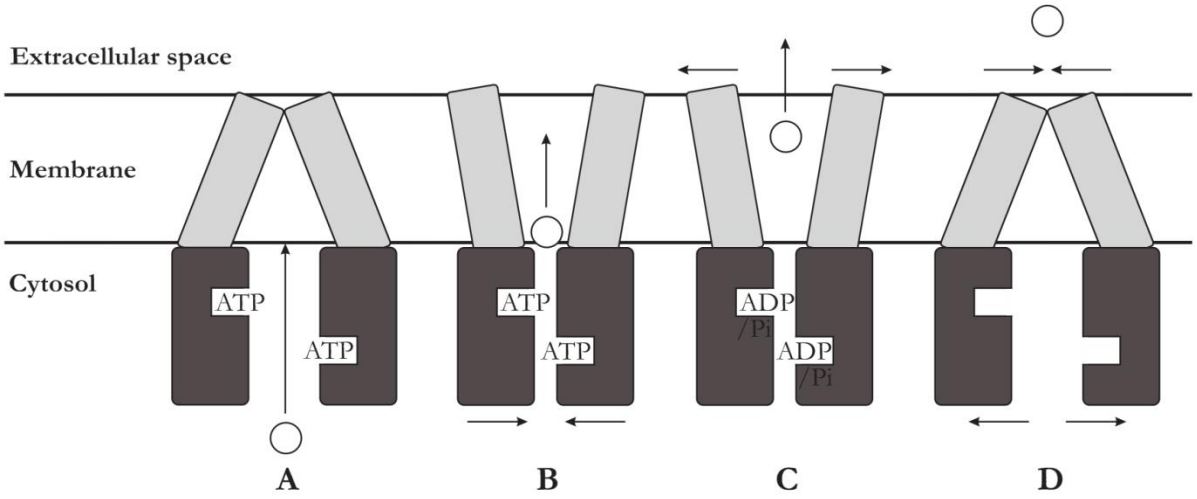

Figure 1.3 Proposed mechanism of action of plasma membrane ABC exporters. (**A**) Resting state: the NBD (dark grey) dimer is in an open position and the TMDs (light grey) are in an inward-facing conformation. (**B**) Substrate binding: the NBD dimer adopts a closed position, allowing for binding and hydrolysis of ATP. (**C**) Substrate export: the TMDs adopt an outward-facing conformation and the substrate is released into the extracellular space. (**D**) Resting state: the NBD dimer returns to an open position, ADP/Pi is released, and the TMDs return to an inward-facing conformation (modified from George & Jones, 2012; 2013).

treatment of infections caused by pathogenic organisms, notably bacteria, fungi, and protozoa (Ouellette et al., 2001; Cannon et al., 2009; Hawkey & Jones, 2009; Morschhäuser, 2010). While MDR can have several causes, it is often mediated by the overexpression of a network of plasma membrane ABC exporters that serve as a first line of defense against xenobiotics. Unlike most ABC transporters, which have limited substrate specificity, those involved in MDR have the ability to export a remarkably large number of substrates, notably xenobiotics of wide-ranging molecular size and chemical structure (Higgins, 2007). This therefore poses major challenges for the development of effective drug treatment plans to combat cancers and pathogenic organisms.

1.2.4 Mammalian P-gp

As an important member of a network that protects cells against the toxigenic effects of xenobiotics, mammalian P-gp is well-known for its prominent role in mediating MDR during chemotherapy (Gottesman et al., 2002; Leslie et al., 2005). P-gp, a member of the ABCB subfamily of ABC transporters, is a 170 kDa full-size protein with its domains joined together in a forward order (Kartner et al., 1983; Gillet et al., 2007). The broad variety of compounds transported by P-gp includes anticancer drugs, cardiac drugs, HIV protease inhibitors, and immunosuppressants (Fromm, 2004). Consequently, it has become one of the best-characterized ABC transporters and is a critical target for the development of effective chemotherapy strategies. Although the crystal structure of human P-gp has not yet been resolved, it shares 87% overall amino acid sequence identity with murine P-gp, whose crystal structure has been resolved. Furthermore, sequence identity within the substrate-binding cavity of both proteins is nearly 100% identical (Aller et al., 2009; Dolghih et al., 2011).

In normal human cells, P-gp has been shown to localize in the ductules of the liver and pancreas, in the medulla and cortex of adrenal glands, at the apical surface of columnar epithelial cells in the small intestine and colon, at the apical surface of bronchial and bronchiolar epithelial cells in the lung, and in the endothelial cells of small blood vessels and capillaries in the brain (Thiebault et al., 1987; Cordon-Cardo et al., 1990; Scheffer et al., 2002). Due to its localization within the cells of barrier and elimination organs, the physiological role of P-gp appears to be in the protection of organs against xenobiotic toxicity through drug excretion (Leslie et al., 2005, Fromm, 2004). As described above, this transporter is also involved in exporting the trichothecene mycotoxin DON from epithelial intestinal cells (Videmann et al., 2007).

1.2.5 Fungal ABC transporters

The phenomenon known as MDR in mammals is referred to as pleiotropic drug resistance (PDR) in fungi (Bauer et al., 1999). A number of P-gp functional homologues have been identified and characterized in fungal species. Homologues CaCdr1p and CaCdr2p of *Candida albicans* and CgCdr1p and CgPdh1p of *Candida glabrata* are often associated with azole antifungal drug resistance during the treatment of infections caused by these major pathogenic fungi (reviewed in Cannon et al., 2009). In the model yeast *Saccharomyces cerevisiae*, homologues Yor1p, Snq2p, and Pdr5p have been associated with the export over one hundred structurally and functionally unrelated compounds (Kolaczkowski et al., 1998).

1.2.6 PDR network in *S. cerevisiae*

S. cerevisiae has a large network of proteins that contribute to PDR. These proteins include Yor1p from the ABCC subfamily of ABC transporters as well as Snq2p, Pdr5p, Pdr10p, Pdr11p, and Pdr15p, all from the ABCG subfamily (Kovalchuk & Driessen, 2010). In *S. cerevisiae*, the expression of proteins from the PDR network is regulated by two homologous zinc

finger transcription factors, Pdr1p and Pdr3p, encoded by the transcriptional regulators *PDR1* and *PDR3*. Both transcription factors recognize the same consensus sequences, known as pleiotropic drug resistance elements (PDREs), which are located in the promoters of their target genes. All targets have at least one PDRE, which can bind either Pdr1p or Pdr3p to activate gene transcription (reviewed in Kolaczkowska & Goffeau, 1999).

Pdr5, Snq2p, and Yor1p are the best-studied transporters from the PDR network. Despite each having distinct substrate specificities, they also show considerable substrate overlap (Kolaczkowski et al., 1998). While none of these proteins are essential for viability, disruption of their corresponding genes has an effect on the PDR network. Kolaczkowska et al. (2008) used isogenic *S. cerevisiae* strains with single and double deletions of Pdr5p, Snq2p, and Yor1p to show that in the absence of one or two of these transporters, there is a compensatory activation of the remaining transporter(s). These strains were exposed to a variety of drugs, each corresponding to a specific substrate for one of the three transporters. In the strains harboring single deletions of Snq2p or Yor1p, increased resistance to the Pdr5p-specific substrates was demonstrated; with more pronounced resistance in the strain with a double deletion of Snq2p and Yor1p. Growth inhibition was observed when the strains harboring a deletion of Pdr5p were grown in Pdr5p-specific substrates. These trends were observed for all isogenic strains. Additionally, increased mRNA and protein levels of the transporters were correlated with increased resistance to their respective substrates. These results demonstrate that while there is a compensatory effect on substrate efflux in absence of a PDR transporter, this will not prevent the growth inhibition by a toxic compound if its specific transporter is absent or inhibited.

1.2.7 Pdr5p function

Pdr5p is the major transporter in exponentially growing *S. cerevisiae* cells, with a reported 42,000 molecules per cell, compared to 1,300 molecules of Snq2p and 3,600 molecules of Yor1p (Ghaemmaghami et al., 2003). This 160 kDa full-sized protein is a member of the ABCG subfamily of ABC transporters and its domains are joined together in a reverse order, which is a unique feature of all transporters in this subfamily (Figure 1.4) (Balzi et al., 1994; Verrier et al., 2008). Pdr5p has a major role in exporting a large number of compounds such as protein synthesis inhibitors, mycotoxins, anticancer drugs, azole antifungals, steroids, and fluorescent dyes from living cells (Figure 1.5) (Kolaczkowski et al., 1996; Egner et al., 1998; Suzuki & Iwahashi, 2012). The ability of Pdr5p to transport the fluorescent dyes rhodamine 6G and rhodamine 123 provides a useful approach to directly visualize substrate transport or inhibition.

Inhibitory compounds can affect ABC transporters in three ways: by interaction with proteins; by changing the level of intracellular ATP; or by increasing membrane permeability (Bartosiewicz & Krasowska, 2009). Human P-gp inhibitors including flavonoids, protein kinase C effectors, and FK506 also have an effect on Pdr5p (reviewed in Hiraga et al., 2005). The Gleddie lab determined that *F. graminearum* produces an inhibitor that blocks DON transport by *S. cerevisiae*, and they have suggested that this inhibitor shares properties with FK506, such as the ability to specifically block Pdr5p function in *S. cerevisiae*. Numerous other Pdr5p-specific inhibitors have been identified including enniatin B, which was isolated from the *Fusarium* species Y-53 by Hiraga et al. (2005). FK506 and enniatin B are both substrates and inhibitors of Pdr5p (Figure 1.6) (Egner et al. 1998; Hiraga et al., 2005). Pdr5p is an effective exporter of DON; however, in the presence of the putative Pdr5p-specific inhibitor produced by *F. graminearum*, its ability to transport DON appears to become impaired.

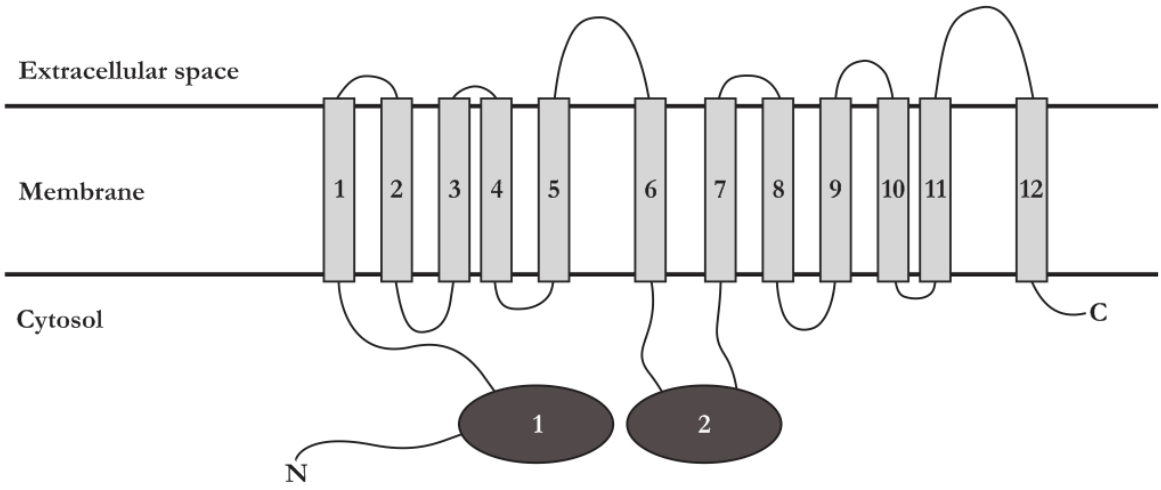

Figure 1.4 Predicted topology model of *S. cerevisiae* ABC transporter Pdr5p. The 12 TMDs are shown as numbered light grey rectangles interlinked by intracellular loops on the cytosolic side of the membrane and extracellular loops on the extracellular side. The two NBDs are shown as numbered dark grey ovals. The domains of Pdr5p are arranged in a reverse order (modified from Rutledge et al., 2011).

A) Cycloheximide **B) Fluconazole** **C) Ketoconazole**

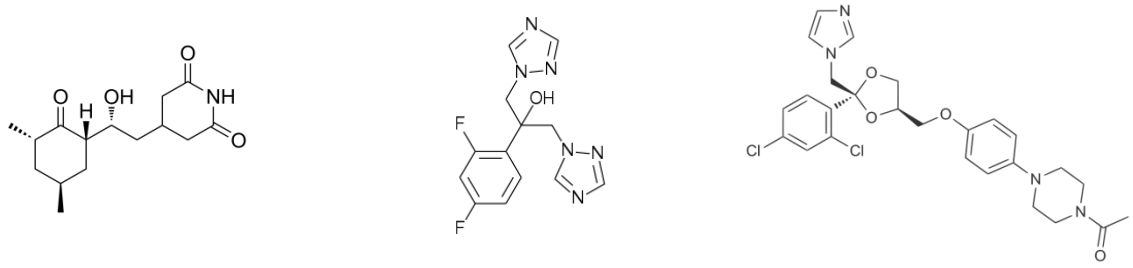

D) Sporidesmin **E) Dexamethasone** **F) Rhodamine 6G**

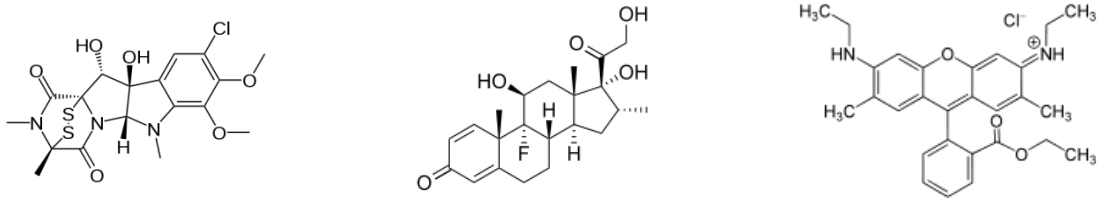

Figure 1.5 Examples of structurally and functionally unrelated substrates transported by *S. cerevisiae* ABC transporter Pdr5p. The structures of the following substrates are presented: (**A**) protein synthesis inhibitor cycloheximide, (**B**) azole antifungal fluconazole, (**C**) azole antifungal ketoconazole, (**D**) mycotoxin sporidesmin, (**E**) steroid dexamethasone, and (**F**) fluorescent dye rhodamine 6G.

FK506

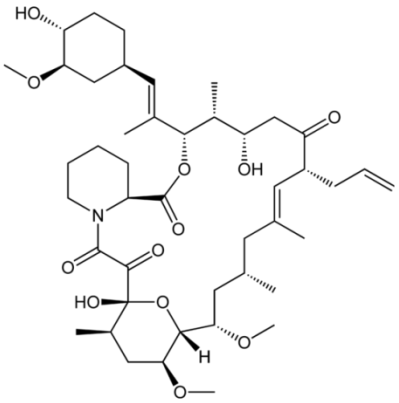

804.02 Da

Enniatin B

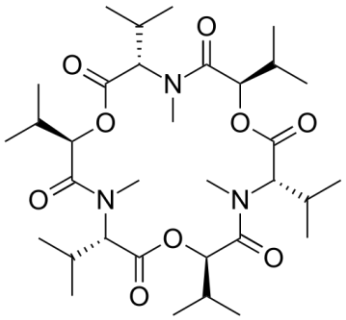

639.82 Da

Figure 1.6 Molecular structure and weight of FK506 and enniatin B. Both compounds are Pdr5p-specific inhibitors.

Unlike P-gp, which has low basal ATP hydrolysis activity in the absence of substrates, Pdr5p continuously displays high ATP hydrolysis activity, whether in the presence or absence of substrates. As suggested by Gupta et al. (2011), this seemingly futile basal activity of Pdr5p could be an adaptive mechanism since *S. cerevisiae* is a single cell organism and encounters much faster-changing environments than multicellular organisms. While its exact physiological role remains unclear, Pdr5p appears to be important in cell detoxification and adaptation to stress (Mamnum et al., 2004). Since it shows substrate overlap with ABC exporters from *Candida* species as well as substrate and inhibitor overlap with P-gp, Pdr5p is an important model transporter for the examination of drug resistance mechanisms in tumours and in pathogenic fungi. Similarly, Pdr5p can be used as a model to study plant resistance to trichothecene mycotoxins.

1.2.8 ABC transporters in plants

Examination of entire genome sequences has revealed that plants have considerably more ABC transporter genes than animals and fungi. In *A. thaliana*, *Oryza sativa*, *Sorghum bicolor*, and *Z. mays*, 130, 128, 121, and 130 respective potential transporters have been identified, compared to 56 in *Drosophila melanogaster*, 49 in *Homo sapiens*, 52 in *Mus musculus*, and 31 in *S. cerevisiae* (Rea, 1999; Xie et al., 2012; Pang et al., 2013). As autotrophs, plants require the function of a specialized membrane transport system to adapt and survive in rapidly and continuously changing environments (Dreyer et al., 1999; Pang et al., 2013). Plant ABC transporters are important members of this system and are essential for the function of numerous plant processes including growth and development regulation, defense against pathogens and herbivores, and protection from toxins, notably herbicides and secondary metabolites (Knöller & Murphy, 2011; Szewczak et al., 2011). In the context of green

biotechnology, plant ABC transporters could be engineered to enhance plant phytoremedation of toxic metals, such as lead or cadmium in contaminated soils, or to improve crop yield through the development of cultivars resistant to drought, salinity, pathogens, and/or pests (Szewczak et al., 2011; Pang et al., 2013).

Despite the importance of mammalian and yeast ABC transporters in toxin resistance, the role of their plant counterparts in this phenomenon remains largely unknown. Substrate specificity between mammalian P-gp and its *A. thaliana* ortholog AtABCB1 differs substantially, as AtABCB1 appears to be primarily involved in cellular efflux of auxin. Multani et al. (2003) demonstrated that disruptions of ABCB1 in *Z. mays* and *S. bicolor* affect growth elongation due to impaired polar auxin transport in the plants. Through the use of HeLa cells expressing AtABCB1, Geisler et al. (2005) showed that while auxin was effluxed, the anticancer drug daunomycin, the anticancer drug analogue BODIPY-vinblastine, and the fluorescent dye rhodamine 123, which are all substrates of P-gp, remained within the cells. Additionally, *A. thaliana* plants overexpressing AtABCB1 have shown resistance to certain herbicides but sensitivity to others (Windsor et al., 2003). Although these findings are restricted to one ABC transporter and a limited number of toxins, they suggest that plant ABC transporters could to be engineered for resistance against herbicides and possibly secondary metabolites, including mycotoxins.

1.3 Yeast as a model for plants

1.3.1 Experimental analysis of ABC transporters

As the first eukaryote to have its genome completely sequenced (Goffeau et al., 1996), *S. cerevisiae* has been used as a major model in systems biology as well as functional genomics and proteomics research in higher organisms (Winzeler et al., 1999; Giaever et al., 2002; Suter et al.,

2006). *S. cerevisiae* is a single-cell eukaryote sharing molecular, genetic, and biochemical characteristics with higher organisms (Yesilirmak & Sayers, 2009). Compared to plants, which have large genomes, *S. cerevisiae* is a relatively simple system with a small compact genome coding for about 6,000 genes, or open reading frames (ORFs), of which less than 7% have introns (Goffeau et al., 1996; Nagy, 2008). Additionally, it has a short doubling time of ninety minutes, it is stable in both haploid and diploid states, and it can easily be manipulated and grown on defined media (Suter et al., 2006). *S. cerevisiae* can therefore easily be used to conduct *in vivo* assays since it gives measurable phenotypes, which can be used for genetic screening.

As a host for heterologous expression, *S. cerevisiae* has been useful in the characterization of plant membrane transporters. Since biochemical and biophysical studies requiring the isolation of plant proteins are often troublesome due to cost and time constraints, *S. cerevisiae* has been widely used as the host organism for heterologous protein expression (Yesilirmak & Sayers, 2009). Another advantage of *S. cerevisiae* is that both overexpression and knockout strains for most annotated or putative *S. cerevisiae* ORFs have been created to form the yeast overexpression and knockout collections.

The genetic activity of an organism can be manipulated experimentally by increasing (overexpressing) or decreasing (knocking out) gene dosage (Niu et al., 2008). By either overexpressing or knocking out a single gene, it becomes possible to study the function of that particular gene as well as the effects of its modification though phenotypic analyses. The *Saccharomyces* genome-deletion project has successfully produced knockout strains for most *S. cerevisiae* ORFs. For each yeast knockout (YKO) strain, a different ORF was replaced by homologous recombination with a kanMX4 selectable resistance gene, thereby conferring strain resistance to the kanamycin analog geneticin (G418) (Winzeler et al., 1999; Giaever et al., 2002).

Using YKO strains for ABC transporter genes, it would be possible to analyze their phenotypes during growth in the presence of a mycotoxin such as DON.

1.3.2 Molecular modeling of Pdr5p

Despite being one of the best-characterized ABC transporters in yeast, a crystal structure of Pdr5p has not yet been resolved; however, the computationally modeled structure of Pdr5 is an important substitute (Rutledge et. al., 2011). The molecular model for Pdr5p is based on the crystal structures of the resolved ABC transporters P-gp of mouse, Sav1866 of *S. aureus*, and Haemolysin B (HlyB) of *E. coli* (Schmitt et al., 2003; Dawson & Locher, 2006; Aller et al., 2009), which were selected due to sequence homology. Furthermore, this model has been validated by functional studies of single amino acid residue substitutions. The NBDs of Pdr5p were modeled in the "open" position using P-gp, and in the "closed" position using HlyB as templates. The TMDs were modeled in the "inward-facing" conformation using P-gp and in the "outward-facing" conformation using Sav1866. From this molecular model of Pdr5p, a large central cavity is observed in both TMD conformations. This is consistent with the crystal structures of P-gp and Sav1866 transporters, which show a large substrate-binding pocket formed by the TMDs.

1.3.3 Identification of TMD amino acid residues implicated in toxin transport

An important objective towards understanding the mechanism of Pdr5p function involves identifying and analyzing individual amino acid residues lining the substrate-binding pocket that affect substrate transport and inhibitor susceptibility. This has been conducted extensively in *S. cerevisiae* using random and site-directed mutagenesis combined with phenotypic screening of the resulting Pdr5p mutants (Egner et al., 1998; 2000; Tutulan-Cunita et al., 2005). Together with molecular modeling, these mutagenesis studies suggest that Pdr5p contains at

least seven different drug-binding sites, located on the hydrophilic face of the substrate-binding pocket. Two of these putative binding sites, located at residues S1360 and T1364 of TMH11, are of particular interest for this study (Figure 1.7). Following the random mutagenesis of *PDR5*, Egner et al. (1998) determined that the S1360F amino acid substitution at residue S1360 enabled Pdr5p to maintain substrate export in the presence of the Pdr5p-specific inhibitory drug FK506. Subsequently, Egner et al. (2000) conducted site directed mutagenesis of S1360 as well as T1364, which corresponds to the residue located one helix turn further up from S1360. The resulting mutants were classified based on their FK506 sensitivity levels as follows: S1360A > WT > S1360T = T1364S > T1364A > T1364F = S1360F. Furthermore, Hiraga et al. (2005) observed that the Pdr5p-specific inhibitor enniatin B had a similar substrate inhibition pattern to that of FK506, with S1360A being more sensitive than the WT, which was more sensitive than S1360F. Since *F. graminearum* produces an inhibitor that appears to share properties with FK506, such as the ability to specifically block Pdr5p, it is therefore possible that specific amino acid substitutions at residues S1360 and/or T1364 could enable Pdr5p to maintain its ability to export trichothecene mycotoxins such as DON in presence of this inhibitory compound. This could provide important details about how Pdr5p could potentially be manipulated to be used as an efficient first line of defense against contamination by *F. graminearum* mycotoxins.

1.4 Hypotheses and Objectives

This project was divided into main two parts:

The first part involved determining whether or not other members of the PDR network, in addition to Pdr5p, were involved in exporting DON and 15A-DON from *S. cerevisiae*. This was done since ABC transporters from the PDR network, notably Pdr5p, Snq2p, and Yor1p, had previously shown overlapping substrate specificities (Kolaczkowski et al., 1998). It was

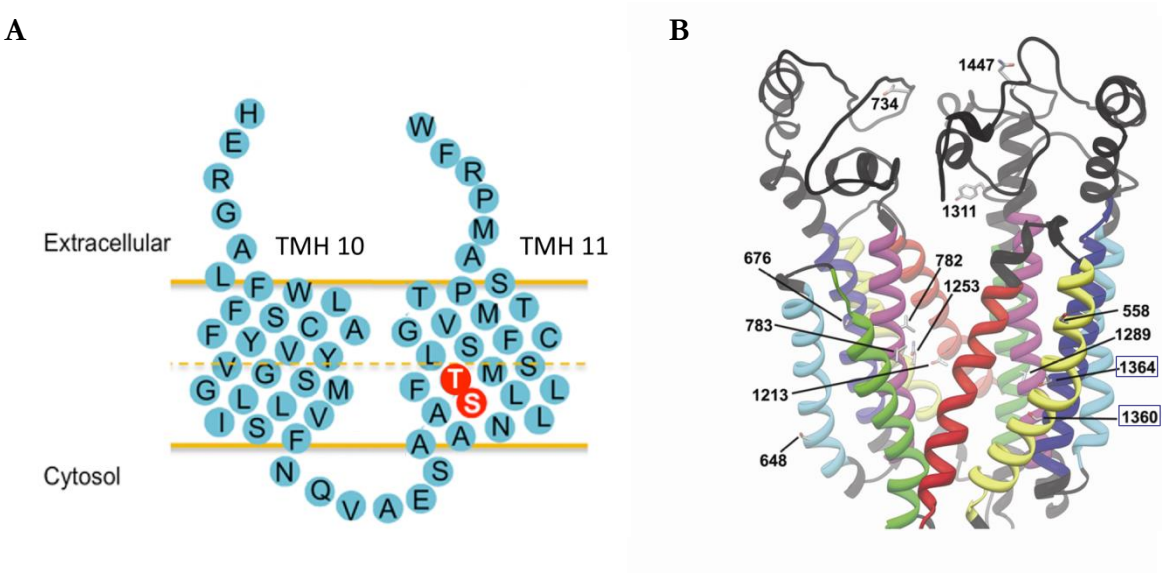

Figure 1.7 Predicted model of the TMHs of *S. cerevisiae* ABC transporter Pdr5p. (**A**) Membrane topology of TMHs 10 and 11 with amino acid residues S1360 and T1364 (shown in red) localized in TMH 11 (modified from Kueppers et al., 2013). (**B**) Structure of the TMHs of Pdr5p with amino acid residues S1360 and T1364, localized in TMH 11 (shown in blue) (modified from Rutledge et al., 2011).

hypothesized that: 1) the plasma membrane of *S. cerevisiae* contains at least one ABC transporter from the PDR network with substrate specificity for DON and 15A-DON; and 2) the absence or inhibition of such transporters will lead to yeast growth inhibition in the presence of either mycotoxin. The objectives of the first part of this thesis were to: 1) identify the ABC transporter(s) from the PDR network with substrate specificity for DON and 15A-DON using *S. cerevisiae* as a model for plants; and 2) determine the importance of any identified transporter in exporting these mycotoxins from the cell.

The second part involved engineering the ABC transporter(s) involved in DON and 15A-DON export in order to maintain efficient mycotoxin export while in the presence of an inhibitory compound such as that produced by *F. graminearum*. Previous studies with Pdr5p had shown that single amino acid substitutions at residue S1360 or T1364 affect substrate specificity and inhibitor susceptibility (Egner et al., 1998; 2000). It was therefore hypothesized that modifying a single amino acid at either of these sites in Pdr5p, or at corresponding sites in any other ABC transporter with substrate specificity to DON and 15A-DON, could modulate insensitivity to the FK506-like inhibitor produced by *F. graminearum* while maintaining efficient export of both mycotoxins. The objectives of the second part of this thesis were to: 1) generate mutants of any important exporter of DON and 15A-DON; and 2) analyze the mutants to determine if any could modulate insensitivity to the *F. graminearum* inhibitory compound while maintaining efficient mycotoxin export.

CHAPTER 2 – MATERIALS AND METHODS

2.1 Yeast strains

The *Saccharomyces cerevisiae* yeast knockout (YKO) strains used in this study were derived from the haploid parental wild-type (WT) strain BY4741 (*Mat**a** his3*Δ*1 leu2*Δ*0 met15*Δ*0 ura3*Δ*0*) (Thermo Scientific). Yeast from the BY4741 and YKO strains were obtained from glycerol stocks stored at -80°C in 96-well plates. The WT *PDR5*- and mutant *PDR5*-expressing yeast transformants used in this study are isogenic and were derived from the Δ*pdr5* YKO strain.

2.2 Growth, selection, and isolation of yeast colonies

Yeast strains were plated onto appropriate growth medium as follows: BY4741, on non-selective yeast peptone dextrose (YPD) agar [1% (w/v) yeast extract, 2% (w/v) peptone, 2% (v/v) dextrose, 2% (w/v) agar]; the YKO strains, on selective YPD agar [1% (w/v) yeast extract, 2% (w/v) peptone, 2% (v/v) dextrose, 2% (w/v) agar, 0.2 μg/μL G418]; and the Δ*pdr5* transformants, on synthetic dropout agar lacking uracil (SD-Ura) {0.17% (w/v) yeast nitrogen base, 0.5% (w/v) ammonium sulphate, 10% (v/v) 10x amino acid dropout solution minus L-Uracil [0.02% (w/v) L-adenine hemisulfate salt, 0.02% (w/v) L-Arginine hydrochloride (HCl), 0.02% (w/v) L-Histidine HCl monohydrate, 0.03% (w/v) L-Isoleucine, 0.1% (w/v) L-Leucine, 0.03% (w/v) L-Lysine HCl, 0.02% (w/v) L-Methionine, 0.05% (w/v) L-Phenylalanine, 0.2% (w/v) L-Threonine, 0.02% (w/v) L-Tryptophan, 0.03% (w/v) L-Tyrosine, 0.15% (w/v) L-Valine], 2% (w/v) agar}.

For the selection and isolation of individual colonies, yeast were streaked onto appropriate media and incubated at 30°C. When most individual colonies reached a diameter of 1-2 mm on the plates, one colony from each yeast strain was re-streaked onto appropriate fresh

agar media and incubated at 30°C to obtain pure clonal isolates. When the majority of clonal isolates reached a diameter of 1-2 mm on the plates, a suitable number were patched, with sterile toothpicks, onto appropriate fresh agar media, as described above, and incubated for a minimum of 48 h at 30°C. All yeast manipulations were performed in a laminar flow hood using aseptic technique.

2.3 Storage and maintenance of confirmed yeast strains

When the identity of a yeast strain was confirmed, either by PCR or by sequencing, as described below in "2.4 Verification of YKO strains" and "2.8 Verification of the Δ*pdr5* transformants", a small quantity of yeast (~2 mm in diameter) corresponding to the confirmed strain was scraped from the media with a sterile toothpick and used to inoculate 5 mL of liquid YPD in sterile 20 mm glass culture tubes. The BY4741 strain and the Δ*pdr5* transformants were grown in non-selective YPD and the YKO strains were grown in selective YPD overnight at 30°C and 300 rpm in an Excella® E24 incubator shaker (New Brunswick). In sterile 2 mL Nalgene® cryogenic vials, 500 μL of overnight yeast culture were added to 500 μL of sterile 30% glycerol. The cryogenic vials were kept at room temperature on a nutating mixer for a minimum of 5 min. The yeast strains were then stored as glycerol stocks in the cryogenic vials at -80°C. Yeast strains were maintained at 4°C as patched colonies on agar plates containing the appropriate media. Every month, strains were patched from the appropriate frozen glycerol stocks, with sterile toothpicks, onto appropriate fresh agar media, as described above, and incubated for a minimum of 48 h at 30°C.

2.4 Verification of YKO strains

Each YKO strain was generated by deleting a single open reading frame (ORF) and replacing it by homologous recombination with a PCR-generated kanMX4 cassette (Figure 2.1)

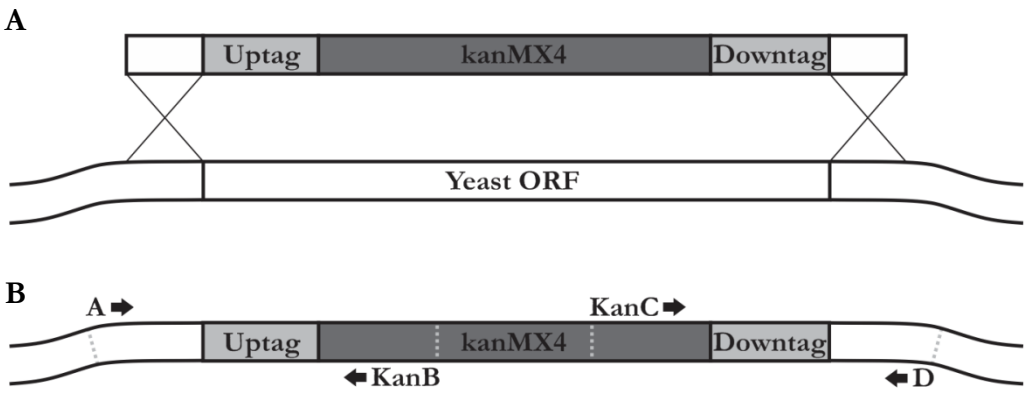

Figure 2.1 Example of a YKO strain. Representation of (**A**) yeast ORF replacement with a PCR-generated kanMX4 cassette, composed of a kanMX4 marker, Uptag, and Downtag, and (**B**) PCR amplification of a DNA sequence upstream from the kanMX4 marker (including the strain-specific Uptag), using the KanB-A primer pair, and PCR amplification of a DNA sequence downstream from the kanMX4 marker (including the strain-specific Downtag), using the KanC-D primer pair (modified from Giaever et al., 2002).

(Giaever et al., 2002). This cassette contains the kanMX4 selectable marker, which confers resistance to G418. PCR amplification can be used to verify the identity of every YKO strain, which each have four 20-bp primer binding sites: "A", "B", "C", and "D". Strain-specific primers ("A" and "D") bind to the A and D sites respectively while primers specific to the kanMX4 marker ("KanB" or "KanC") bind to the B and C sites respectively. The A-KanB primer pair amplifies a DNA fragment upstream from the kanMX4 marker, including a strain-specific region of the kanMX4 cassette known as the "Uptag". The D-KanC primer pair amplifies a DNA fragment downstream from the kanMX4 marker, including a strain-region of the kanMX4 cassette known as the "Downtag". PCR amplification using these strain-specific primer pairs was conducted to verify the identity of each YKO strain used in this study.

2.5 Preparation of genomic DNA (gDNA)

Crude genomic DNA (gDNA) preparations were made from each YKO strain using a protocol adapted from Lõoke et al. (2011). Yeast (~2 mm in diameter) from a single patched colony of each YKO strain was scraped from the media with a 100 μL plastic pipette tip and suspended in a 0.5 mL tube containing 100 μL of a LiOAc-SDS lysis solution (200mM LiOAc and 1% SDS). After incubation for 15 min at 70°C in a water bath, 300μL of 95% ethanol was added to the tube to precipitate the gDNA. The tube was briefly vortexed for 5-10 s, and centrifuged at 15,000 *g* for 3 min. The supernatant was removed and the precipitated gDNA was dissolved in 100μL TE (Tris-EDTA) buffer [10mM Tris-HCl (pH 8) and 1mM EDTA (pH 8)], centrifuged at 15,000 *g* for 1 min, and stored at -20°C.

2.5.1 PCR amplification

All PCR primers used to verify the identity of the YKO strains used in this study were purchased from Sigma-Aldrich and reconstituted to 100 μM in TE buffer (Table 2.1). The

Table 2.1 Primers used for the PCR verification of all YKO strains used in this study. KanB and KanC, which are specific to the kanMX4 marker, were paired respectively with the strain-specific A and D primers to amplify a fragment of DNA from each YKO strain.

PCR Primer	Primer Sequence (5' → 3')	Expected PCR Product Size (bp)
KanB	CTGCAGCGAGGAGCCGTAAT	
PDR5-A	TTGAACGTAATCTGAGCAATACAAA	578
PDR10-A	GTACTACTACAGAATTGGTCGGCAT	577
PDR11-A	CACTTTTGTTTCCTACAACTTCCAC	678
PDR12-A	TCTCGACGGTTCTTATGATTATTTC	635
PDR15-A	GAGGGAAAAGAATACTGCTACTGCT	593
PDR18-A	TATCCGGGAATTCTGATATTTTACA	528
ADP1-A	GGTAATTTCTTTCTCGATAAGAGGC	660
AUS1-A	CTGAAGATCACTCCATATACAGGCT	685
SNQ2-A	CACCACTTTTTATGCTTGTATATGCT	667
YOR1-A	TTTCCTACAAATAGATCTGCTGTCC	606
YOL075c-A	ACGTATTGGAAGATACAGGTTCAGA	627
KanC	TGATTTTGATGACGAGCGTAAT	
PDR5-D	TCACACTAAATGCTGATGCCTATAA	886
PDR10-D	TCACTGCAGATGTTAATAGATCCAA	967
PDR11-D	GATGCAAATCAAGGAATGTTCTAAT	995
PDR12-D	TCAAACTTCCTTTTGAAGGTGATAG	934
PDR15-D	GAATAATCCAGTTCGACTCTGAAAA	943
PDR18-D	TTGGGATTATGTGTTTATAGCCTTG	943
ADP1-D	GTCTCTGACAGGTTGGAGTACAGAG	1026
AUS1-D	ACTCTGAGAAACAACAAAATAACGG	908
SNQ2-D	GTTTAGCTTGTACTTGCAACACCTT	944
YOR1-D	ATTTGAAATATCCTTCGGTTTTAGG	1011
YOL075c-D	TGATGTTAAAGCTGAAAATGTCAAG	946

sequence for each of these primers was obtained from the Saccharomyces Genome Deletion Project website (http://www-sequence.stanford.edu/group/yeast_deletion_project/downloads.html#strainsavail). PCR amplification was done in 52 μL reactions in 0.2 mL PCR tubes containing the following materials: 10 μL of 5x Green GoTaq® Reaction Buffer (Promega; Cat. no. M3005), 2 μL of 10 mM A or D primer, 2 μL of 10mM KanB or KanC primer, 1 μL of dNTP mix (10 mM each), 0.25 μL of 5 units/μL GoTaq® DNA Polymerase (Promega; Cat. no. M3005), 5 μL of gDNA template, and 31.75 μL of PCR-H_2O. A positive control (+) was prepared by adding gDNA from a previously confirmed YKO strain. A negative control (-) was prepared by substituting the gDNA template with PCR-H_2O. PCR amplification was carried out in a Mastercycler® gradient thermocycler (Eppendorf) as follows: initial denaturation at 95°C for 1 min, 35 × (denaturation at 95°C for 1 min, annealing at 50°C for 1 min, extension at 72°C for 1 min), and final extension at 72°C for 7 min.

2.5.2 Analysis of PCR products

PCR products (20 μL) were loaded on a 1% (w/v) agarose gel containing 1x Tris-acetate-EDTA (TAE) buffer (40mM Tris-acetate and 1mM EDTA) with SYBR® Safe DNA gel stain [1:10,000 (v/v) dye-to-gel ratio; Life Technologies™; Cat. no. S33102]. A DNA ladder [2.4 μL of 0.5 μg/μL GeneRuler™ DNA Ladder Mix (100-10,000 bp) (Thermo Scientific; Cat. no. SM0331), 2.4 μL of 6x DNA loading dye (Thermo Scientific; Cat. no. SM0331), and 9.6 μL of PCR-H_2O] was also loaded on the gel. After 1 h of electrophoresis at 100 V (constant voltage), DNA bands were visualized and photographed under ultraviolet (UV) transillumination using a ChemiDoc™ XRS+ imaging system with Image Lab™ software (Bio-Rad). The band sizes were then compared to the expected PCR product sizes specified on the Saccharomyces

Genome Deletion Project website (http://www-sequence.stanford.edu/group/yeast_deletion_project/downloads.html#strainsavail).

2.6 Site-directed mutagenesis of the *PDR5* gene

Gene cassettes containing the indigenous *PDR5* promoter with its three PDREs, the *PDR5* gene, and the three prime untranslated region (3' UTR) of *PDR5* were constructed and sequence-verified. The cassettes, containing either the WT *PDR5* gene or a mutant *PDR5* gene coding a serine (S) to phenylalanine (F) substitution at residue S1360F (referred to as the S1360F mutant), were individually cloned into the p416CYC1 plasmid (DualSystems Biotech), replacing the CYC1 promoter and CYC1 terminator. The p416CYC1 plasmid is a low-copy-number CEN/ARS yeast expression vector containing URA3 as a selectable marker for uracil biosynthesis. Plasmids were expressed from a low-copy-number vector to best-replicate natural expression levels of *PDR5*. Human influenza hemagglutinin (HA) epitope-tagged versions were developed by inserting the HA coding sequence at the N-terminus coding sequence of both *PDR5* gene cassettes. These cassettes were also individually cloned into the p416CYC1 plasmid vector. All manipulations described above with the *PDR5* gene were performed by the Gleddie lab. All other mutant *PDR5* genes coding single amino acid substitutions at residue S1360 and T1364 were generated by *in vitro* site-directed mutagenesis of the WT *PDR5* HA-tagged gene. Cassettes containing the *PDR5* promoter with its three PDREs, one of the mutant *PDR5* genes, and the 3' UTR of *PDR5* were sequence-verified and individually cloned into the p416CYC1 plasmid using the GeneArt® Mutagenesis Service (Life Technologies). Each plasmid was individually transformed into the Δ*pdr5* YKO strain as described below. In total, 38 *PDR5* mutants coding for every single amino acid substitution at residue S1360 and T1364 were generated.

2.7 Transformation of yeast

Each p416CYC1 plasmid was individually introduced into the Δ*pdr5* YKO strain by transformation using a protocol adapted from Amberg et al. (2005). Prior to transformation, yeast from the PCR-verified Δ*pdr5* YKO colony underwent Western blot analysis, as described below in "2.9 Yeast protein extract preparation and Western blot analysis", to confirm the absence of Pdr5p expression. For each transformation, freshly grown yeast (~2 mm in diameter) from the PCR-verified Δ*pdr5* colony was scraped from the media with a 100 μL plastic pipette tip and suspended in a 1.5 mL microcentrifuge tube containing the following materials: 3 μL of 10 mg/mL denatured herring testes carrier DNA (previously denatured in a boiling water bath for 5 min), 1μL of plasmid DNA, and 100 μL of fresh transformation mix (0.4 M fresh sterile LiOAc and 40% PEG-3350, plus 7.7 μL of β-mercaptoethanol per mL of transformation mix). An empty plasmid (E) DNA control was also prepared. A no DNA control (-) was prepared by substituting the plasmid DNA with sterile Milli-Q-H_2O (MQ-H_2O). Suspended cells were vortexed for 5-10 s then incubated for 30 min at 37°C in a water bath. The cells were pelleted by centrifugation at 3,000 rpm for 4 min and resuspended in 100 μL sterile MQ-H_2O. The cells were then plated and grown on SD-Ura agar as described above in "2.2 Growth, selection, and isolation of yeast colonies" to select for Δ*pdr5* colonies transformed with the p416CYC1 plasmid. Growth assays in liquid culture were conducted as described below in "2.11 Growth assays" with 15A-DON (25 μg/mL) to screen sister clones from each Δ*pdr5* transformation. Growth phenotypes were visually inspected and sister clones were grown until four from each transformation demonstrated a similar phenotype.

2.8 Verification of the *Δpdr5* transformants

2.8.1 Plasmid rescue

Plasmid rescue was conducted against phenotypically-verified sister clones from each Δ*pdr5* transformant to recover the *PDR5* gene and to verify the identity of each transformant. Plasmid DNA was rescued with the QIAprep® Spin Miniprep Kit (Qiagen; Cat. no. 27104) using a protocol adapted from the Gottschling Lab. Yeast cells were grown overnight as described above in "2.3 Storage and maintenance of confirmed yeast strains". For each overnight culture, 1.5 mL of cells were transferred to 1.5 mL microcentrifuge tubes and pelleted by centrifugation at 3,800 *g* for 5 min. The supernatants were removed and the pellets were resuspended in 250 μL of resuspension buffer P1, and then transferred to 2 mL screw-capped tubes containing 250 μL of 425-600 μm acid-washed glass beads (Sigma-Aldrich; Cat. no. G8772). Yeast cells were lysed for 45 s at level 6 in a Fast-Prep Machine (MP Biomedicals); 250 μL of lysis buffer P2 were added and the tubes were slowly inverted 6 times; then 350 μL of neutralization buffer N3 were added and the tubes were slowly inverted 6 times. The mixture was centrifuged at maximum speed for 10 min, and then the supernatants were applied to QIAprep spin columns. The columns were centrifuged at maximum speed for 60 s, the flow-through was discarded, and retained plasmid DNA was washed with 750 μL of wash buffer PE. The columns were then centrifuged at maximum speed for 60 s, the flow-through was discarded, and the columns were centrifuged at maximum speed for an additional 2 min. The columns were placed in clean 1.5 mL microcentrifuge tubes, and the plasmid DNA was eluted from the membrane of the columns into the tubes by adding 50 μL of elution buffer (EB), incubating for 1 min at room temperature, and then centrifuging at maximum speed for 1 min.

Plasmid DNA concentrations were determined using a NanoDrop spectrophotometer (Thermo Scientific).

2.8.2 PCR amplification

PCR was performed to amplify an 870 bp fragment of *PDR5* from plasmid recovered from each Δ*pdr5* transformant. The following primer pair was designed using PrimerSelect (DNAStar®), ensuring that the primers flanked the coding sequences of amino acid residues S1360 and T1364 of Pdr5p: forward *PDR5* primer (5'-GGTCAGTATTCGTCTATTCCAGCA-3') and reverse *PDR5* primer (5'-ATACCATAATTTCTCCATCTCT-3'). The primers were purchased from IDT and reconstituted to 100μM in TE buffer. PCR reactions were set up in a UV-irradiated laminar flow hood with UV-irradiated materials and equipment (pipettes, tips, PCR tubes, and PCR-H_2O). PCR amplification was done in 50 μL reactions in 0.2 mL PCR tubes containing the following materials: 5 μL of 10x High Fidelity PCR Buffer (Life Technologies™; Cat. no. 11304), 1 μL of dNTP mix (10 mM each), 2 μL of 50 mM $MgSO_4$ (Life Technologies™; Cat. no. 11304), 0.2 μL of Platinum® Taq DNA Polymerase High Fidelity (Life Technologies™; Cat. no. 11304), 1 μL of *PDR5* primer mix (10 mM each), 3 μL of plasmid DNA, and 37.8 μL of PCR-H_2O. A no DNA control was prepared by substituting the plasmid DNA with sterile PCR-H2O. PCR amplification was carried out in a Mastercycler® gradient thermocycler (Eppendorf) as follows: initial denaturation at 94°C for 2 min, 35 × (denaturation at 94°C for 15 s, annealing at 45°C for 30 s, extension at 68°C for 1.5 min), and final extension at 68°C for 7 min.

2.8.3 Analysis of PCR products

In 0.5 mL tubes, 2μL of 6x DNA loading dye (Thermo Scientific; Cat. no. SM0331) were added to 18 μL of PCR product. These products were analyzed as described above in "2.5.2 Analysis of PCR products". These PCR products were then prepared for sequencing.

2.8.4 Sequencing

Prior to setting up the sequencing reactions PCR products were treated with ExoSAP-IT® (Affymetrix; Cat. no. 78201). In 0.2 mL PCR tubes, 2 μL of ExoSAP-IT® reagent were added to 5 μL of PCR product. Cleanup of the PCR products (elimination of unincorporated primers and dNTPs) by ExoSAP-IT® was carried out in a Masetercycler® gradient thermocycler (Eppendorf) with incubation at 37°C for 15 min followed by inactivation of the enzyme at 80°C for 15 min. A forward and reverse sequencing reaction was performed on each ExoSAP-IT®-treated PCR product. The following primers were designed to cover a length of 328 bp within the PCR-amplified fragment using PrimerSelect (DNAStar®), ensuring that they flanked the coding sequences of amino acid residues S1360 and T1364 of Pdr5p: forward primer (5'-ATTTCATTTATCTTCGCTCAA-3') and reverse primer (5'-ATACCATAATTTCTCCATCTCT-3'). The primers were purchased from Sigma-Aldrich and reconstituted to 100μM in TE buffer. Sequencing reactions were done in a volume of 10 μL in 0.2 mL PCR tube strips containing the following materials: 1.75 μL of BigDye® Terminator v3.1 5x Sequencing Buffer (Life Technologies™; Cat. no. 4337454), 0.5 μL of BigDye® Terminator v3.1 Ready Reaction Mix (Life Technologies ™; Cat. no. 4337454), 0.5 μL of 3.2μM forward or reverse primer, 1 μL of ExoSAP-IT®-treated PCR product, and 6.25 μL of PCR-H_2O. The sequencing reactions were carried out in a Mastercycler® gradient thermocycler (Eppendorf) as follows: initial denaturation at 95°C for 3 min, 40 × (denaturation at 95°C for 30 s, annealing at 50°C for 15 s,

extension at 60°C for 2 min). The sequencing reactions were run by the ECORC Microbial Molecular Technologies Laboratory (MMTL) group, Ottawa.

2.8.5 Analysis of sequences

Contiguous sequence results from the forward and reverse products of each sequencing reaction were received from the ECORC MMTL group, Ottawa and assembled using SeqMan Pro (DNAStar®) to generate a consensus sequence for each *PDR5* gene fragment. Generation of the reverse complement sequence and translation to amino acids was done using SeqBuilder (DNAStar®). Alignment of all amino acid sequences was done in MegAlign (DNAStar®) using the ClustalW method. Verification of the aligned amino acids at residues S1360 and T1364 was done to confirm that each Δ*pdr5* transformant had been transformed with the correct amino acid-substituted *PDR5* gene.

2.9 Yeast protein extract preparation and Western blot analysis

2.9.1 Protein extract preparation

Whole-cell protein extracts were prepared for Western blot analysis of Pdr5p expression using a protocol adapted from von der Haar (2007). Yeast cells were grown overnight as described above in "2.3 Storage and maintenance of confirmed yeast strains". About 24 h later, 0.5-1.5 μL of overnight yeast culture were used to inoculate 10 mL of liquid YPD in a new set of sterile yeast culture tubes, and the cultures were grown overnight again at 30°C and 300 rpm in an Excella® E24 incubator shaker (New Brunswick). In semimicro disposable 1.5 mL cuvettes (Fisher Scientific), yeast cells from each culture were diluted 10-fold in sterile MQ-H_2O. The cuvettes were slowly inverted 15-20 times and placed in a Genesys Uv spectrophotometer (Thermo Scientific) to measure the optical density of the cultures at 600 nm

(OD_{600}). Cultures were grown until they reached an OD_{600} of 3.5 in log phase growth. Considering that cultures with an OD_{600} of 1.0 contain 3×10^7 cells/mL, 10^8 cells were then transferred to 2 mL screw-capped tubes containing a volume of 75 µL of 425-600 µm acid-washed glass beads (Sigma-Aldrich; Cat. no. G8772). Cells were pelleted by centrifugation at 3,800 *g* for 5 min, then the supernatants were removed, and the pellets were resuspended in 1 mL of sterile ice cold MQ-H_2O. Cells were pelleted by centrifugation at 3,800 *g* for 5 min, the supernatants were removed, and the pellets were quick-frozen in liquid nitrogen. The pellets were thawed on ice and resuspended in 100 µL of lysis buffer [8 M urea, 0.1 M NaOH, 50 mM EDTA, and 2% SDS, plus 20 µL β-mercaptoethanol and one cOmplete™, Mini, EDTA-free protease inhibitor cocktail tablet (Roche; Cat. no. 04693159001) per mL of lysis buffer]. Cells were lysed for 45 s at level 6 in a Fast-Prep Machine (MP Biomedicals). After incubation for 10 min at 55°C in a water bath, 2.5 µL of 4 M acetic acid were added, and the tubes were vortexed for 30 s. After incubation for 10 min at 55°C in a water bath, lysates were cleared by centrifugation at maximum speed for 5 min. The supernatants were transferred to sterile 1.5 mL tubes and then centrifuged at maximum speed for 2.5 min. After adding 25 µL of loading buffer [0.25 M Tris-HCl (pH 6.8), 50% glycerol, and 0.05% bromophenol blue], the tubes were gently mixed for 30 s and then centrifuged at maximum speed for 2.5 min. The protein extracts were aliquoted to 0.5 mL tubes and stored at -20°C.

2.9.2 SDS-polyacrylamide gel electrophoresis (SDS-PAGE) and protein transfer

Proteins were prepared for SDS-PAGE by incubating protein extracts for 5 min at 55°C in a water bath. Afterward, 2.5 µL of each extract were loaded on 4-15% 15-well Mini-PROTEAN® TGX™ precast gels (Bio-Rad; Cat. no. 456-1086) or 4-15% 26-well Criterion™ TGX™ precast gels (Bio-Rad; Cat. no. 567-1085). A prestained protein marker [2.5 µL Precision

Plus Protein™ All Blue Standard (10-250 kDa) (Bio-Rad)] was also loaded on the gels. Empty wells were loaded with 2.5 μL of 1:5 (v/v) diluted loading buffer. Proteins were separated by SDS-PAGE at 200 V (constant voltage) in a Mini-PROTEAN® Tetra Cell (Bio-Rad) for 35 min or in a Criterion™ Cell (Bio-Rad) for 45 min, then blotted onto 0.2 μm polyvinylidene difluoride (PVDF) membranes [Trans-Blot® Turbo™ PVDF Transfer Packs (Bio-Rad; Cat. no. 170-4157)] using a Trans-Blot® Turbo™ Blotting System (Bio-Rad). Proteins separated on Mini-PROTEAN® gels were blotted using the High MW protocol (10 min, 1.3 A) and proteins separated on Criterion™ gels were blotted using the Turbo protocol (7 min, 2.5 A). Following protein transfer, blots were air-dried on Whatman paper for 1 h.

2.9.3 Western blot analysis

After 1 h of drying, blots were reactivated with 100% methanol for 20 s. The reactivated membranes were then placed in 1x Tris-buffered saline (TBS) [50 mM Tris-HCl (pH 7.5) and 150 mM NaCl] for 5 min. Membranes were then blocked overnight at 4°C in blocking buffer (RBB) [1% blocking reagent (Roche; Cat. no. 11096176001) prepared in maleic acid buffer (pH 7.5) and 1x TBS]. Blots were then removed from RBB and incubated for 1 h in TBS-RBB solution (1x TBS and 0.5 % blocking buffer) containing affinity-purified goat polyclonal IgG antibody directed either against a peptide mapping at the N-terminus (yN-18; final dilution 1:500; Santa Cruz Biotechnology; Cat. no. sc-27253) or C-terminus of Pdr5p (yC-18; final dilution 1:500; Santa Cruz Biotechnology; Cat. no. sc-27255) and mouse monoclonal IgG loading control antibody directed against human beta actin (final dilution 1:1000; abcam®; Cat. no. ab8224). Following incubation, blots were washed 2 × 10 min in TBS-Tween solution (1x TBS and 0.1% Tween 20) and then 2 × 10 min in TBS-RBB solution. Blots were then incubated for 45 min in TBS-RBB solution containing HRP-conjugated affinity-isolated rabbit

anti-goat polyclonal IgG antibody (final dilution 1:120,000; Sigma-Aldrich; Cat. no. A5420) and HRP-conjugated AffiniPure rabbit anti-mouse IgG antibody (final dilution 1:60,000; Jackson ImmunoReseach; Cat. no. 315-035-003). Following incubation, antibody binding was detected by enhanced chemiluminescence (ECL) using the Clarity™ Western ECL system (Bio-Rad; Cat. no. 170-5061). After 5 min of incubation in the ECL substrate, blots were exposed for 5 min and photographed using a ChemiDoc™ XRS+ imaging system with Image Lab™ software (Bio-Rad). Protein bands were detected and quantified using the ImageLab™ software. Ratios of Pdr5p-to-actin were determined by dividing the relative quantity of Pdr5p by the relative quantity of actin from each lane. Proteins separated on the blots were then visualized by staining. After rinsing the blot in H_2O, it was stained for 5 min with Coomassie Brilliant Blue solution [50% (v/v) methanol, 7% (v/v) acetic acid, 0.1% (w/v) Coomassie Brilliant Blue R-250 stain (Bio-Rad)], destained for 5 min in destain solution [50% (v/v) methanol, 7% (v/v) acetic acid], rinsed in H_2O, and air-dried on Whatman paper.

2.10 Chemicals and fungal metabolites

Working solutions of G418 (100 mg/mL; BioShop®; Cat. no. GEN418.5), FK506 (20 mg/mL; LC Laboratories; Cat. no. F-4900), and enniatin B (2 mg/mL; Sigma-Aldrich; Cat. no. E5411) were prepared in 100% DMSO. *Fusarium graminearum* culture filtrates, DON, and 15A-DON were gifts from Dr. Barb Blackwell (ECORC AAFC, Ottawa), and *F. avenaceum* culture filtrates were gifts from Dr. Linda Harris (ECORC AAFC, Ottawa). *F. graminearum* culture filtrates were collected from the 15A-DON-producing strain DAOM 233423 grown in culture. High-performance liquid chromatography (HPLC) was used to quantify 15A-DON. Two ethyl-acetate extracts of culture filtrate (11A, prepared in 2011, and 12A, prepared in 2012) were used in this study. *F. avenaceum* culture filtrates were collected from the LH_27 and LH_36 strains

grown in culture. Working solutions of DON (25 mg/mL), 15A-DON (25 mg/mL), and both preparations of *F. graminearum* culture filtrate (24.23 mg/mL) were prepared in 100% DMSO.

2.11 Growth assays

Growth assays in liquid culture were performed to analyze the effects of selected toxins on the growth rate of *S. cerevisiae* strains.

2.11.1 Preparation of yeast cells

Yeast cells were grown overnight as described above in "2.3 Storage and maintenance of confirmed yeast strains". In semimicro disposable 1.5 mL cuvettes (Fisher Scientific), yeast cells from each culture were diluted 10-fold in sterile MQ-H_2O. The cuvettes were slowly inverted ~20 times and placed in a Genesys Uv spectrophotometer (Thermo Scientific) to measure the optical density of the cultures at 600 nm (OD_{600}). In a new set of sterile yeast culture tubes, the overnight cultures were diluted to an OD_{600} of 0.1 in 5 mL of liquid YPD and grown for 4 h, again at 30°C and 300 rpm in an Excella® E24 incubator shaker (New Brunswick), allowing the cells to return to log phase growth. The optical density of these cultures was then determined, as described above, without diluting the cultures in sterile MQ-H_2O. In sterile tubes, the cultures were then diluted to an OD_{600} of 0.1 in an appropriate volume of liquid YPD. The tubes were slowly inverted ~20 times.

2.11.2 Preparation of the negative control and treatments

The negative control and treatments were prepared in sterile tubes at 2x the final required concentration. DMSO was used as the negative control. The negative control and toxins added to each treatment were diluted in an equal volume of YPD. The percentage of DMSO was kept constant at 2.5% in all tubes.

2.11.3 Assay set-up

In sterile Nunc™ MicroWell™ 96-well plates (Thermo Scientific), 50 µL of cells at an OD_{600} of 0.1 were aliquoted to each designated well, then 50 µL of negative control or treatment was aliquoted to each designated well, for a total volume of 100 µL per well and a total of 2 or 3 technical replicates according to the assay. The plates were then covered with a Nunc™ Microplate Lid (Thermo Scientific) and sealed with parafilm. The growth rate for each strain was recorded, according to OD_{600} values measured by an Eon™ Microplate Spectrometer (BioTek®), using the Gen5™ 2.0 data analysis software (BioTek®). OD_{600} values were recorded every 10 min for 20 h, after 5 min of constant shaking (1,000 Hz) then 5 min of incubation at 30°C. Resulting growth curves (Figure 2.2) were analysed to compare technical replicates and to determine growth rate variation between cells grown in the presence or absence of a toxin.

2.11.4 Data analysis

Area under the curve (AUC) was calculated by integration of the growth curves using the Gen5™ 2.0 data analysis software (BioTek®). Relative growth ratios (%) were determined by dividing the AUC of treated cells by the AUC of control cells and multiplying the values by 100. Relative growth ratios were expressed as the mean, plus and minus the standard error of the mean (±SEM). Data were evaluated for equality of variance prior to statistical analysis. Data were then analyzed by 1-way analysis of variance (ANOVA), followed by Tukey's honestly significant difference (HSD) test with significance accepted at $P<0.05$. Statistical analysis was performed using the statistical software R (R Project).

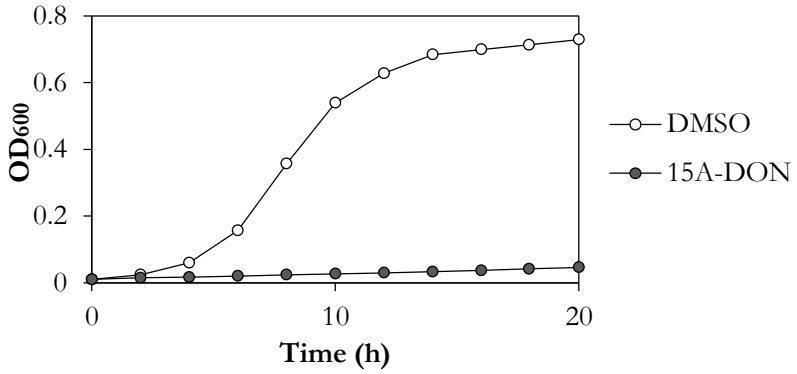

Figure 2.2 Example of growth curves determined from the OD_{600} values of Δ*pdr5* YKO cells grown for 20 h in DMSO or in 15A-DON (25 μg/mL).

CHAPTER 3 – RESULTS

3.1 Transport of trichothecene mycotoxins by Pdr5p

Pdr5p is a member of the pleiotropic drug resistance (PDR) subfamily of ATP-binding cassette (ABC) transporters and has a major role in the PDR network, which mediates toxin export. Previous studies have identified Pdr5p as a major exporter of *Fusarium graminearum* mycotoxins, notably deoxynivalenol (DON) and 15-acetyl-deoxynivalenol (15A-DON); however, it was unclear whether additional members of the PDR network were also involved in *F. graminearum* mycotoxin export. To assess this, yeast knockout (YKO) strains lacking the individual genes responsible for expressing each ABC transporter with a known or putative role in the PDR network (Table 3.1) were phenotypically screened in DON and 15A-DON.

PCR was performed to confirm the identity of each YKO strain analyzed in this study. All strains apart from Δ*pdr10* were positively confirmed using the KanB-A primer pairs (Figure 3.1A). All strains including Δ*pdr10* were positively confirmed using the KanC-D primer pairs (Figure 3.1B).

Growth assays of these YKO strains were conducted in liquid culture to determine the importance of each absent transporter in exporting DON or 15A-DON from living cells. When grown in the presence of a toxin, the level of growth inhibition of a YKO strain can be used to indicate the importance of its absent transporter in exporting that particular toxin. The more the growth of a YKO strain is inhibited, the greater the importance of the absent transporter in exporting the toxin. The concentrations of DON and 15A-DON used for these growth assays were previously shown to have comparable inhibitory effects on the wild-type (WT) strain BY4741 grown in liquid culture. Apart from Δ*pdr5*, whose growth was markedly reduced and almost completely inhibited in the presence of either DON or 15A-DON, no

Table 3.1 *Saccharomyces cerevisiae* ABC transporters with known or putative roles in the PDR network.

Standard Name[a]	Systematic Name[a]	Subcellular location[b]	Protein Molecules per Cell[c]	Function[a,b]
Pdr5p	Yor153wp	PM	42,000	PDR network transporter; export of numerous chemicals (e.g. anticancer drugs, antibiotics, mycotoxins, azole antifungals).
Pdr10p	Yor328wp	PM	No data	PDR network transporter.
Pdr11p	Yil013cp	PM	No data	PDR network transporter; sterol uptake.
Pdr12p	Ypl058cp	PM	752	Export of weak organic acids (e.g. sorbate, benzoate).
Pdr15p	Ydr406wp	PM	No data	PDR network transporter; general stress response factor involved in cellular detoxification.
Pdr18p	Ynr070wp	PM	No data	PDR network transporter.
Adp1p	Ycr011cp	ERM	339	Unknown.
Aus1p	Yor011wp	PM	No data	Sterol uptake.
Snq2p	Ydr011wp	PM	1,300	PDR network transporter; export of singlet oxygen species (e.g. cercosporin).
Yor1p	Ygr281wp	PM	3,610	PDR network transporter; export of numerous organic anions (e.g. oligomycin).
Unidentified	Yol075cp	PM	No data	Unknown.

PM, Plasma Membrane; ERM, Endoplasmic Reticulum Membrane.
References: [a] Saccharomyces Genome Database, [b] UniProt, [c] Ghaemmaghami et al. (2003).

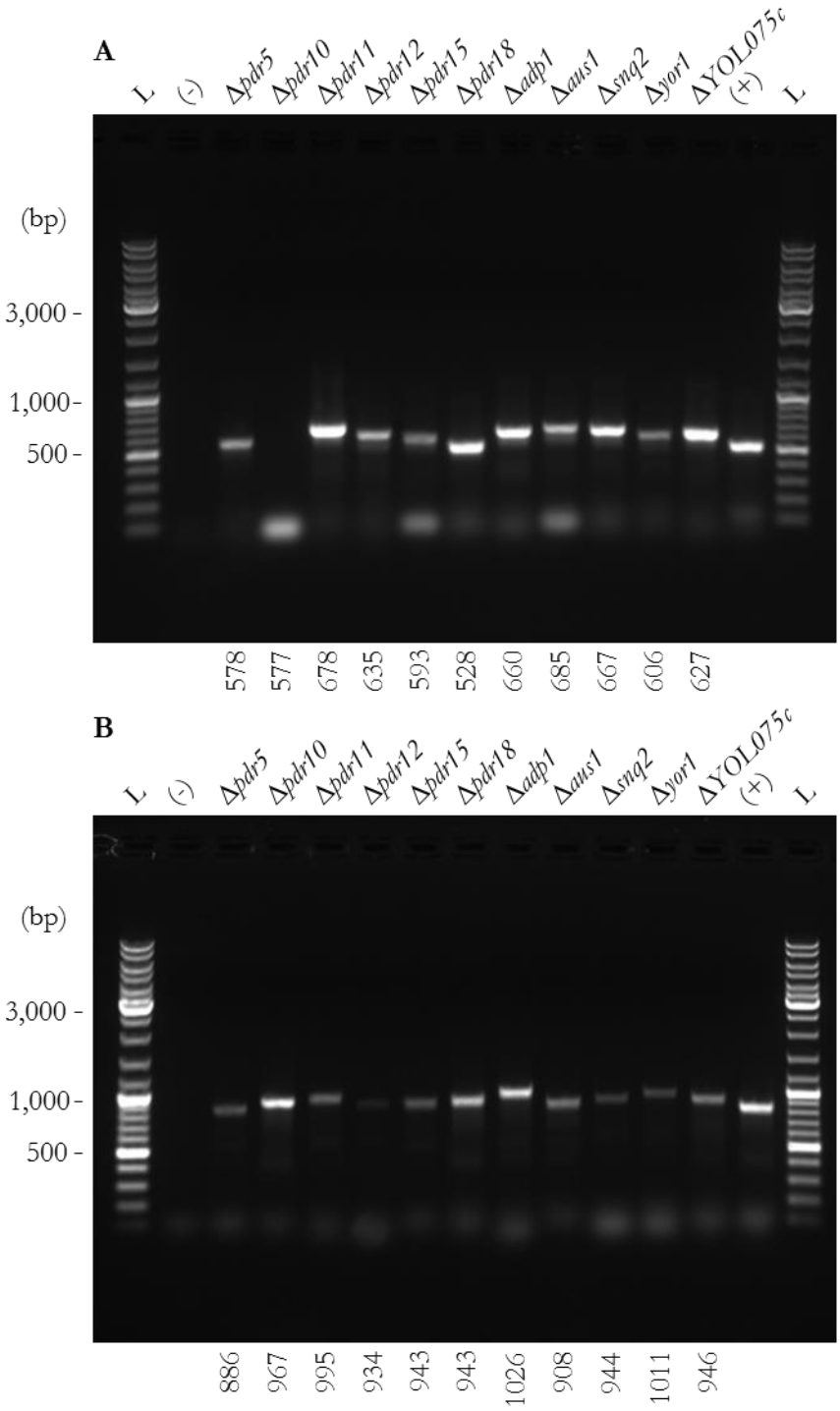

Figure 3.1 PCR validation of the YKO strains used in this study. For each strain, gDNA was used for PCR amplification using (**A**) the A-KanB primer pairs and (**B**) the D-KanC primer pairs. The expected size of each PCR product is indicated below each panel. Lanes L: DNA ladder, lane (-): negative control, and lane (+) positive control.

significant growth effects were observed in the remaining YKO strains when compared to BY4741 (Figure 3.2).

To best replicate the natural contamination conditions of a eukaryotic cell by *F. graminearum* trichothecene mycotoxins, the YKO strains were grown in the presence of *F. graminearum* culture filtrate preparation 11A (Figure 3.3). Briefly, this culture filtrate contained all the compounds produced and secreted by *F. graminearum*, including trichothecenes (primarily 15A-DON) and the FK506-like compound. *F. graminearum* culture filtrate can be used in conjunction with yeast cells to simulate fungal crop infection. Of the 11 YKO strains assayed, Δ*pdr5* was the only strain that showed a drastic growth reduction in culture filtrate. In fact, its growth was nearly completely inhibited. Growth of the WT strain BY4741 and of the ten other YKO strains was slightly decreased in culture filtrate, while growth of each of these strains had been unaffected in DON and 15A-DON.

Of the 11 YKO strains analyzed, Δ*pdr5* was the only strain that demonstrated severe growth inhibition in the presence of DON, 15A-DON, or *F. graminearum* culture filtrate. Western blot analysis was performed to explicitly demonstrate that Pdr5p was not being expressed by this strain. With the WT strain BY4741 as a positive control for Pdr5p expression, Pdr5p was detected using antibodies directed either against a peptide mapping at the N-terminus (yN-18; Figure 3.4A) or C-terminus (yC-18; Figure 3.4B) of Pdr5p. Both antibodies detected a single band of ~150 kDa in the WT, while no bands were detected in Δ*pdr5*.

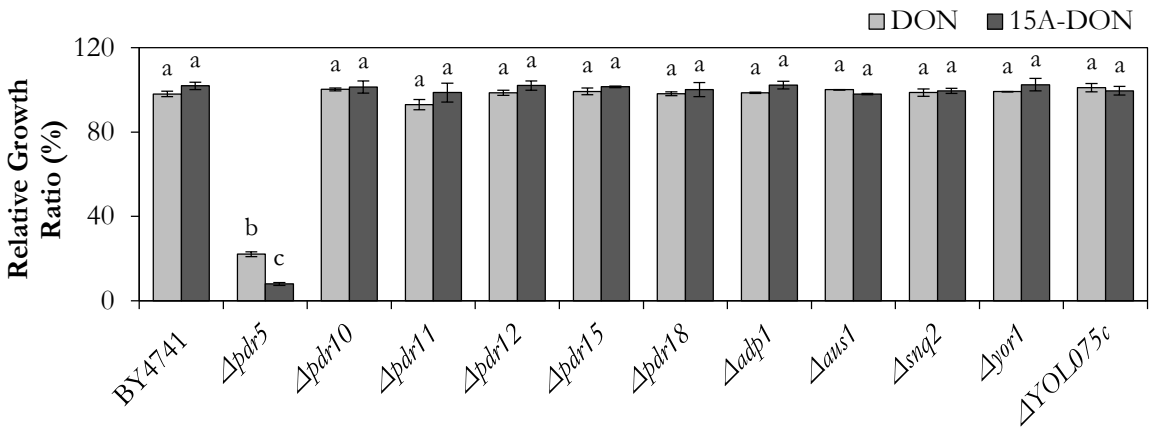

Figure 3.2 Relative growth ratio (%) of YKO strains in DON and 15A-DON. Yeast strains were grown for 20 h in DON (125 μg/mL) or 15A-DON (25 μg/mL). Relative growth ratios were determined by dividing the growth rates of treated cells by the growth rates of untreated cells. All data are expressed as means ±SEM (n≥3). Bars with the same letter are not significantly different ($P<0.05$).

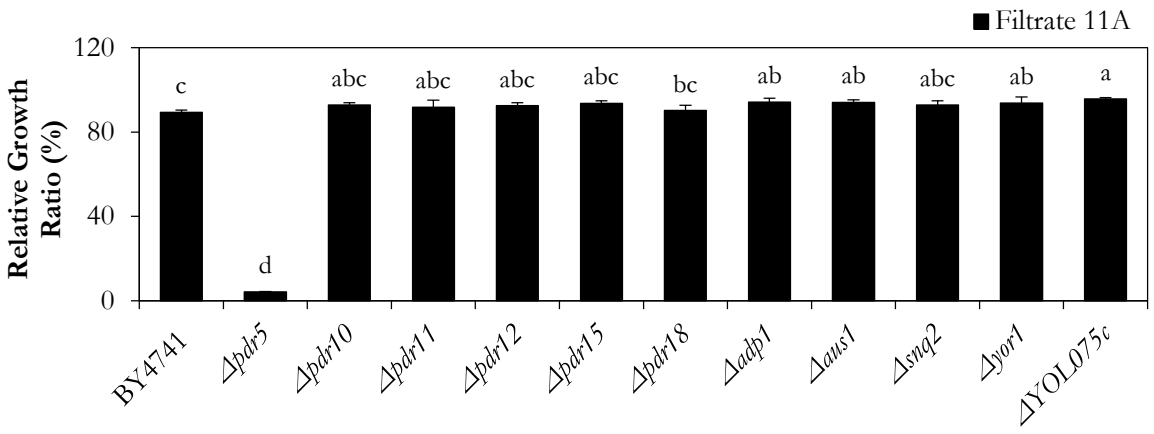

Figure 3.3 Relative growth ratio (%) of YKO strains in *F. graminearum* culture filtrate 11A. Yeast strains were grown for 20 h in filtrate containing a 15A-DON concentration of 100 μg/mL. Relative growth ratios were determined by dividing the growth rates of treated cells by the growth rates of untreated cells. All data are expressed as means ±SEM (n≥3). Bars with the same letter are not significantly different (P<0.05).

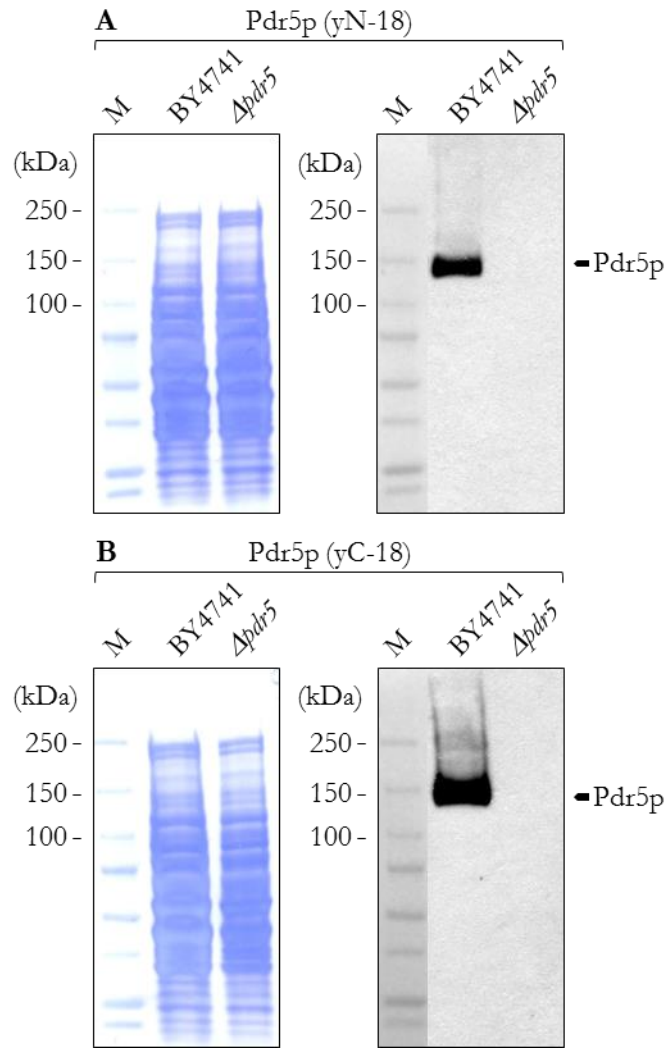

Figure 3.4 Western blot analysis of Pdr5p expression in WT yeast strain BY4741 and YKO strain Δ*pdr5*. Pdr5p was detected using (**A**) an antibody directed against an N-terminal peptide of Pdr5p (yN-18) and (**B**) an antibody directed against a C-terminal peptide of Pdr5p (yC-18). Proteins were stained with Coomassie Brilliant Blue. Lanes M: protein marker.

3.2 Pdr5p mutant S1360F: effects on substrate transport and inhibitor sensitivity

Yeast lacking the expression of Pdr5p is unable to grow in the presence of the trichothecenes DON or 15A-DON, nor in the presence of *F. graminearum* culture filtrate. Experimental results obtained from the Gleddie lab indicate that trichothecene export by yeast expressing Pdr5p is blocked by an FK506-like inhibitor produced by *F. graminearum*. Furthermore, FK506 has been identified as a Pdr5p- specific inhibitor. Taken together, these results indicate that the inhibitory compound produced by *F. graminearum* blocks trichothecene export by specifically inhibiting Pdr5p.

Egner et al. (1998) demonstrated that a serine (S) to phenylalanine (F) amino acid substitution at residue S1360 of Pdr5p (referred to as the S1360F Pdr5p mutant) mediates Pdr5p insensitivity to FK506; however, it decreases the specificity of Pdr5p for substrates such as the azole antifungals ketoconazole and itraconazole, the protein synthesis inhibitor cycloheximide, and the fluorescent dyes rhodamine 6G and rhodamine 123. The S1360F Pdr5p mutant was selected for the present study to determine its potential role in mediating insensitivity to the FK506-like compound produced by *F. graminearum* and to determine whether it could retain the ability to export the trichothecene mycotoxins DON and 15A-DON. WT Pdr5p and the S1360F Pdr5p mutant were individually introduced into the Δ*pdr5* YKO strain by transformation of plasmids.

In a study by Ernst et al. (2008), it was determined that an N-terminal histidine epitope-tag had no effect on the function or expression of the Pdr5p mutants that they tested. Based on these results and in anticipation of potential immunological analyses of the S1360F Pdr5p mutant such as Western blotting, hemagglutinin (HA) epitope-tagged versions of both *PDR5* gene variants were constructed by inserting the HA coding sequence at the N-terminus coding

sequence of both genes. Plasmids created with these HA-tagged *PDR5* gene variants were also individually introduced by transformation into the Δ*pdr5* YKO strain.

The complete nucleotide sequence of the HA-tagged and non-tagged *PDR5* gene variants had been verified by sequencing prior to their cloning into the plasmid vector. To verify the identity of each Δ*pdr5* transformant, plasmid rescue was conducted against one clone from each transformation to recover the *PDR5* gene variant. PCR amplification of a fragment of *PDR5* recovered from each clone was then performed. As shown in Figure 3.5, a strong single band was clearly visible at 870 bp, corresponding to the expected size of the PCR-amplified fragment of *PDR5*. A faint band was noticeable in the empty plasmid control (E), which is the Δ*pdr5* YKO strain transformed with an empty plasmid. This was likely caused by aerosol contamination during plasmid rescue, as the plasmids from each clone were recovered concurrently. No bands were detected in the negative control (-), indicating that contamination did not occur during PCR reaction set up. Since contamination of the empty plasmid control was minimal, it was deduced that any cross-contamination between the other plasmids would have also been minimal. Additionally, recovered plasmid DNA was not used for further applications and was solely used to verify that each Δ*pdr5* transformant was expressing the correct coding sequence at residue S1360 of Pdr5p.

These amplified fragments of *PDR5* were used as templates for forward and reverse sequencing reactions. The aligned amino acid sequences obtained for each clone were identical, apart from a single phenylalanine (F) substitution at residue S1360 in the clones expressing the HA-tagged and non-tagged S1360F *PDR5* gene variants (Figure 3.6).

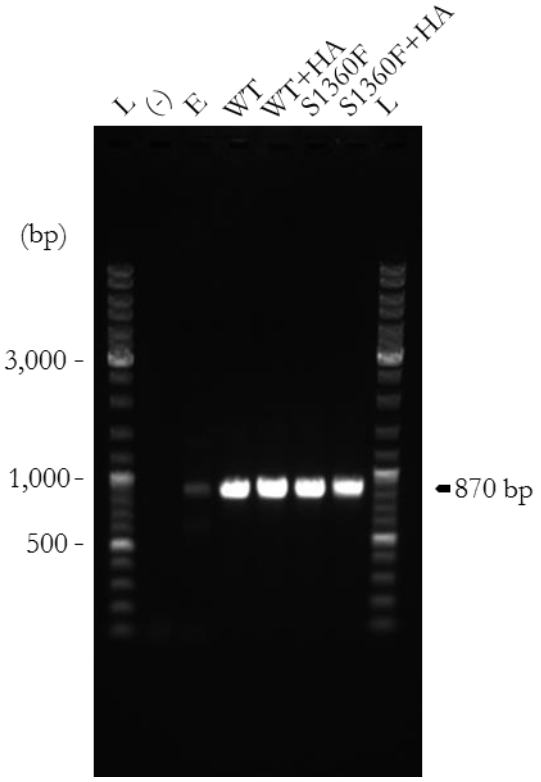

Figure 3.5 PCR amplification of an 870 bp fragment of *PDR5* from plasmid DNA, recovered from one clone from each Δ*pdr5* transformation expressing WT or S1360F mutant Pdr5p. L: DNA ladder, lane (-): negative control, lane (E): empty plasmid control, and +HA: HA-tagged *PDR5* genes.

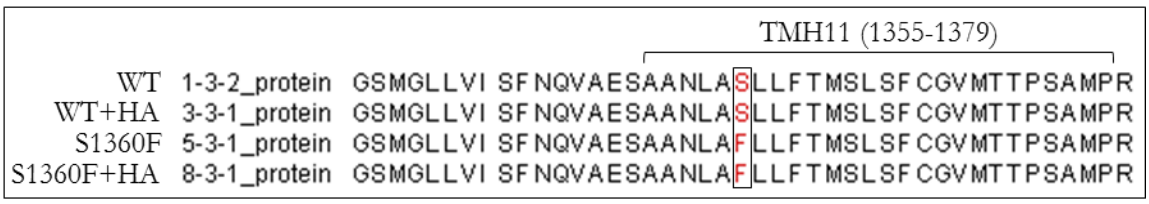

Figure 3.6 A portion of the aligned amino acid sequences obtained following the sequencing of a fragment of *PDR5*, recovered from one clone from each Δ*pdr5* transformation expressing WT or S1360F mutant Pdr5p. The putative sequence of TMH 11, as delimited by Rutledge et al. (2011), between amino acid residues 1355-1379 is shown. Amino acid residues at position S1360 are highlighted.

Western blot analysis was then performed, using protein extracts from the clones listed in Figure 3.6, to determine their Pdr5p expression levels. The antibody directed against a peptide mapping at the C-terminus (yC-18) of Pdr5p detected a single band of ~150 kDa in all clones (Figure 3.7). This band was completely absent in the empty plasmid control (E). The relative quantity of actin in all protein extracts was around a value of 1.00. Additionally, expression of the S1360F Pdr5p mutant was about two times higher than that of WT Pdr5p. This same trend was observed with either the HA-tagged or non-tagged proteins (n=3).

Growth assays of the Δ*pdr5* transformants expressing HA-tagged and non-tagged WT Pdr5p and S1360F Pdr5p mutant were then conducted in liquid culture. These transformants were grown in DON or 15A-DON to compare the ability of their expressed Pdr5p to export either mycotoxin. Additionally, these transformants were grown in DON or 15A-DON with the addition of FK506 to compare the ability of their expressed Pdr5p to export these mycotoxins in the presence of a Pdr5p-specific inhibitor (Figure 3.8).

No differences were observed in the yeast growth rates under any treatment, when comparing the transformants expressing non-tagged WT Pdr5p (WT) or HA-tagged WT Pdr5p (WT+HA). Likewise, no differences were observed in the yeast growth rates under any treatment, when comparing the transformants expressing the non-tagged S1360F Pdr5p mutant (S1360F) or the HA-tagged S1360F Pdr5p mutant (S1360F+HA). The HA tag therefore did not have an effect on the function of Pdr5p, as indicated by Ernst et al. (2008). FK506 alone had no growth effects on any of the transformants, including the empty vector control (E). DON or 15A-DON alone had no growth effects on the transformants expressing WT and WT+HA Pdr5p. Both mycotoxins had significant negative growth effects on the transformants expressing the S1360F and S1360F+HA Pdr5p mutants. Furthermore, these negative growth

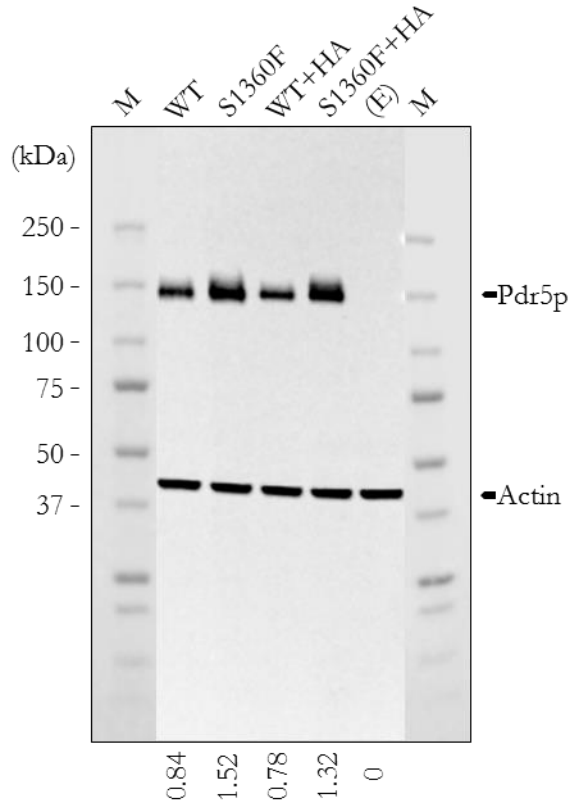

Figure 3.7 Western blot analysis of Pdr5p expression in clones from each Δ*pdr5* transformation. Pdr5p was detected using an antibody directed against a C-terminal peptide of Pdr5p (yC-18). Ratios of Pdr5p to actin are indicated below the panel. Lanes M: protein marker, lane (E): empty plasmid control, and +HA: HA-tagged Pdr5p. (n=3).

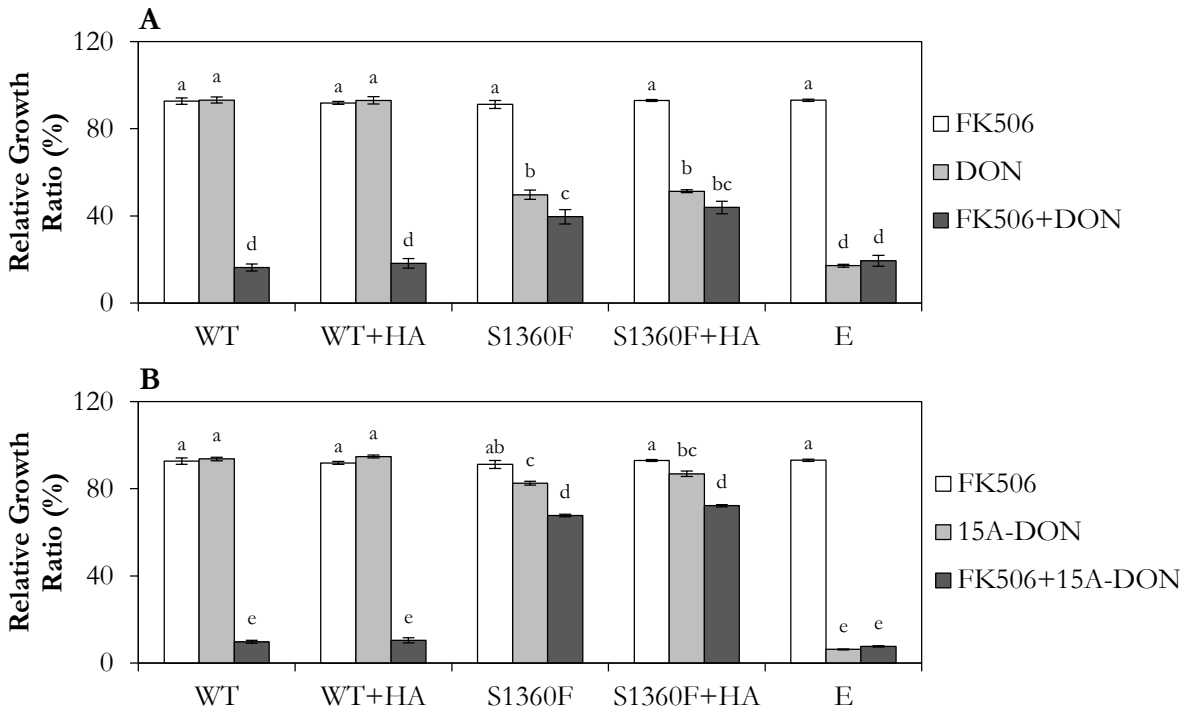

Figure 3.8 Relative growth ratio (%) of Δ*pdr5* transformants expressing WT Pdr5p and the S1360F Pdr5p mutant in (**A**) FK506+DON or (**B**) FK506+15A-DON. Yeast strains were grown for 20 h in FK506 (20 μg/mL), DON (125 μg/mL), FK506+DON (20 μg/mL+125 μg/mL), 15A-DON (25 μg/mL), or FK506+15A-DON (20 μg/mL+25 μg/mL). +HA: HA-tagged Pdr5p. An empty plasmid control (E) was also grown. All data are expressed as means ±SEM (n=3). In each panel, bars with the same letter are not significantly different ($P<0.05$).

effects were significantly greater in DON than in 15A-DON. In DON or 15A-DON alone, or when FK506 was added to either mycotoxin, growth of the empty plasmid control (E) was nearly completely inhibited. Similarly, when FK506 was added to either DON or 15A-DON, growth of the transformants expressing WT or WT+HA Pdr5p was nearly completely inhibited. On the contrary, when FK506 was added to either mycotoxin, growth reduction of the transformants expressing the S1360F and S1360F+HA Pdr5p mutants was minimal when compared to their growth in DON or 15A-DON alone and when compared to the transformants expressing WT or WT+HA Pdr5p. It does appear, however, that relative to the growth inhibitory effects caused by DON or 15A-DON alone, the combination of DON and FK506 had slightly smaller growth inhibitory effects than the combination of 15A-DON and FK506.

Simulation of yeast cell infection by *F. graminearum* was done by conducting growth assays in liquid culture using fungal culture filtrate 11A (Figure 3.9). The Δ*pdr5* transformant expressing WT+HA Pdr5p maintained a high level of growth in fungal filtrate; however, growth of the S1360F+HA Pdr5p mutant or the empty vector control (E) was nearly completely inhibited. Growth inhibition of the transformants expressing WT+HA Pdr5p or the S1360F+HA Pdr5p mutant was also concentration-dependant. For both transformants, growth inhibition was significantly reduced when they were grown in fungal filtrate containing a 15A-DON concentration of 300 μg/mL compared to 100 μg/mL. Growth inhibition of the empty plasmid control was identical with either concentration.

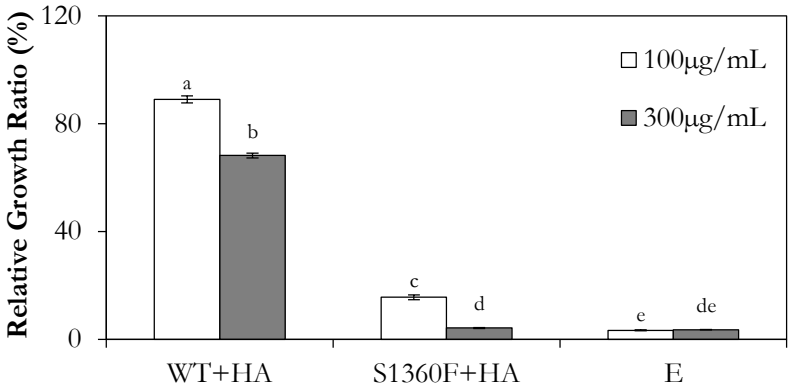

Figure 3.9 Relative growth ratio (%) of Δ*pdr5* transformants expressing WT Pdr5p and the S1360F Pdr5p mutant in *F. graminearum* culture filtrate containing a 15A-DON concentration of 100 μg/mL or 300 μg/mL. +HA: HA-tagged Pdr5p. An empty plasmid control (E) was also grown. All data are expressed as means ±SEM (n=3). Bars with the same letter are not significantly different ($P<0.05$).

3.3 Single amino acid substitutions at residues S1360 and T1364 of Pdr5p

Despite demonstrating a relatively high level of insensitivity to FK506, the S1360F Pdr5p mutant was unable to export DON or 15A-DON as efficiently as WT Pdr5p. Additionally, the S1360F Pdr5p mutant could not mediate resistance to *F. graminearum* culture filtrate. Despite the lack of success with this mutant, other mutants have been identified and could be involved in *F. graminearum* resistance. Egner et al. (2000) determined that the S1360A/T and T1364A/F/S single amino acid substitutions had either a positive, negative, or neutral effect on the function of Pdr5p. Since S1360 and T1364 have been identified as important amino acid residues in determining the ability of Pdr5p to mediate substrate specificity or to prevent inhibitor susceptibility, these two residues were selected for this study to determine their potential role in mediating Pdr5p resistance against *F. graminearum*. For this study, *in vitro* mutagenesis of the WT *PDR5* gene was performed to generate 19 *PDR5* S1360 variants, each coding for a different single amino acid substitution at residue S1360 of Pdr5p, and 19 *PDR5* T1364 variants, each coding for a different single amino acid substitution at residue T1364 or Pdr5p, for a total of 38 *PDR5* variants.

Since the N-terminal HA tag did not affect the expression or function of the S1360F Pdr5p mutant when compared with the non-tagged S1364F Pdr5p mutant, all 38 *PDR5* variants were HA-tagged. As described previously, each of the sequence-verified HA-tagged *PDR5* variants were individually introduced by transformation into the Δ*pdr5* YKO strain. The identity of each Δ*pdr5* transformant was then verified by using two sister clones from each transformation. For each clone, the expected 870 bp fragment of recovered *PDR5* was amplified (Figures 3.10 & 3.11) then sequenced. The aligned amino acid sequences for each clone were identical, apart from a single amino acid substitution at residue S1360 in clones

expressing a S1360 mutation (Figure 3.12) or at residue T1364 in clones expressing a T1364 mutation (Figure 3.13). Additionally, the sequences from the two sister clones from each transformation were identical.

Western blot analysis was then performed using protein extracts from one of each of the sister clones listed in Figures 3.12 and 3.13 to determine their Pdr5p expression levels. The antibody directed against a peptide mapping at the C-terminus (yC-18) of Pdr5p detected a single band of ~150 kDa in all clones (Figure 3.14). The band was completely absent in the empty plasmid control (E). Although a band is not visible on the blot shown in Figure 3.14B in the lane corresponding to the T1364D mutant, a single faint band of ~150 kDa was visible when the blot was overexposed. The relative quantity of actin in all protein extracts was around a value of 1.00. Consistently, variation in the expression of Pdr5p mutants at both residues was observed (n=3).

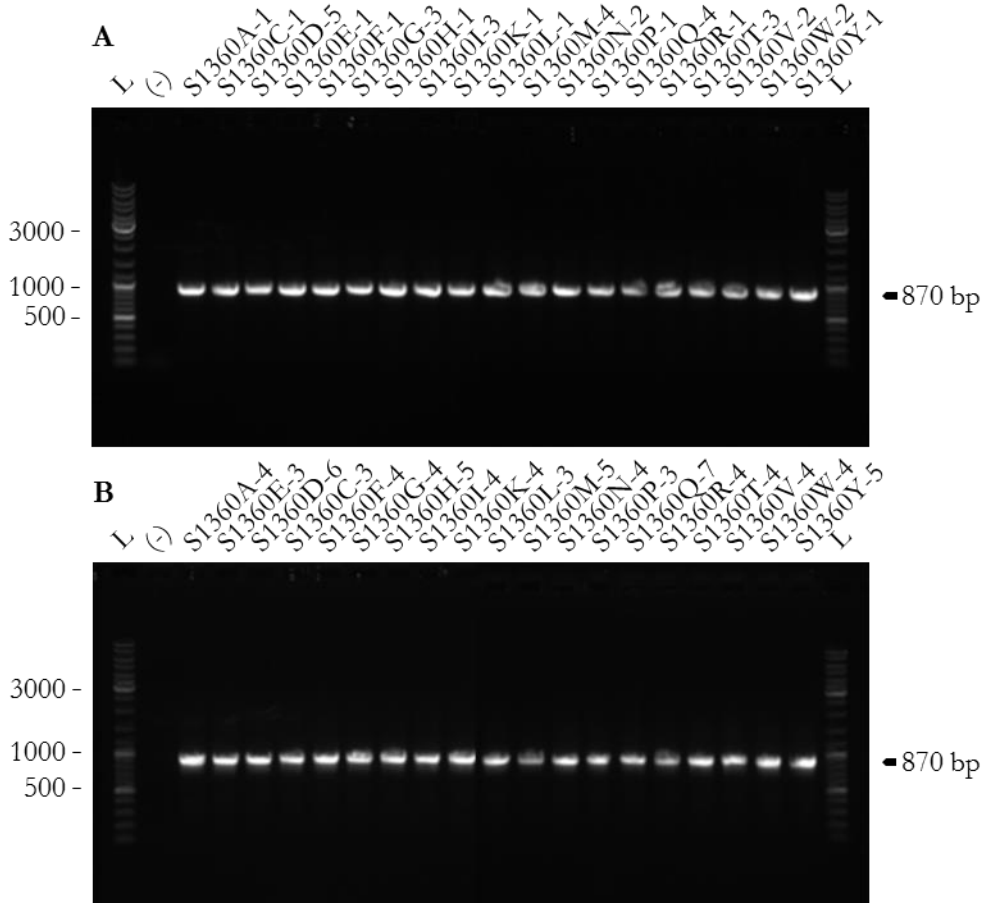

Figure 3.10 PCR amplification of an 870 bp fragment of *PDR5* from plasmid DNA, recovered from two sister clones (**A** & **B**) from each Δ*pdr5* transformation expressing a S1360 Pdr5p mutant. L: DNA ladder, lane (-): negative control.

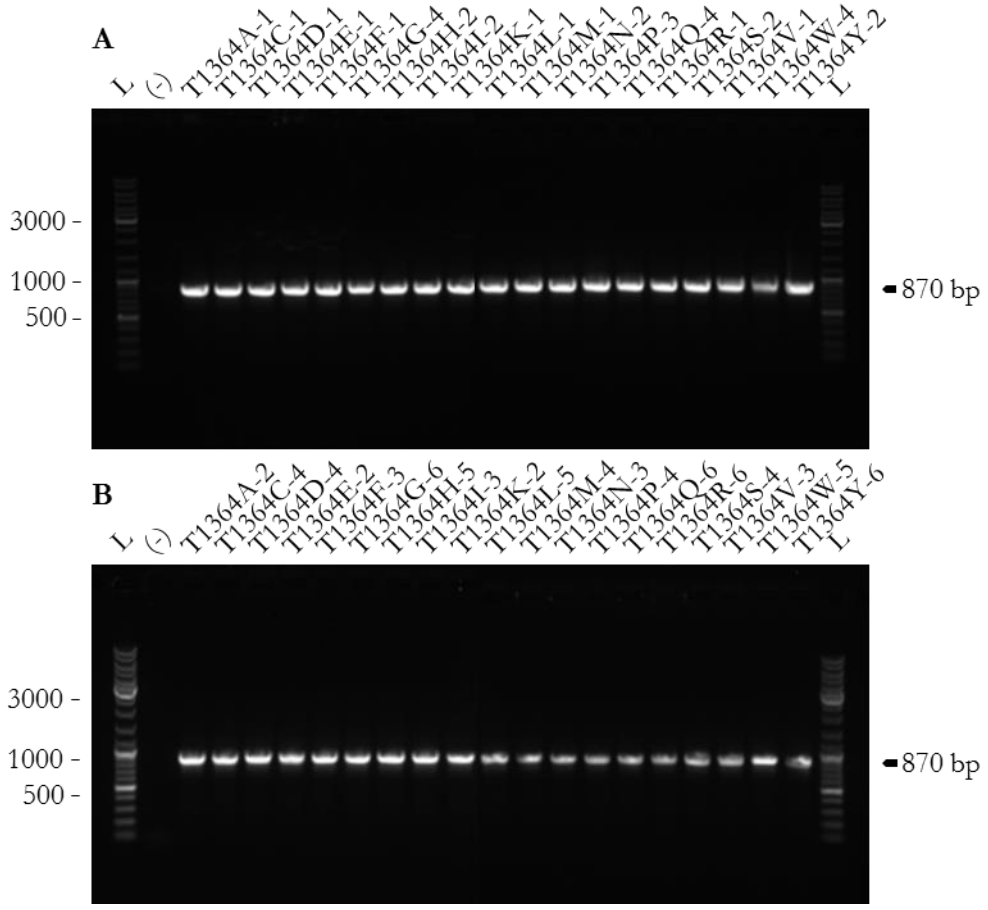

Figure 3.11 PCR amplification of an 870 bp fragment of *PDR5* from plasmid DNA, recovered from two sister clones (**A** & **B**) from each Δ*pdr5* transformation expressing a T1364 Pdr5p mutant. L: DNA ladder, lane (-): negative control.

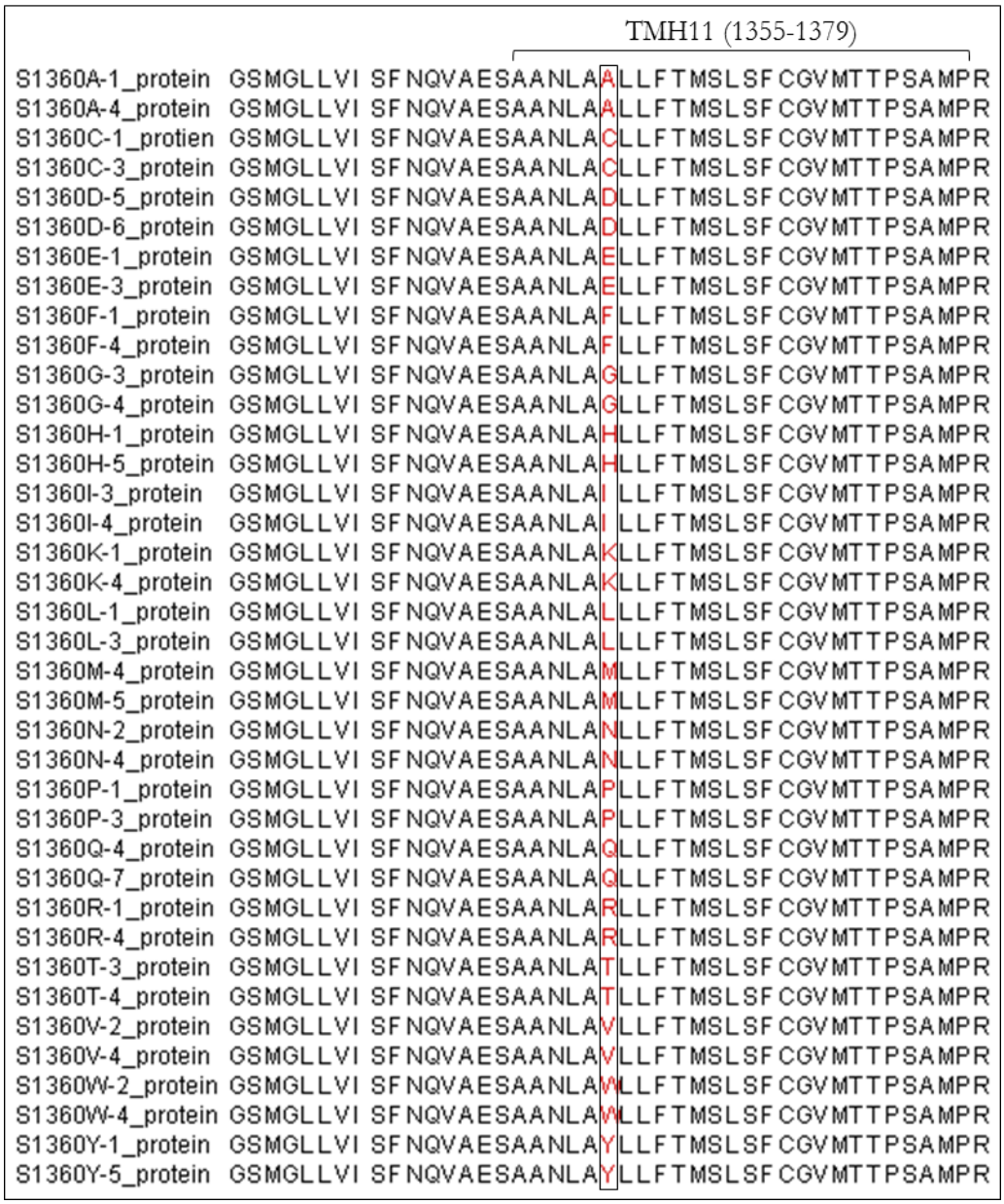

Figure 3.12 A portion of the aligned amino acid sequences obtained following the sequencing of a fragment of *PDR5*, recovered from two sister clones from each Δ*pdr5* transformation expressing a S1360 Pdr5p mutant. The sequence of TMH11, as delimited by Rutledge et al. (2011), between amino acid residues 1355-1379 is shown. Amino acid residues at position S1360 are highlighted.

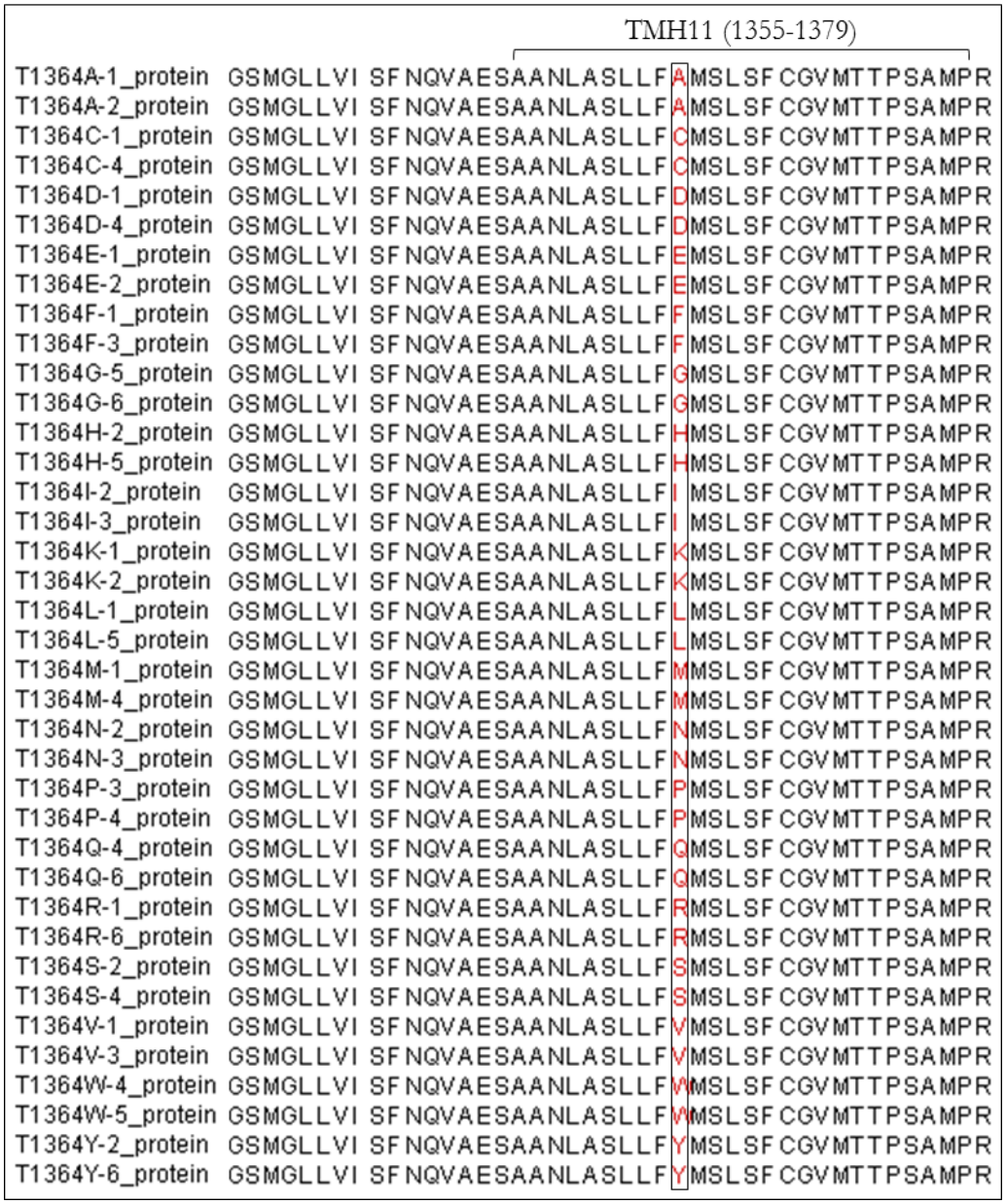

Figure 3.13 A portion of the aligned amino acid sequences obtained following the sequencing of a fragment of *PDR5*, recovered from two sister clones from each Δ*pdr5* transformation expressing a T1364 Pdr5p mutant. The sequence of TMH11, as delimited by Rutledge et al. (2011), between amino acid residues 1355-1379 is shown. Amino acid residues at position T1364 are highlighted.

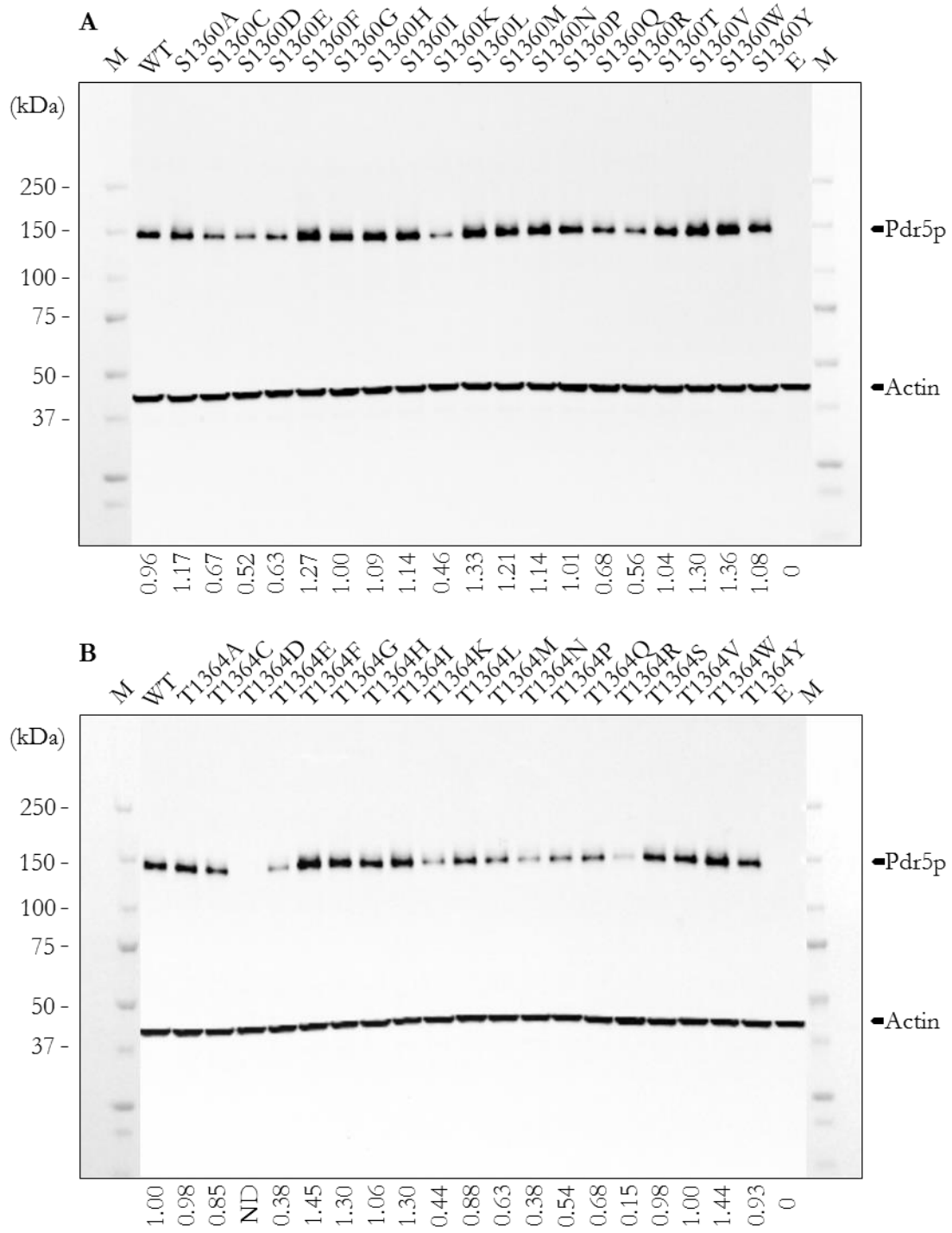

Figure 3.14 Western blot analysis of Pdr5p expression in clones from each Δ*pdr5* transformation expressing (**A**) a S1360 Pdr5p mutant or (**B**) a T1364 Pdr5p mutant. Pdr5p was detected using an antibody directed against a C-terminal peptide of Pdr5p (yC-18). Ratios of Pdr5p to actin are indicated below the panel. Lanes M: protein marker, lane (E): empty plasmid control, and +HA: HA-tagged Pdr5p. (n=3).

3.4 Growth of the S1360 and T1364 Pdr5p mutants

3.4.1 Growth in DON and 15A-DON

To determine the ability of each S1360 or T1364 Pdr5p mutant to export trichothecene mycotoxins produced by *F. graminearum*, growth assays were performed by growing each transformant in liquid culture with DON or 15A-DON (Figures 3.15 & 3.17). When compared to the transformant expressing WT Pdr5p, growth of most of the Pdr5p mutant transformants was unaffected or marginally affected by DON or 15A-DON.

The transformants were then arranged in descending order based on their relative growth ratios in DON or 15A-DON, and then they were subjectively classified according to the ability of their expressed S1360 or T1364 Pdr5p mutant to export either mycotoxin (Figures 3.16 & 3.18). Apart from the S1360F, S1360W, and T1364D mutants, which demonstrated an intermediate level of DON and 15A-DON export, all other mutants maintained a high level of export for both mycotoxins. The S1360F mutant maintained a greater level of 15A-DON export compared to that of DON, while the S1360W mutant maintained a greater level of DON export compared to that of 15A-DON. No obvious differences in DON or 15A-DON export were observed for the T1364D mutant. Differences observed between Pdr5p mutants for all growth treatments will be addressed in the discussion.

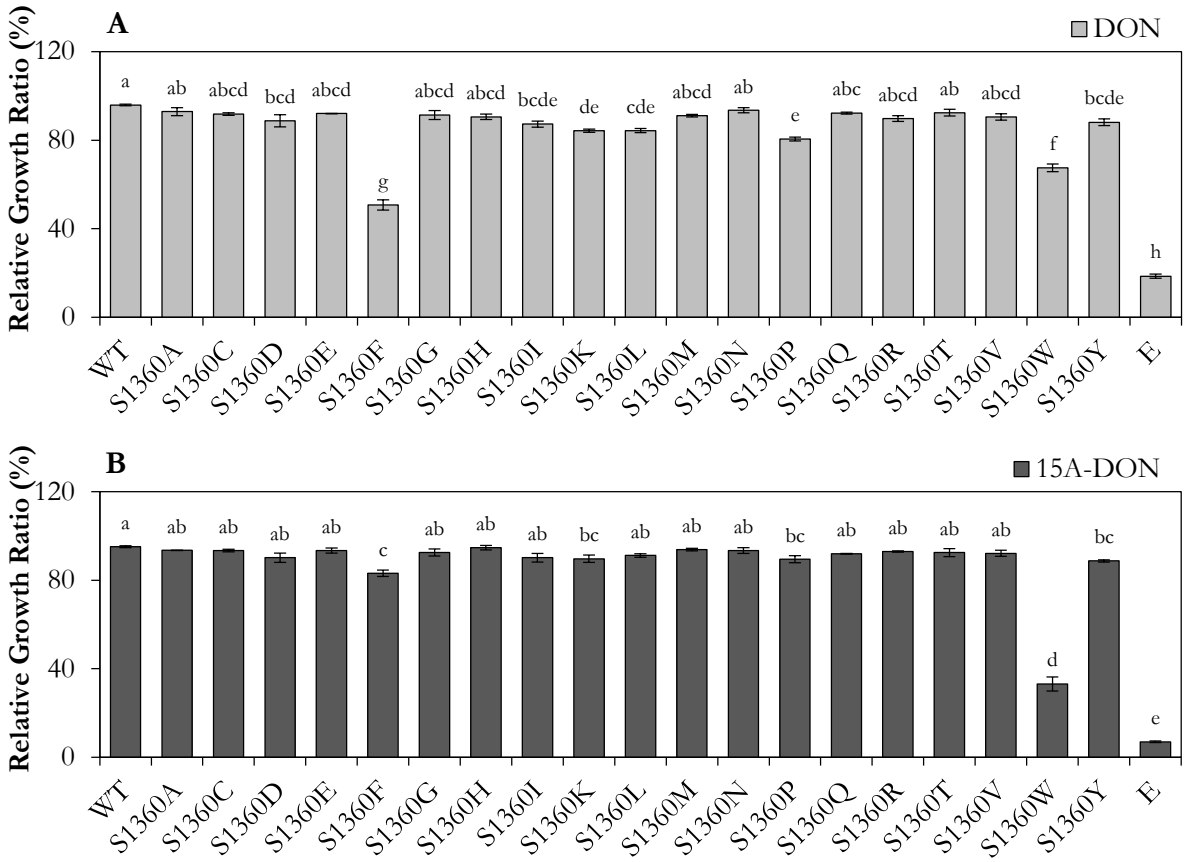

Figure 3.15 Relative growth ratios (%) of S1360 Pdr5p mutant transformants in DON or 15A-DON. Each transformant, expressing a S1360 Pdr5p mutant (designated by the single-letter code of the substituted amino acid), the transformant expressing wild-type Pdr5p (WT), and an empty plasmid control (E) were grown for 20 h in (**A**) DON (125 μg/mL) or (**B**) 15A-DON (25 μg/mL). Relative growth ratios were determined by dividing the growth rates of treated cells by the growth rates of untreated cells. All data are expressed as means ±SEM (n≥3). In each panel, bars with the same letter are not significantly different (P<0.05).

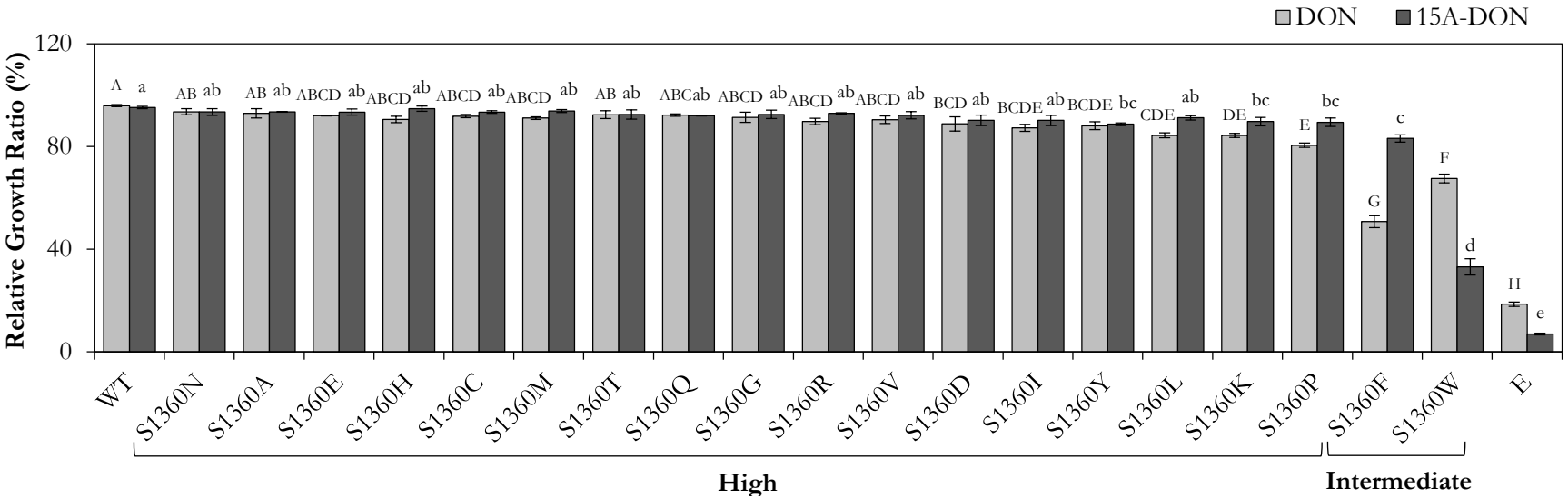

Figure 3.16 Classification of the S1360 Pdr5p mutant transformants grown in DON or 15A-DON. Transformants shown in Figure 3.15 were arranged in descending order based on their relative growth ratios (%) after growth in DON (125 μg/mL) or 15A-DON (25 μg/mL). Each transformant was then subjectively classified according to the ability of their expressed S1360 Pdr5p mutant to export either mycotoxin at a high, intermediate, or low level. The transformant expressing wild-type Pdr5p (WT) and the empty plasmid control (E) were added to compare their growth ratios to those of each transformant expressing a S1360 Pdr5p mutant. All data are expressed as means ±SEM (n≥3). Bars with the same letter within each group (uppercase for DON and lowercase for 15A-DON) are not significantly different ($P<0.05$).

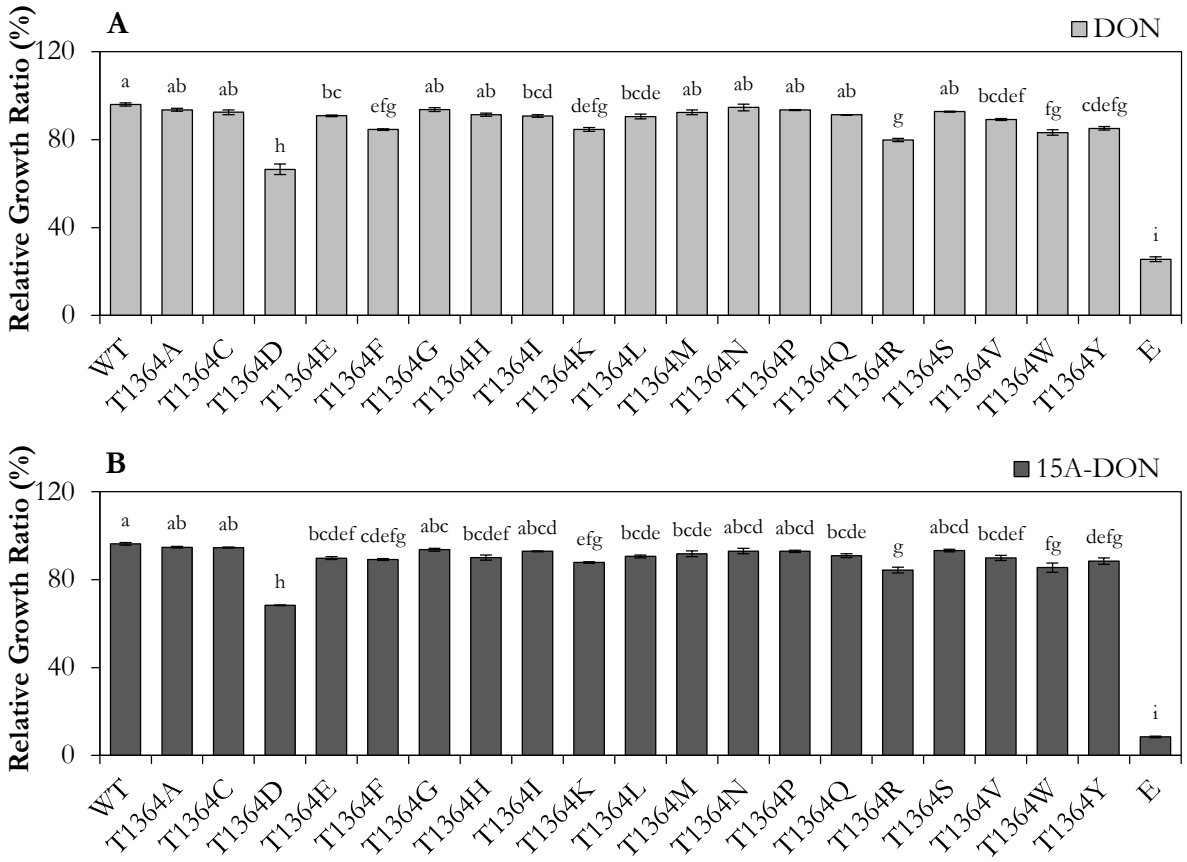

Figure 3.17 Relative growth ratios (%) of T1364 Pdr5p mutant transformants in DON or 15A-DON. Each transformant, expressing a T1364 Pdr5p mutant (designated by the single-letter code of the substituted amino acid), the transformant expressing wild-type Pdr5p (WT), and an empty plasmid control (E) were grown for 20 h in (**A**) DON (125 μg/mL) or (**B**) 15A-DON (25 μg/mL). Relative growth ratios were determined by dividing the growth rates of treated cells by the growth rates of untreated cells. All data are expressed as means ±SEM (n≥3). In each panel, bars with the same letter are not significantly different ($P<0.05$).

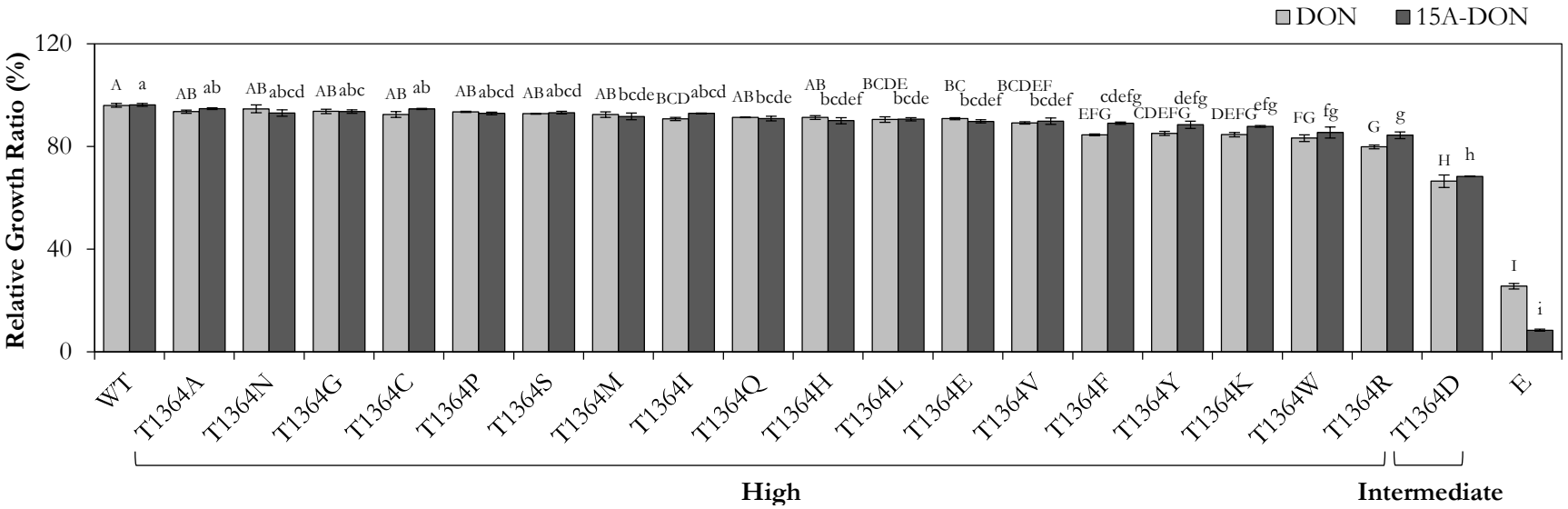

Figure 3.18 Classification of the T1364 Pdr5p mutant transformants grown in DON or 15A-DON. Transformants shown in Figure 3.17 were arranged in descending order based on their relative growth ratios (%) after growth in DON (125 μg/mL) or 15A-DON (25 μg/mL). Each transformant was then subjectively classified according to the ability of their expressed T1364 Pdr5p mutant to export either mycotoxin at a high, intermediate, or low level. The transformant expressing wild-type Pdr5p (WT) and the empty plasmid control (E) were added to compare their growth ratios to those of each transformant expressing a T1364 Pdr5p mutant. All data are expressed as means ±SEM (n≥3). Bars with the same letter within each group (uppercase for DON and lowercase for 15A-DON) are not significantly different ($P<0.05$).

3.4.2 Growth in DON and 15A-DON in the presence of FK506

The main objective of this study was to determine the ability of each S1360 or T1364 Pdr5p mutant to export DON or 15A-DON in the presence of the FK506-like inhibitor produced by *F. graminearum*. Since the identity of this inhibitory compound remains unknown, FK506 was used as a substitute. Growth assays were performed by growing each transformant in liquid culture with FK506+DON or FK506+15A-DON (Figures 3.19 & 3.22). FK506 alone did not have a major effect on growth of the transformants. The overall growth trends for all transformants were very similar in both mycotoxins with the addition of FK506. As described above, growth of the transformant expressing WT Pdr5p was drastically reduced in FK506+DON and FK506+15A-DON. Although growth of certain S1360 or T1364 Pdr5p mutant transformants was also compromised, many of the transformants were capable of maintaining growth in FK506+DON and FK506+15A-DON.

The transformants were then arranged in descending order based on their relative growth ratios in FK506+DON and FK506+15A-DON, and then they were subjectively classified according to the ability of their expressed S1360 or T1364 Pdr5p mutant to export either mycotoxin in the presence of FK506 (Figures 3.20 & 3.23). There were mutants at both residues that maintained a high level of DON and 15A-DON export in the presence of FK506. There were mutants at residue S1360 that demonstrated a low level of mycotoxin export, comparable to that of WT Pdr5p, in the presence of FK506, while none of the mutants at residue T1364 demonstrated a low level of DON and 15A-DON export in the presence of FK506. Additionally, as observed in DON or 15A-DON alone, the S1360F mutant maintained a greater level of 15A-DON export compared to that of DON, while the S1360W mutant maintained a greater level of DON export compared to that of 15A-DON.

Transformants expressing S1360 or T1364 Pdr5p mutants that maintained a high level of DON and 15A-DON export in the presence of FK506 were grown again in 15A-DON alone and in 15A-DON+FK506 (Figures 3.21 & 3.24). The mycotoxin 15A-DON was selected for these assays since it is noticeably more toxic than DON and a smaller quantity is required to cause considerable impact on growth of the WT Pdr5p strain. While the concentration of FK506 remained the same as in the previous growth assays, the concentration of 15A-DON was increased by a factor of 12. Despite this very high concentration of 15A-DON, several transformants expressing S1360 or T1364 Pdr5p mutants were able to maintain a level of 15A-DON export comparable to that of the transformant expressing WT Pdr5p. In 15A-DON+FK506, growth of the transformant expressing WT Pdr5p was nearly completely inhibited. Although their growth was negatively affected, various transformants, notably those expressing Pdr5p mutants S1360H/N/Q and T1364C/E/N/P, were capable of growing in 15A-DON+FK506.

3.4.3 Growth in *F. graminearum* culture filtrate

Growth assays with the transformants expressing S1360 Pdr5p mutants and T1364 Pdr5p mutants were conducted in liquid culture to determine the potential ability of any of the 38 mutants to mediate increased yeast resistance to *F. graminearum* culture filtrate when compared to WT Pdr5p. Growth assays were repeated with two culture filtrate preparations: 11A (prepared in 2011) and 12A (prepared in 2012). None of the transformants expressing a S1360 Pdr5p mutant (Figure 3.25) or a T1364 Pdr5p mutant (Figure 3.28) grew significantly better than the transformant expressing WT Pdr5p in filtrate 11A or 12A. As stated previously, the culture filtrate used for these growth assays contained all the compounds produced and secreted by *F. graminearum* grown in culture. It is therefore possible that certain unidentified

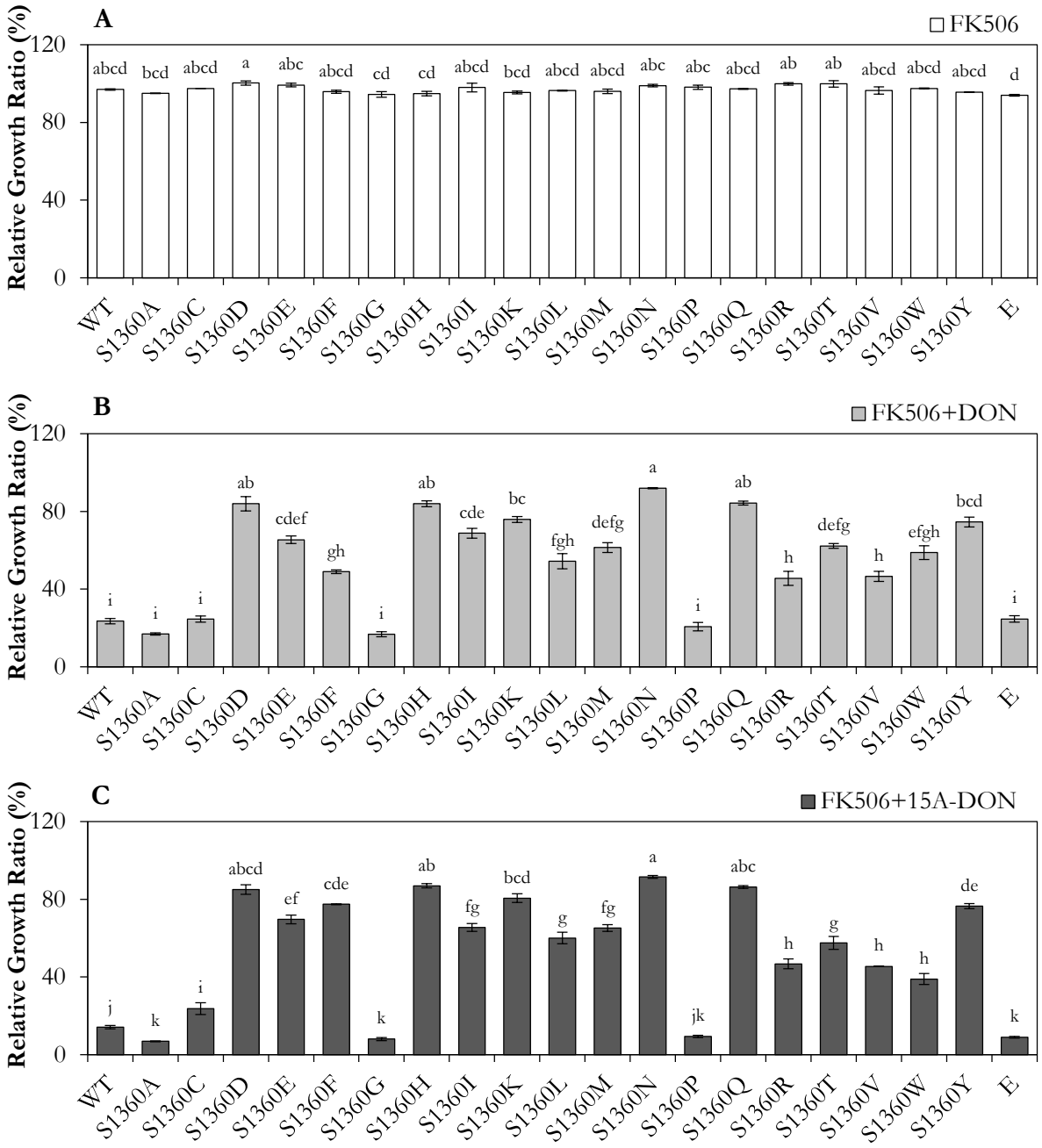

Figure 3.19 Relative growth ratios (%) of S1360 Pdr5p mutant transformants in FK506, FK506+DON, or FK506+15A-DON. Each transformant, expressing a S1360 Pdr5p mutant (designated by the single-letter code of the substituted amino acid), the transformant expressing wild-type Pdr5p (WT), and an empty plasmid control (E) were grown for 20 h in (**A**) FK506 (20 μg/mL), (**B**) FK506+DON (20 μg/mL+125 μg/mL), or (**C**) FK506+15A-DON (20 μg/mL+25 μg/mL). Relative growth ratios were determined by dividing the growth rates of treated cells by the growth rates of untreated cells. All data are expressed as means ±SEM (n≥3). In each panel, bars with the same letter are not significantly different ($P<0.05$).

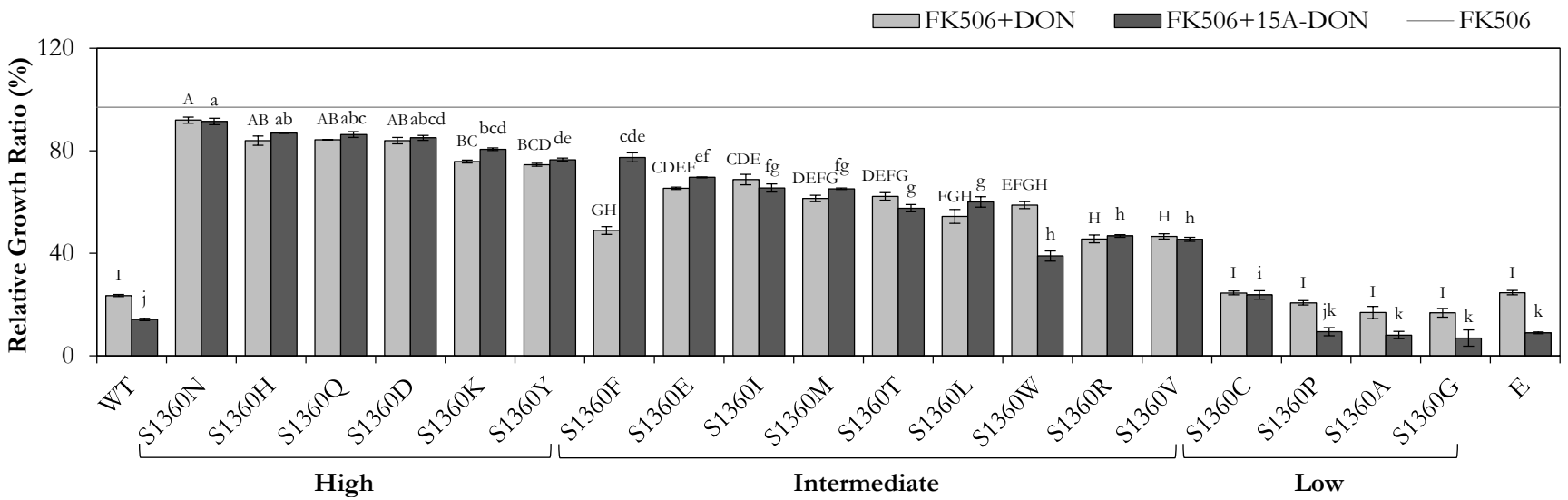

Figure 3.20 Classification of the S1360 Pdr5p mutant transformants grown in FK506+DON, or FK506+15A-DON. Transformants shown in Figure 3.19 were arranged in descending order based on their relative growth ratios (%) after growth in FK506+DON (20 μg/mL+125 μg/mL) or FK506+15A-DON (20 μg/mL+25 μg/mL). Each transformant was then subjectively classified according to the ability of their expressed S1360 Pdr5p mutant to export either mycotoxin at a high, intermediate, or low level in the presence of FK506. The average of the relative growth ratio of all transformants in FK506 alone is indicated by the grey line. The transformant expressing wild-type Pdr5p (WT) and the empty plasmid control (E) were added to compare their growth ratios to those of each transformant expressing a T1364 Pdr5p mutant. All data are expressed as means ±SEM (n≥3). Bars with the same letter within each group (uppercase for FK506+DON and lowercase for FK506+15A-DON) are not significantly different ($P<0.05$).

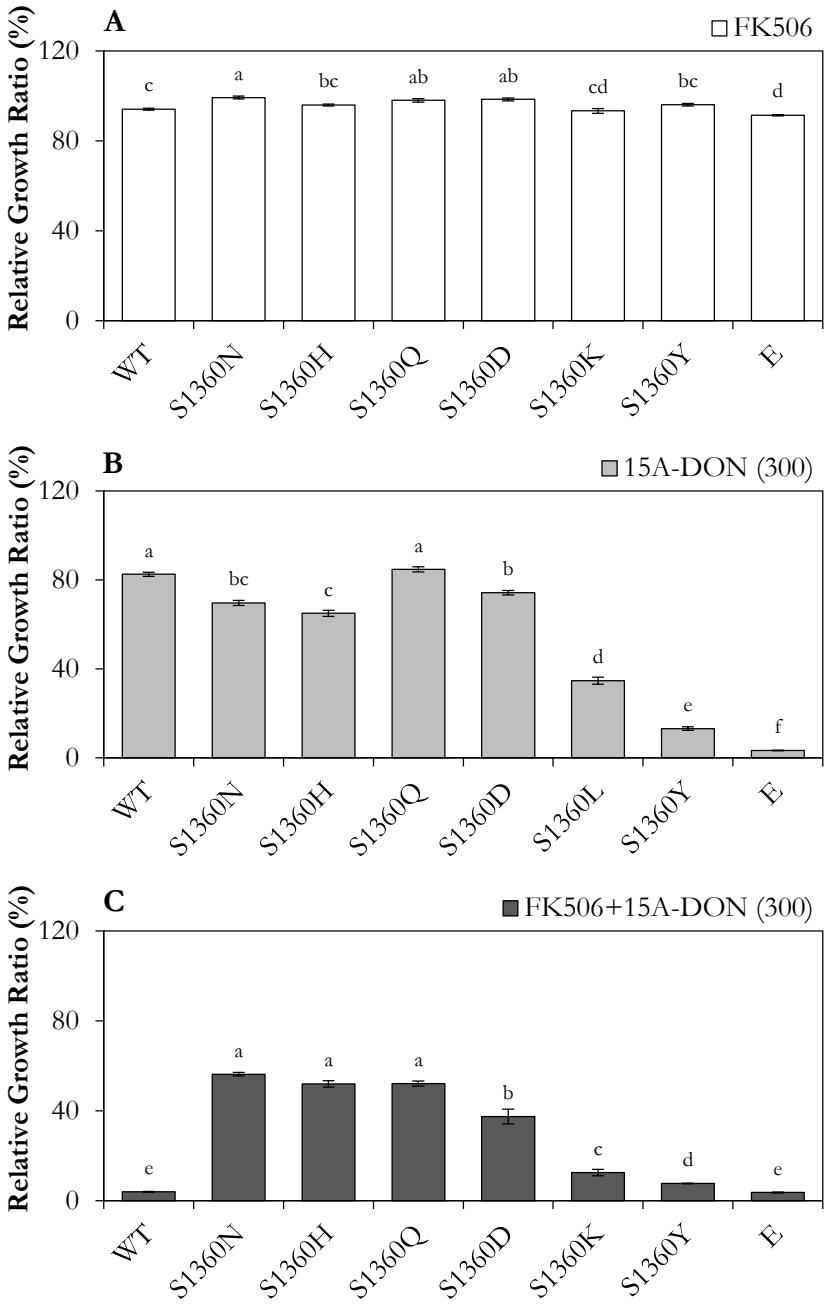

Figure 3.21 Relative growth ratios (%) of transformants expressing S1360 Pdr5p mutants classified as maintaining a high level of export of either DON or 15A-DON in the presence of FK506. Each transformant, expressing a S1360 Pdr5p mutant (designated by the single-letter code of the substituted amino acid), the transformant expressing wild-type Pdr5p (WT), and an empty plasmid control (E) were grown for 20 h in (**A**) FK506 (20 μg/mL), (**B**) 15A-DON (300 μg/mL), or (**C**) FK506+15A-DON (20 μg/mL+300 μg/mL). Relative growth ratios were determined by dividing the growth rates of treated cells by the growth rates of untreated cells. All data are expressed as means ±SEM (n≥3). In each panel, bars with the same letter are not significantly different ($P<0.05$).

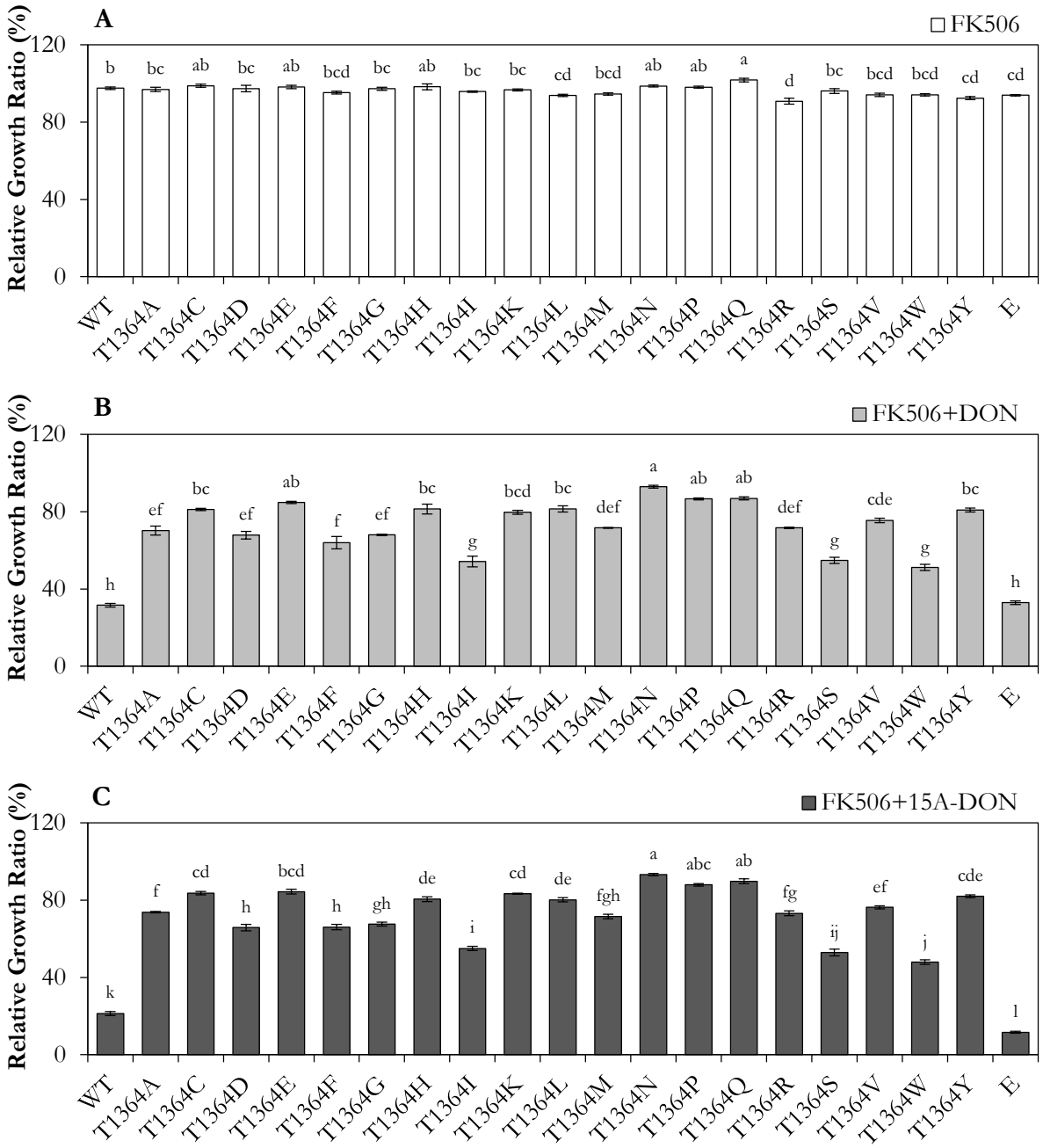

Figure 3.22 Relative growth ratios (%) of T1364 Pdr5p mutant transformants in FK506, FK506+DON, or FK506+15A-DON. Each transformant, expressing a T1364 Pdr5p mutant (designated by the single-letter code of the substituted amino acid), the transformant expressing wild-type Pdr5p (WT), and an empty plasmid control (E) were grown for 20 h in (**A**) FK506 (20 μg/mL), (**B**) FK506+DON (20 μg/mL+125 μg/mL), or (**C**) FK506+15A-DON (20 μg/mL+25 μg/mL). Relative growth ratios were determined by dividing the growth rates of treated cells by the growth rates of untreated cells. All data are expressed as means ±SEM (n≥3). In each panel, bars with the same letter are not significantly different ($P<0.05$).

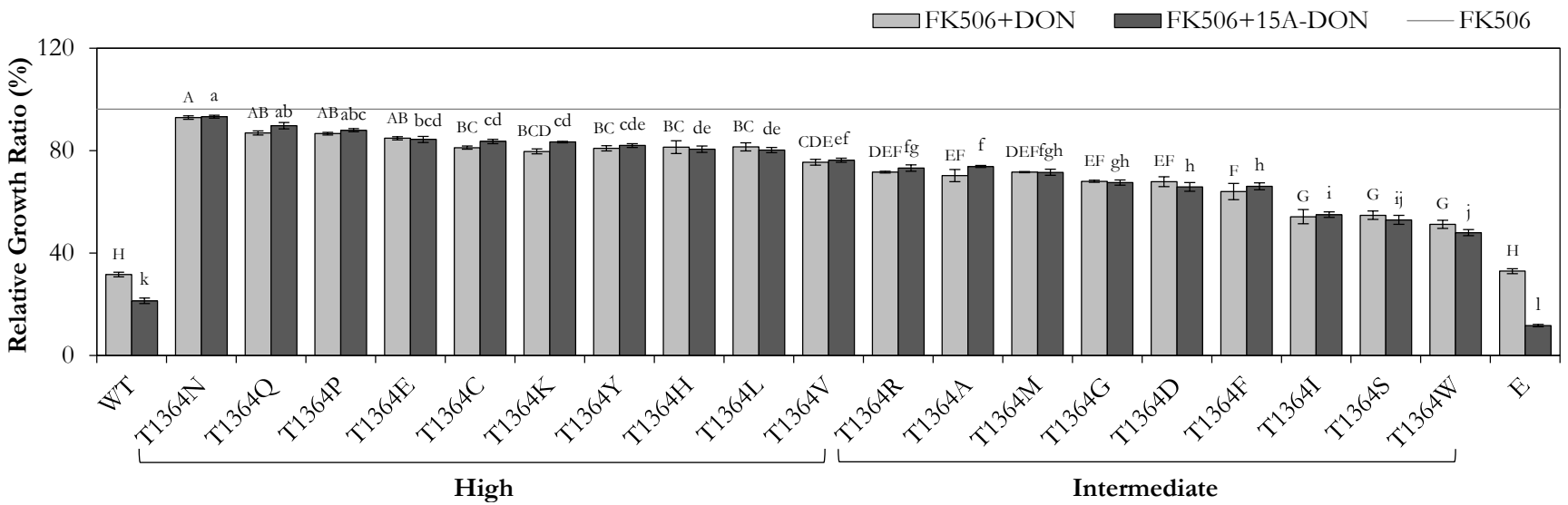

Figure 3.23 Classification of the T1364 Pdr5p mutant transformants grown in FK506+DON, or FK506+15A-DON. Transformants shown in Figure 3.22 were arranged in descending order based on their relative growth ratios (%) after growth in FK506+DON (20 μg/mL+125 μg/mL) or FK506+15A-DON (20 μg/mL+25 μg/mL). Each transformant was then subjectively classified according to the ability of their expressed T1364 Pdr5p mutant to export either mycotoxin at a high, intermediate, or low level in the presence of FK506. The average of the relative growth ratio of all transformants in FK506 alone is indicated by the grey line. The transformant expressing wild-type Pdr5p (WT) and the empty plasmid control (E) were added to compare their growth ratios to those of each transformant expressing a T1364 Pdr5p mutant. All data are expressed as means ±SEM (n≥3). Bars with the same letter within each group (uppercase for FK506+DON and lowercase for FK506+15A-DON) are not significantly different ($P<0.05$).

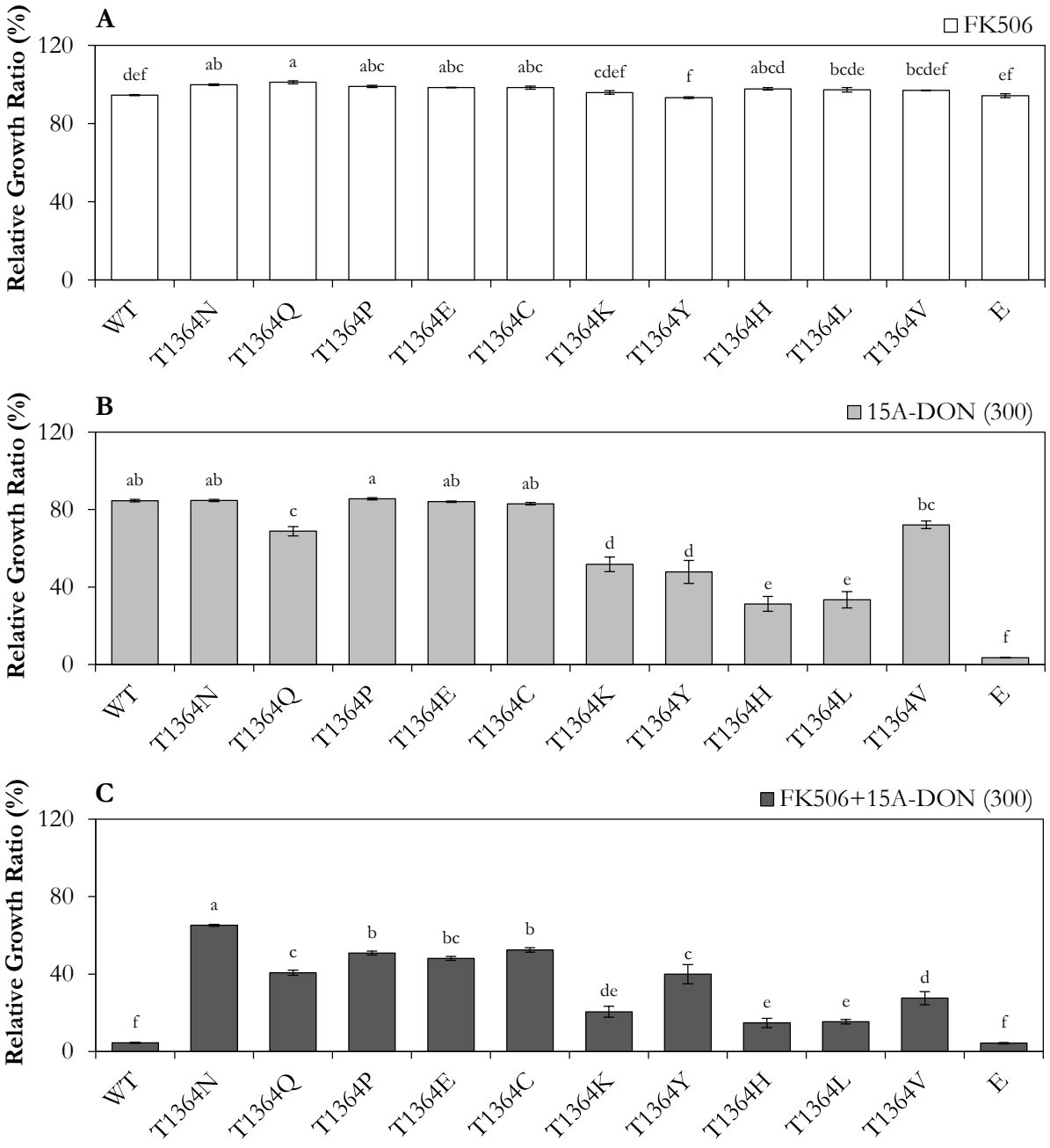

Figure 3.24 Relative growth ratios (%) of transformants expressing T1364 Pdr5p mutants classified as maintaining a high level of export of either DON or 15A-DON in the presence of FK506. Each transformant, expressing a T1364 Pdr5p mutant (designated by the single-letter code of the substituted amino acid), the transformant expressing wild-type Pdr5p (WT), and an empty plasmid control (E) were grown for 20 h in (**A**) FK506 (20 μg/mL), (**B**) 15A-DON (300 μg/mL), or (**C**) FK506+15A-DON (20 μg/mL+300 μg/mL). Relative growth ratios were determined by dividing the growth rates of treated cells by the growth rates of untreated cells. All data are expressed as means ±SEM (n≥3). In each panel, bars with the same letter are not significantly different ($P<0.05$).

compounds in the culture filtrate were having unknown effects on the function of Pdr5p. The overall growth trends for each transformant were very similar with both filtrates; however, filtrate 11A had a more pronounced growth inhibitory effect on every transformant. Filtrate 11A was therefore possibly more toxic than filtrate 12A. This difference was likely caused by normal variability in the exact composition of different filtrate preparations.

The transformants were then arranged in descending order based on their relative growth ratios in both filtrates, and then they were subjectively classified according to the ability of their expressed S1360 or T1364 Pdr5p mutant to mediate yeast resistance against filtrate 11A (Figures 3.26 & 3.29). The S1360F/P/W/Y mutants provided low yeast resistance to filtrate 11A. The S1360W mutant was the only mutant that caused low resistance to filtrate 12A. Yeast expressing the T1364D/R mutants demonstrated low resistance to filtrate 11A; however, they were more resistant than yeast expressing S1360F/P/W/Y. None of the S1360 or T1364 transformants that mediated high yeast resistance to filtrate 11A grew significantly better than WT Pdr5p; therefore, eight top S1360 (Figure 3.27) and T1364 (Figure 3.30) transformants were selected and grown in both filtrates containing a higher concentration of 15A-DON. Once again, none of the transformants grew significantly better than the WT.

3.4.4 Growth in DON and 15A-DON in the presence of enniatin B

Enniatin B is a Pdr5p-specific inhibitor produced by *F. avenaceum*, a *Fusarium* species that infects cereal grains in the Western Canadian Prairie provinces (Hiraga et al., 2005; Gräfenhan et al., 2013). As a result, it was a biologically relevant inhibitor to analyze in this study. To determine the ability of each S1360 or T1364 Pdr5p mutant to export known concentrations of DON or 15A-DON in the presence of a known *Fusarium* species Pdr5p-specific inhibitor, growth assays were performed by growing each transformant in liquid culture with enniatin

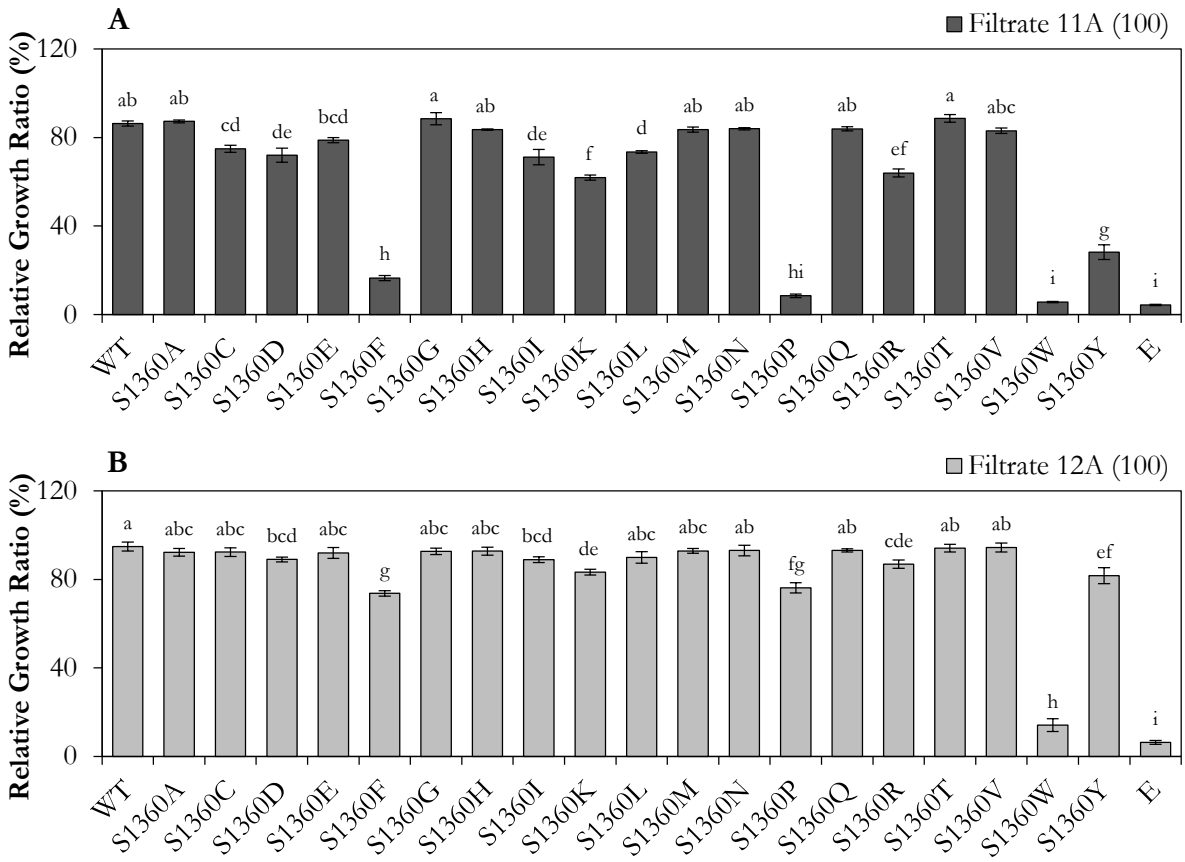

Figure 3.25 Relative growth ratios (%) of S1360 Pdr5p mutant transformants in *F. graminearum* culture filtrate. Each transformant, expressing a S1360 Pdr5p mutant (designated by the single-letter code of the substituted amino acid), the transformant expressing wild-type Pdr5p (WT), and an empty plasmid control (E) were grown for 20 h in (**A**) filtrate 11A or (**B**) filtrate 12A, each containing a concentration of 100 μg/mL 15A-DON. Relative growth ratios were determined by dividing the growth rates of treated cells by the growth rates of untreated cells. All data are expressed as means ±SEM (n≥3). In each panel, bars with the same letter are not significantly different ($P<0.05$).

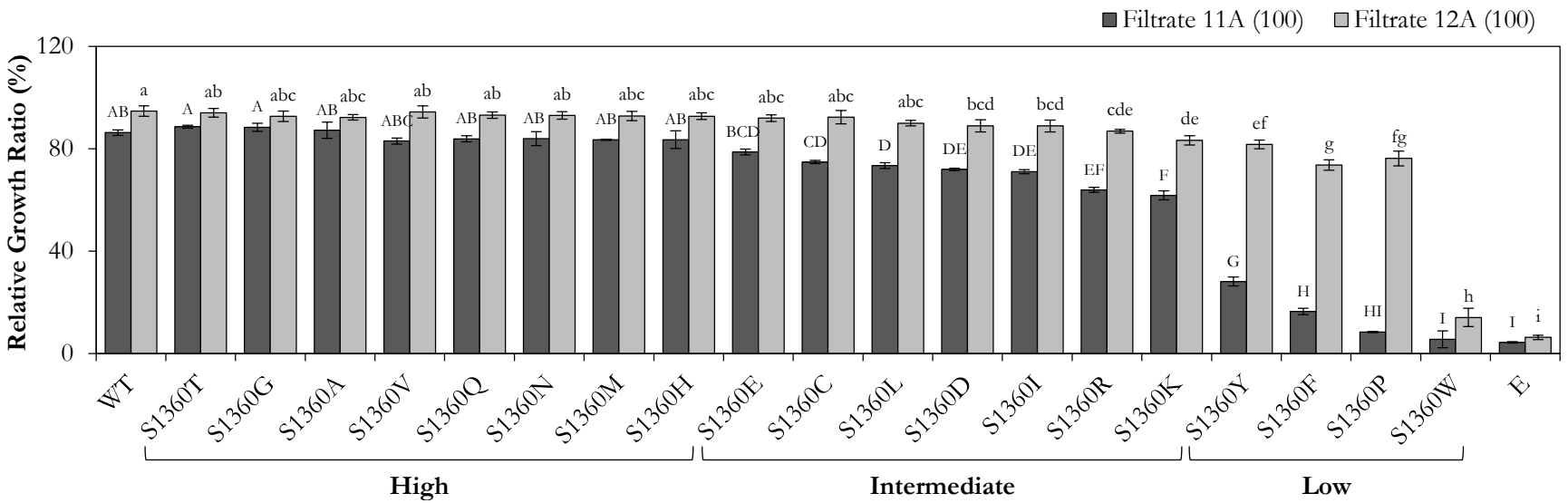

Figure 3.26 Classification of the S1360 Pdr5p mutant transformants grown in *F. graminearum* culture filtrate. The transformants shown in Figure 3.25 were arranged in descending order based on their relative growth ratios (%) after growth in filtrate 11A or filtrate 12A, each containing a concentration of 100 μg/mL 15A-DON. Each transformant was then subjectively classified according to the ability of their expressed S1360 Pdr5p mutant to mediate high, intermediate, or low resistance to filtrate 11A. The transformant expressing wild-type Pdr5p (WT) and the empty plasmid control (E) were added to compare their growth ratios to those of each transformant expressing a S1360 Pdr5p mutant. All data are expressed as means ±SEM (n≥3). Bars with the same letter within each group (uppercase for filtrate 11A and lowercase for filtrate 12A) are not significantly different ($P<0.05$).

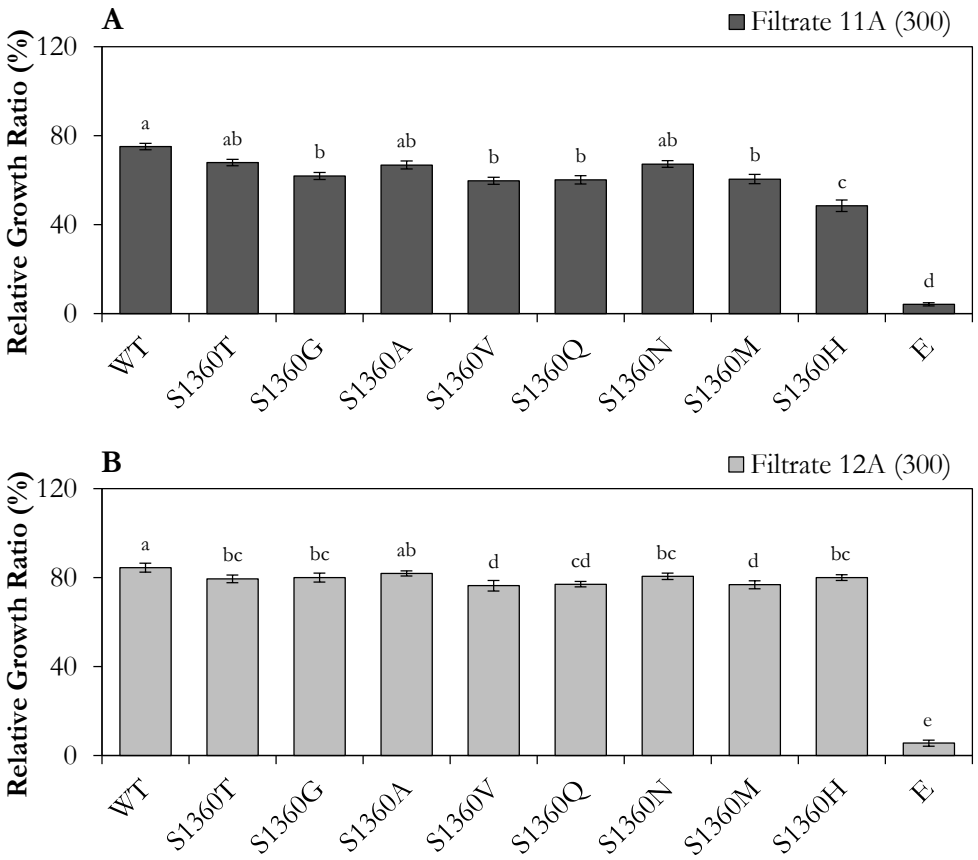

Figure 3.27 Relative growth ratios (%) of transformants expressing S1360 Pdr5p mutants classified as demonstrating a high level of resistance to *F. graminearum* culture filtrate 11A. Each transformant, expressing a S1360 Pdr5p mutant (designated by the single-letter code of the substituted amino acid), the transformant expressing wild-type Pdr5p (WT), and an empty plasmid control (E) were grown for 20 h in (**A**) filtrate 11A or (**B**) filtrate 12A, each containing a concentration of 300 μg/mL 15A-DON. Relative growth ratios were determined by dividing the growth rates of treated cells by the growth rates of untreated cells. All data are expressed as means ±SEM (n≥3). In each panel, bars with the same letter are not significantly different ($P<0.05$).

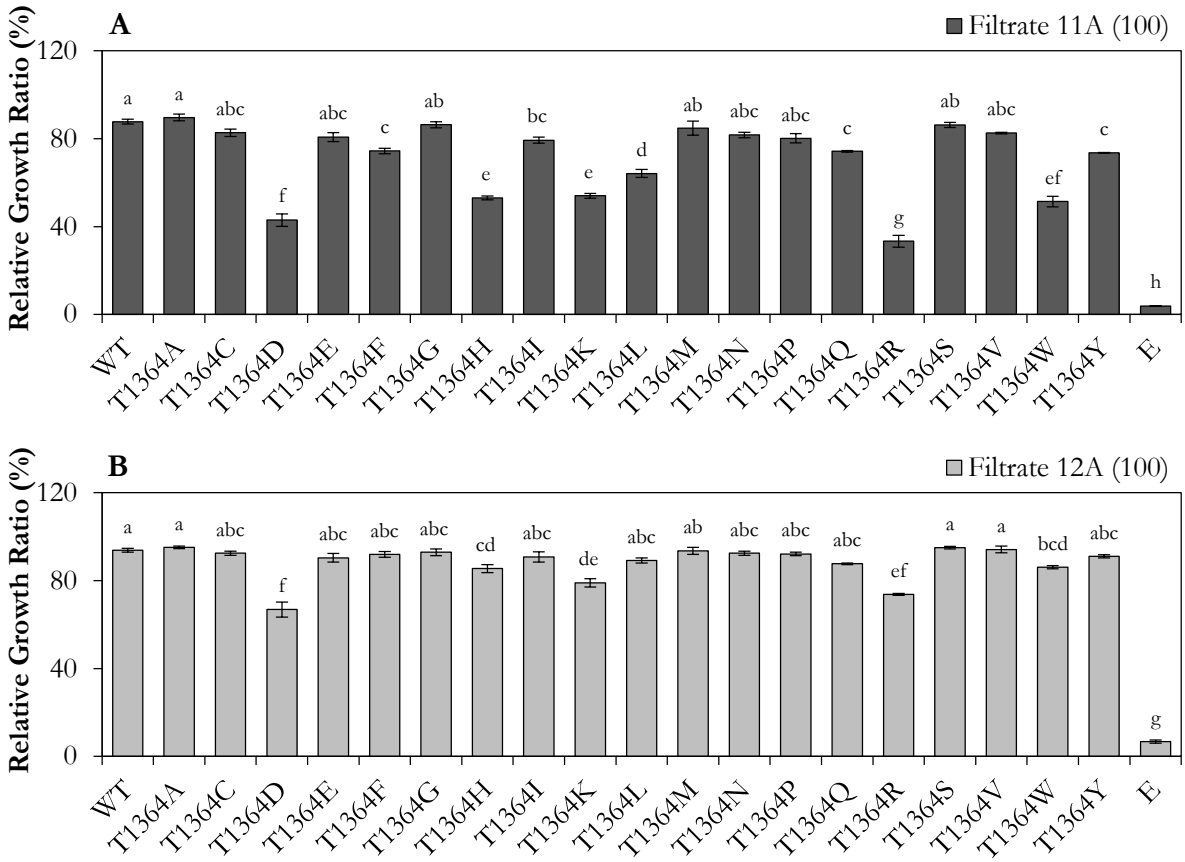

Figure 3.28 Relative growth ratios (%) of T1364 Pdr5p mutant transformants in *F. graminearum* culture filtrate. Each transformant, expressing a T1364 Pdr5p mutant (designated by the single-letter code of the substituted amino acid), the transformant expressing wild-type Pdr5p (WT), and an empty plasmid control (E) were grown for 20 h in (**A**) filtrate 11A or (**B**) filtrate 12A, each containing a concentration of 100 µg/mL 15A-DON. Relative growth ratios were determined by dividing the growth rates of treated cells by the growth rates of untreated cells. All data are expressed as means ±SEM (n≥3). In each panel, bars with the same letter are not significantly different ($P<0.05$).

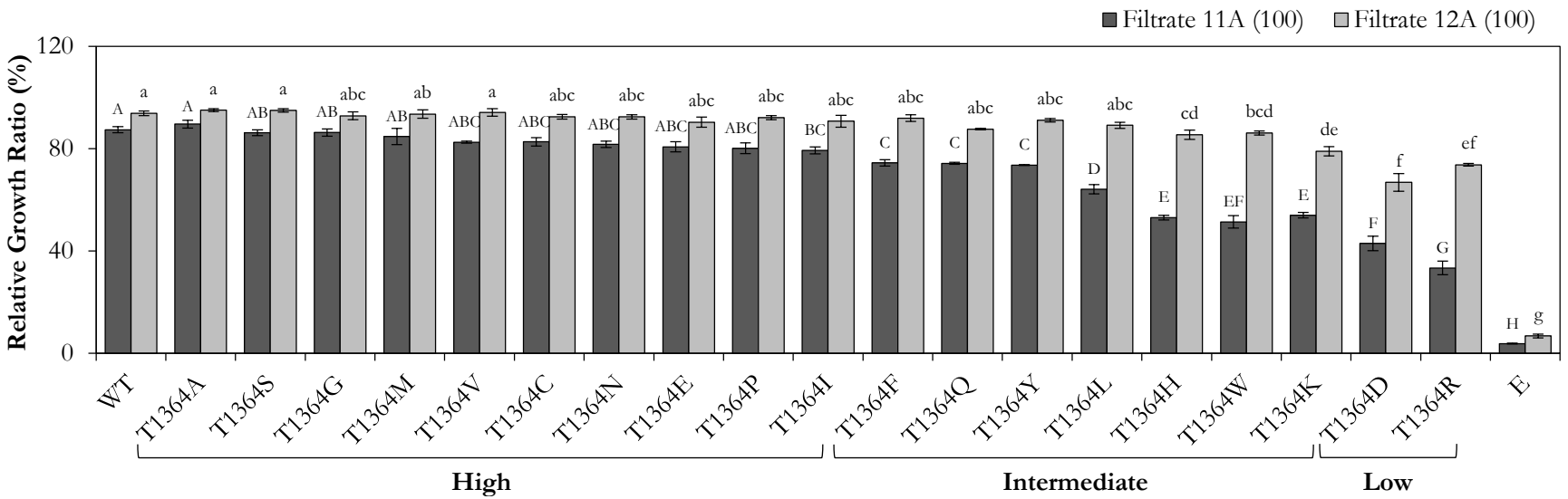

Figure 3.29 Classification of the T1364 Pdr5p mutant transformants grown in *F. graminearum* culture filtrate. The transformants shown in Figure 3.28 were arranged in descending order based on their relative growth ratios (%) after growth in filtrate 11A or filtrate 12A, each containing a concentration of 100 μg/mL 15A-DON. Each transformant was then subjectively classified according to the ability of their expressed T1364 Pdr5p mutant to mediate high, intermediate, or low resistance to filtrate 11A. The transformant expressing wild-type Pdr5p (WT) and the empty plasmid control (E) were added to compare their growth ratios to those of each transformant expressing a T1364 Pdr5p mutant. All data are expressed as means ±SEM (n≥3). Bars with the same letter within each group (uppercase for filtrate 11A and lowercase for filtrate 12A) are not significantly different ($P<0.05$).

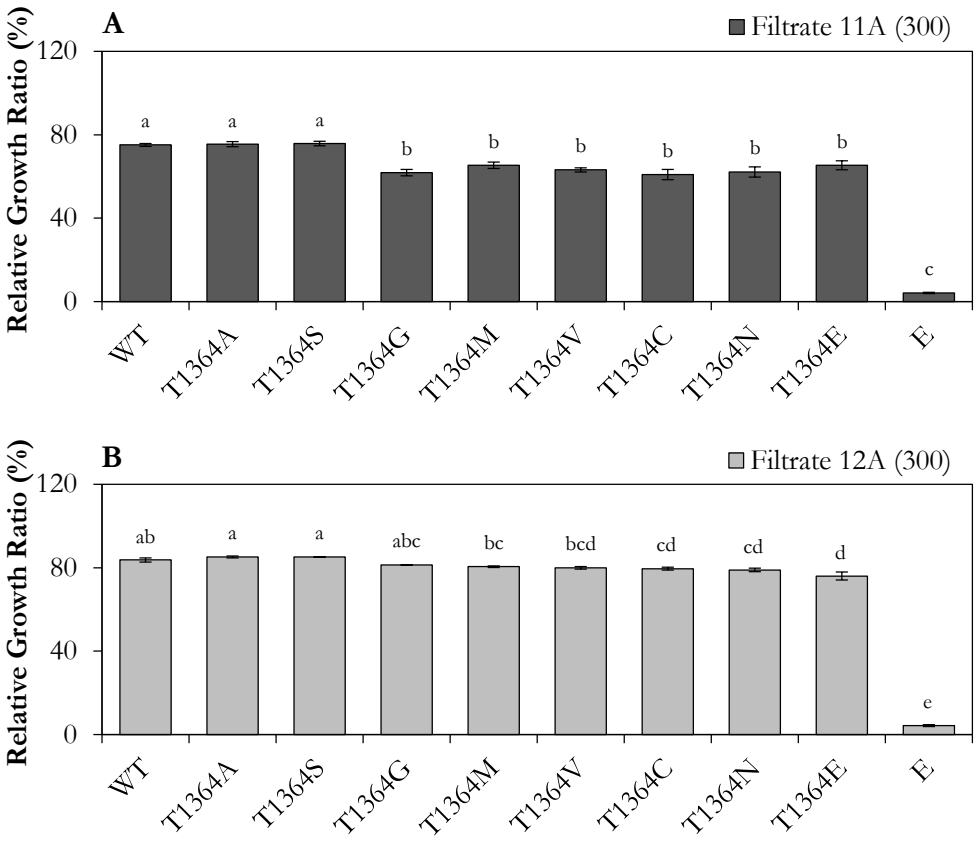

Figure 3.30 Relative growth ratios (%) of transformants expressing T1364 Pdr5p mutants classified as demonstrating a high level of resistance to *F. graminearum* culture filtrate 11A. Each transformant, expressing a T1364 Pdr5p mutant (designated by the single-letter code of the substituted amino acid), the transformant expressing wild-type Pdr5p (WT), and an empty plasmid control (E) were grown for 20 h in (**A**) filtrate 11A or (**B**) filtrate 12A, each containing a concentration of 300 μg/mL 15A-DON. Relative growth ratios were determined by dividing the growth rates of treated cells by the growth rates of untreated cells. All data are expressed as means ±SEM (n≥3). In each panel, bars with the same letter are not significantly different (P<0.05).

B+DON or enniatin B+15A-DON (Figures 3.31 & 3.34). Enniatin B alone did not have a major effect on growth of the transformants. The overall growth trends for all transformants were very similar in both mycotoxins with the addition of enniatin B. Furthermore, certain S1360 or T1364 Pdr5p transformants were capable of maintaining a significantly higher level of growth in enniatin B+DON or enniatin B+15A-DON when compared to the transformant expressing WT Pdr5p.

The transformants were then arranged in descending order based on their relative growth ratios in enniatin B+DON or enniatin B+15A-DON, and then they were subjectively classified according to the ability of their expressed S1360 or T1364 Pdr5p mutant to export either mycotoxin in the presence of enniatin B (Figures 3.32 & 3.35). Mutants at both residues maintained a high level of DON and 15A-DON export in the presence of enniatin B. Few mutants at either residue demonstrated a low level of mycotoxin export in the presence of enniatin B. As observed in DON or 15A-DON alone, the S1360F mutant maintained a greater level of 15A-DON export compared to that of DON.

Transformants expressing S1360 or T1364 Pdr5p mutants that maintained a high level of DON and 15A-DON export in the presence of FK506 were grown again in 15A-DON alone and in 15A-DON+FK506 (Figures 3.33 & 3.36). While the concentration of enniatin B remained the same as in the previous growth assays, the concentration of 15A-DON was increased by a factor of 12. At this very high concentration of 15A-DON, certain transformants expressing S1360 or T1364 Pdr5p mutants were able to maintain a level of 15A-DON export comparable to that of the transformant expressing WT Pdr5p. In 15A-DON+enniatin B, growth of the transformant expressing WT Pdr5p was nearly completely inhibited. Although their growth was negatively affected, various transformants, notably those expressing Pdr5p

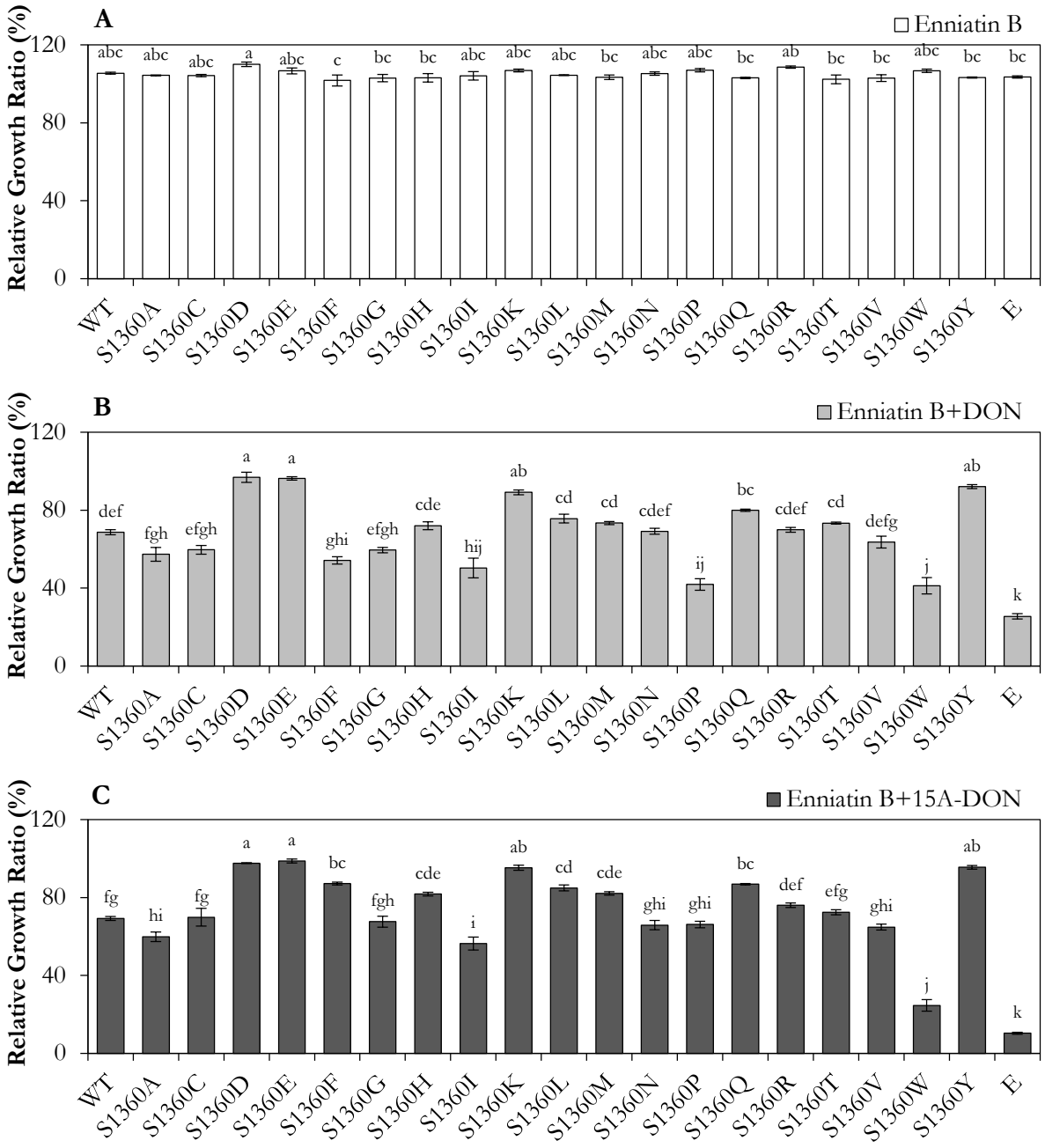

Figure 3.31 Relative growth ratios (%) of S1360 Pdr5p mutant transformants in enniatin B, enniatin B+DON, or enniatin B+15A-DON. Each transformant, expressing a S1360 Pdr5p mutant (designated by the single-letter code of the substituted amino acid), the transformant expressing wild-type Pdr5p (WT), and an empty plasmid control (E) were grown for 20 h in (**A**) enniatin B (20 μg/mL), (**B**) enniatin B+DON (20 μg/mL+125 μg/mL), or (**C**) enniatin B+15A-DON (20 μg/mL+25 μg/mL). Relative growth ratios were determined by dividing the growth rates of treated cells by the growth rates of untreated cells. All data are expressed as means ±SEM (n≥3). In each panel, bars with the same letter are not significantly different ($P<0.05$).

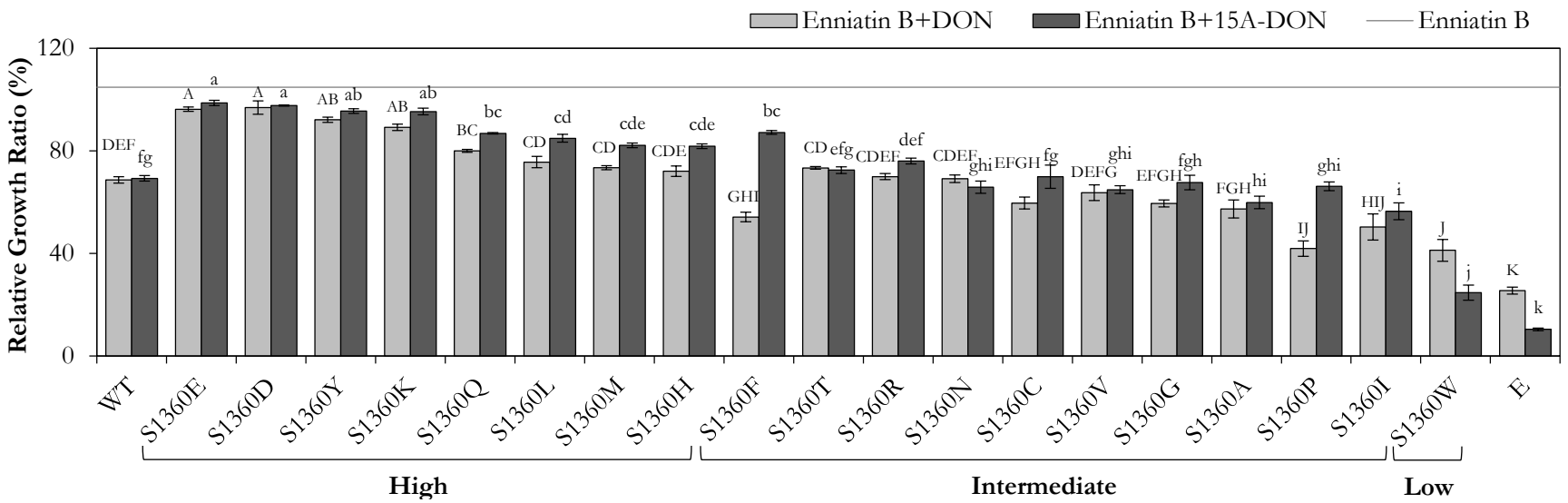

Figure 3.32 Classification of the S1360 Pdr5p mutant transformants grown in enniatin B+DON, or enniatin B+15A-DON. Transformants shown in Figure 3.31 were arranged in descending order based on their relative growth ratios (%) after growth in enniatin B+DON (20 μg/mL+125 μg/mL) or enniatin B+15A-DON (20 μg/mL+25 μg/mL). Each transformant was then subjectively classified according to the ability of their expressed S1360 Pdr5p mutant to export either mycotoxin at a high, intermediate, or low level in the presence of enniatin B. The average of the relative growth ratio of all strains in enniatin B alone is indicated by the grey line. The wild-type (WT) strain the empty plasmid control (E) were added to compare their growth ratios to those of each mutant. All data are expressed as means ±SEM (n≥3). Bars with the same letter within each group (uppercase for enniatin B+DON and lowercase for enniatin B+15A-DON) are not significantly different ($P<0.05$).

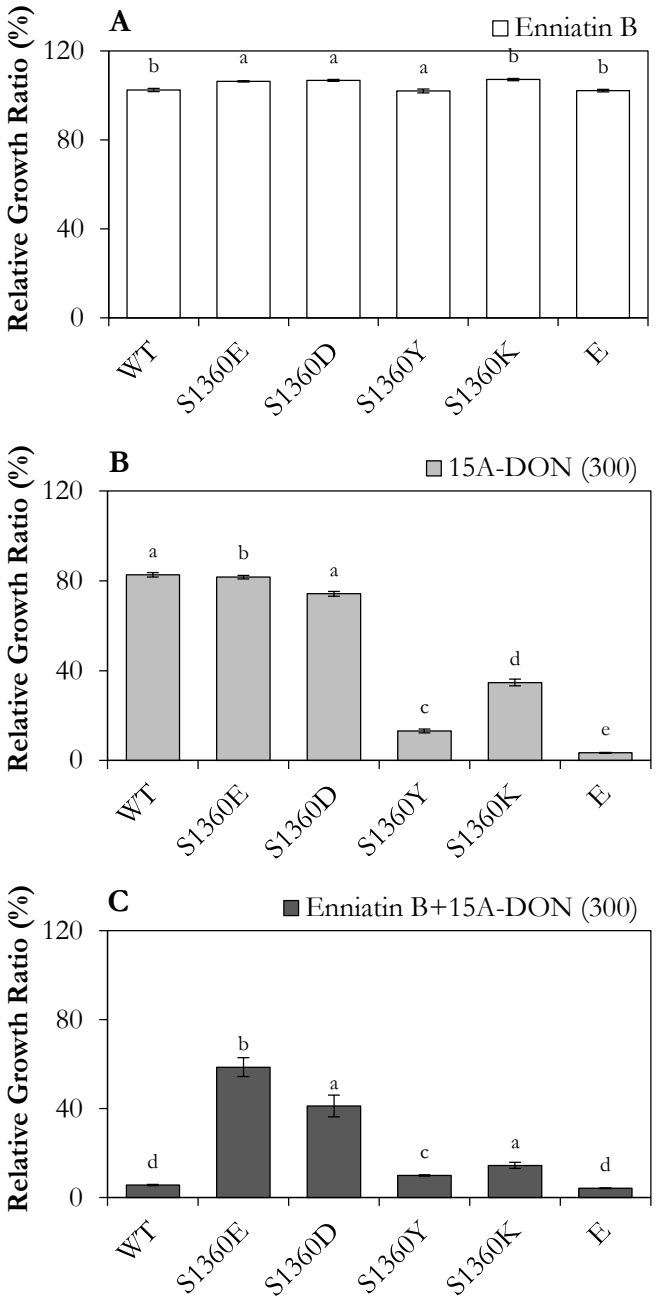

Figure 3.33 Relative growth ratios (%) of transformants expressing S1360 Pdr5p mutants classified as demonstrating a high level of resistance to either DON or 15A-DON in the presence of enniatin B. Each transformant, expressing a S1360 Pdr5p mutant (designated by the single-letter code of the substituted amino acid), the transformant expressing wild-type Pdr5p (WT), and an empty plasmid control (E) were grown for 20 h in (**A**) enniatin B (20 μg/mL), (**B**) 15A-DON (300 μg/mL), or (**C**) enniatin B+15A-DON (20 μg/mL+300 μg/mL). Relative growth ratios were determined by dividing the growth rates of treated cells by the growth rates of untreated cells. All data are expressed as means ±SEM (n≥3). In each panel, bars with the same letter are not significantly different ($P<0.05$).

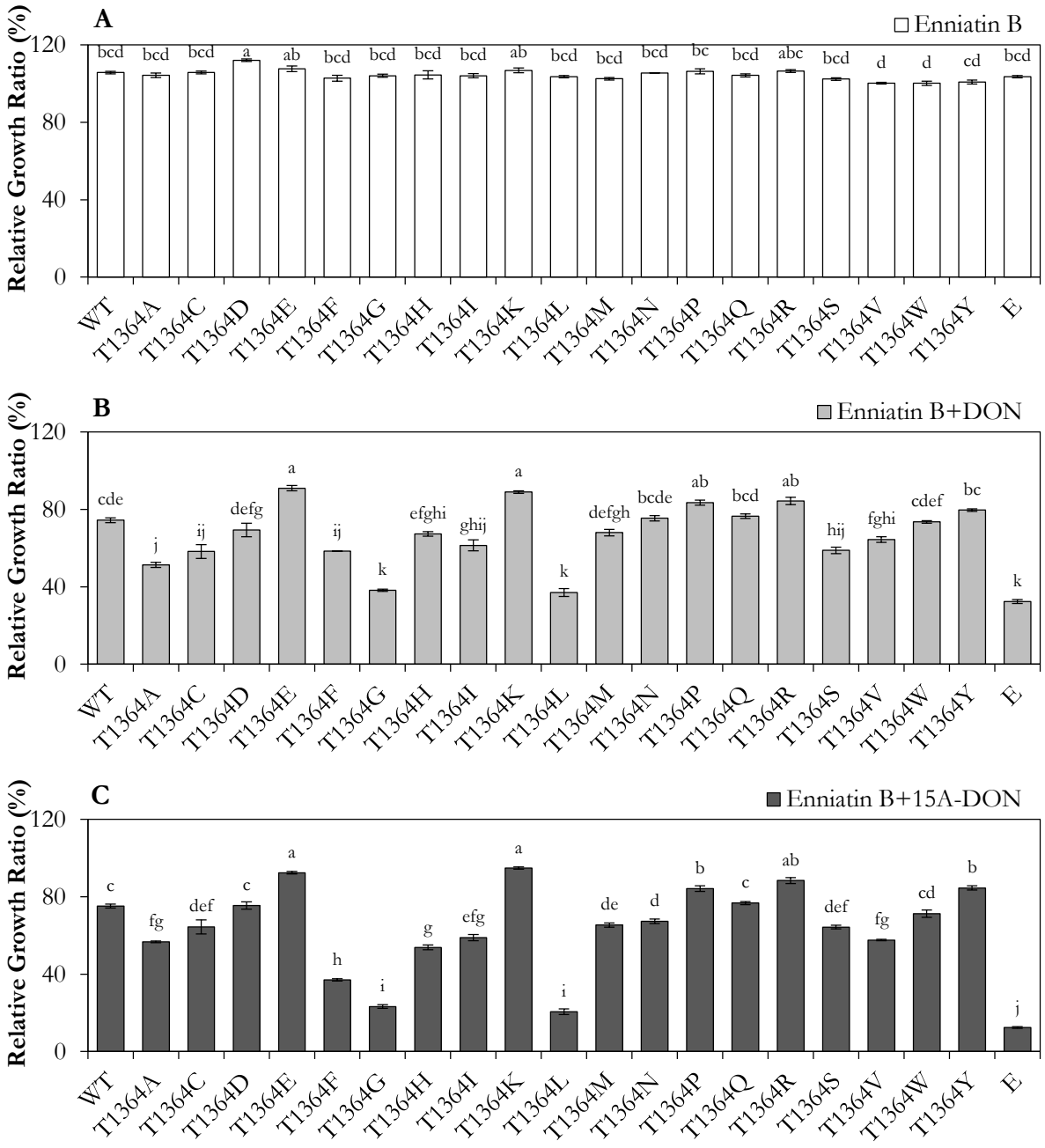

Figure 3.34 Relative growth ratios (%) of S1360 Pdr5p mutant transformants in enniatin B, enniatin B+DON, or enniatin B+15A-DON. Each transformant, expressing a S1360 Pdr5p mutant (designated by the single-letter code of the substituted amino acid), the transformant expressing wild-type Pdr5p (WT), and an empty plasmid control (E) were grown for 20 h in (**A**) enniatin B (20 μg/mL), (**B**) enniatin B+DON (20 μg/mL+125 μg/mL), or (**C**) enniatin B+15A-DON (20 μg/mL+25 μg/mL). Relative growth ratios were determined by dividing the growth rates of treated cells by the growth rates of untreated cells. All data are expressed as means ±SEM (n≥3). In each panel, bars with the same letter are not significantly different ($P<0.05$).

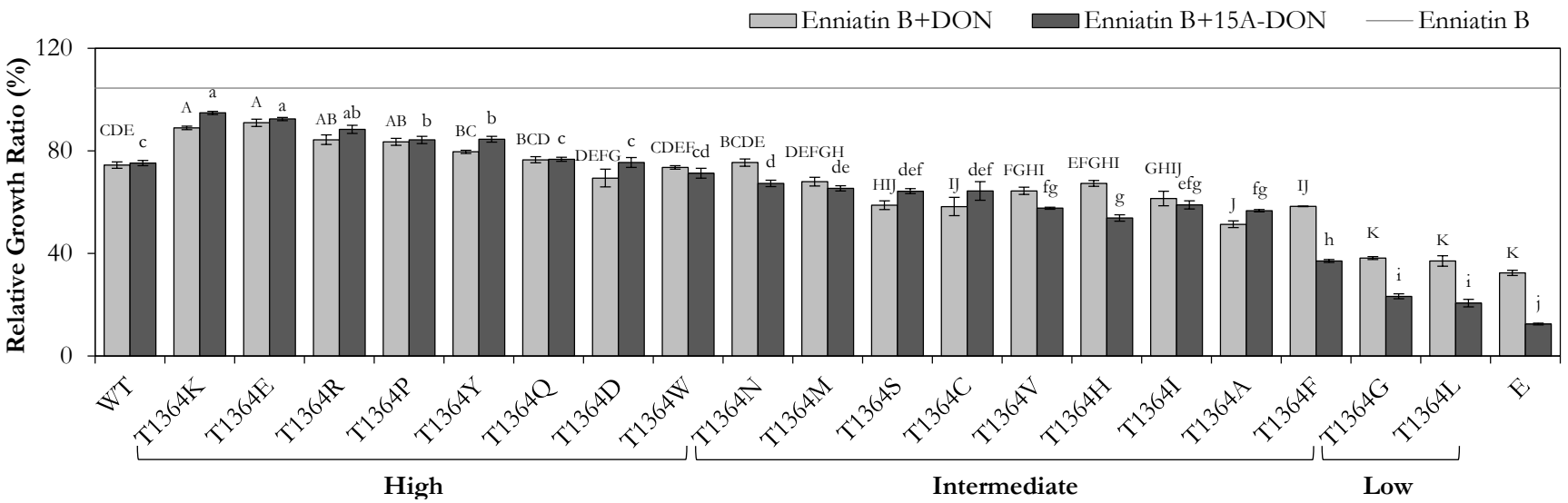

Figure 3.35 Classification of the T1364 Pdr5p mutant transformants grown in enniatin B+DON, or enniatin B+15A-DON. Transformants shown in Figure 3.34 were arranged in descending order based on their relative growth ratios (%) after growth in enniatin B+DON (20 μg/mL+125 μg/mL) or enniatin B+15A-DON (20 μg/mL+25 μg/mL). Each transformant was then subjectively classified according to the ability of their expressed T1364 Pdr5p mutant to export either mycotoxin at a high, intermediate, or low level in the presence of enniatin B. The average of the relative growth ratio of all strains in enniatin B alone is indicated by the grey line. The wild-type (WT) strain the empty plasmid control (E) were added to compare their growth ratios to those of each mutant. All data are expressed as means ±SEM (n≥3). Bars with the same letter within each group (uppercase for enniatin B+DON and lowercase for enniatin B+15A-DON) are not significantly different ($P<0.05$).

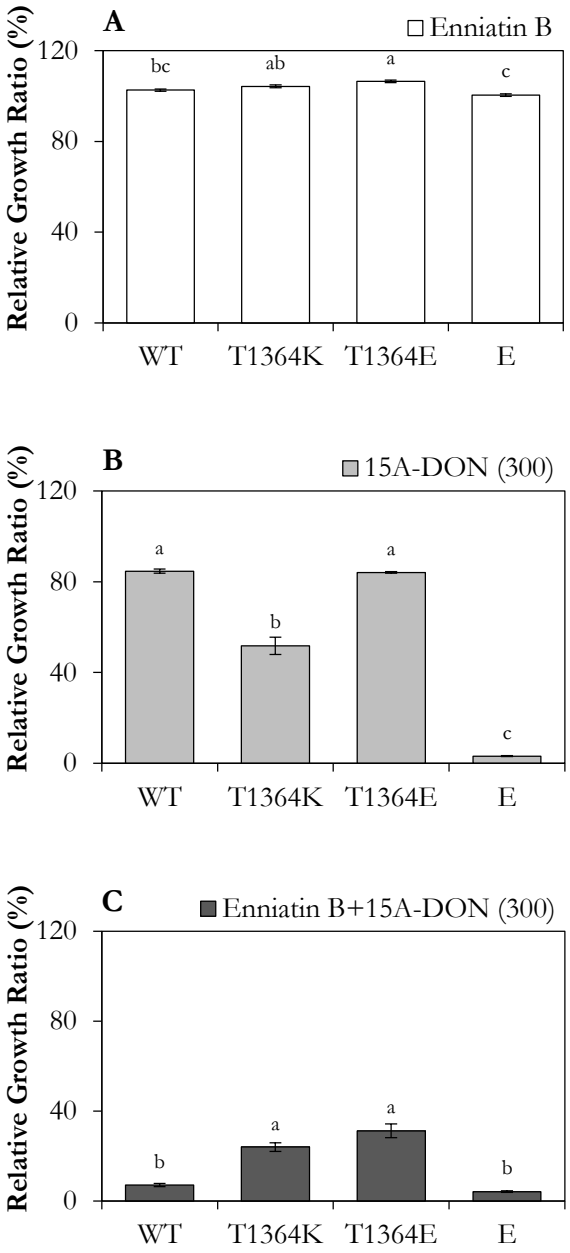

Figure 3.36 Relative growth ratios (%) of transformants expressing T1364 Pdr5p mutants classified as demonstrating a high level of resistance to either DON or 15A-DON in the presence of enniatin B. Each transformant, expressing a T1364 Pdr5p mutant (designated by the single-letter code of the substituted amino acid), the transformant expressing wild-type Pdr5p (WT), and an empty plasmid control (E) were grown for 20 h in (**A**) enniatin B (20 μg/mL), (**B**) 15A-DON (300 μg/mL), or (**C**) enniatin B+15A-DON (20 μg/mL+300 μg/mL). Relative growth ratios were determined by dividing the growth rates of treated cells by the growth rates of untreated cells. All data are expressed as means ±SEM (n≥3). In each panel, bars with the same letter are not significantly different ($P<0.05$).

mutants S1360D/E, were capable of growing in 15A-DON+enniatin, while growth of the mutants at residue T1364 was inhibited.

3.5 Preliminary growth assays of S1360D and S1360E in *F. avenaceum* filtrate

The Pdr5p mutants S1360D and S1360E appear to be involved in modulating insensitivity towards enniatin B. To further assess the importance of these two Pdr5p mutants, preliminary growth assays were performed by growing both transformants, expressing either of these mutants, in liquid culture with *F. avenaceum* filtrate. Briefly, this filtrate contained all compounds produced and secreted by *F. avenaceum*, including enniatin variants such as enniatin B. Since *F. avenaceum* does not produce trichothecene mycotoxins, 15A-DON was added to the culture filtrate. Culture filtrates produced by *F. avenaceum* strains LH_27 and LH_36 grown in culture were used.

Concentrations of 25 or 50 μg/mL 15A-DON alone did not have a large impact on yeast growth (Figure 3.37A). The transformant expressing WT Pdr5p demonstrated drastic growth inhibition in filtrate LH_36 and was nearly completely inhibited in filtrate LH_27 (Figure 3.37B). At 50 μg/mL 15A-DON, transformants expressing either the S1360D or S1360E Pdr5p mutants maintained a high level of growth in filtrate LH_36; however, their growth was drastically reduced in filtrate LH_27. At 25 μg/mL 15A-DON, growth of the mutants in LH_27 was similar to that at 50 μg/mL 15A-DON in filtrate LH_36. While doubling the concentration of 15A-DON had little growth effect on either mutant in the absence of filtrate, it caused substantial growth reduction in both mutants when filtrate LH_27 was added.

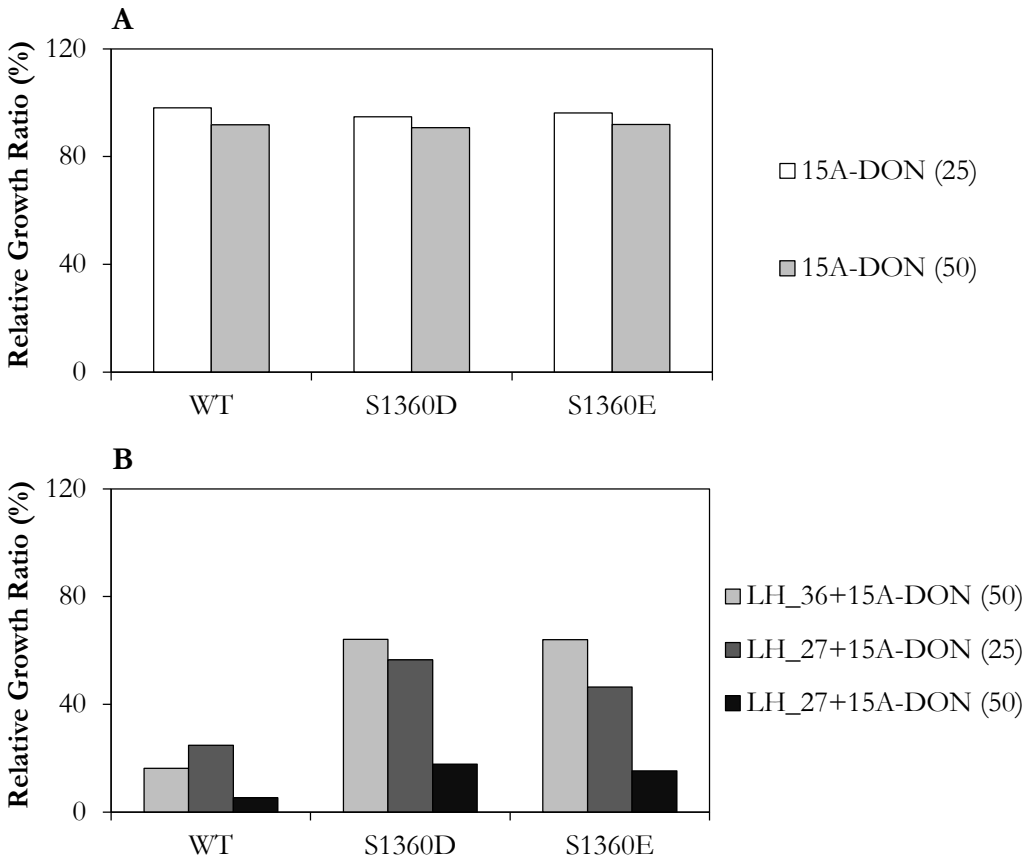

Figure 3.37 Relative growth ratios (%) of transformants expressing WT, S1360D, or S1360E Pdr5p in *F. avenaceum* filtrate LH_27 or LH_36 with 15A-DON. (**A**) Each transformant was grown for 20 h in 25 μg/mL 15A-DON, 50 μg/mL 15A-DON, (**B**) 1 μg/μL filtrate LH_36 with 50 μg/mL 15A-DON, 1 μg/μL filtrate LH_27 with 25 μg/mL 15A-DON, or 1 μg/μL filtrate LH_27 with 50 μg/mL 15A-DON. Relative growth ratios were determined by dividing the growth rates of treated cells by the growth rates of untreated cells. (n=1).

CHAPTER 4 – DISCUSSION

Saccharomyces cerevisiae ATP-binding cassette (ABC) transporters from the pleiotropic drug resistance (PDR) network are involved in exporting hundreds of cytotoxic compounds from the cell (Kolaczkowski et al., 1998). Furthermore, Pdr5p, which is a member of this network, has an essential role in mediating the resistance of *S. cerevisiae* to trichothecene mycotoxins produced by *Fusarium* species. It was therefore hypothesized that the plasma membrane of *S. cerevisiae* contains at least one ABC transporter from the PDR network with substrate specificity for the *Fusarium graminearum* trichothecene mycotoxins deoxynivalenol (DON) and 15-acetyl-deoxynivalenol (15A-DON) and that the absence or inhibition of this/these transporter(s) would lead to yeast growth inhibition in the presence of either mycotoxin. It was also hypothesized that if specific transporters could be identified, they could then be mutagenized to become insensitive to the inhibitory compound produced by *F. graminearum* while maintaining substrate specificity for DON.

To address the hypotheses for the first part of this project, all known or putative transporters from the PDR network were analyzed for their ability to export both DON and its acetylated derivative 15A-DON out of living cells. The results showed that Pdr5p is the main exporter of both mycotoxins. This transporter was, therefore, the focus of the remainder of this thesis. The Gleddie lab determined that *F. graminearum* produces an inhibitory compound that blocks DON export by *S. cerevisiae*. Furthermore, they suggested that this compound shares properties with FK506, such as the ability to specifically block the function of Pdr5p. Previous mutagenesis studies conducted on Pdr5p determined that single amino acid substitutions at residue S1360 or T1364 are capable of generating Pdr5p insensitivity to FK506 (Egner et al., 1998; 2000). These substitutions, however, affect transporter specificity for Pdr5p-specific

substrates such as the azole antifungals ketoconazole and itraconazole, the protein synthesis inhibitor cycloheximide, and the fluorescent dyes rhodamine 6G and rhodamine 123 (Egner et al., 1998; 2000). To address the hypothesis for the second part of this project, Pdr5p mutants with single amino acid substitutions at residue S1360 or T1364 were generated, individually expressed in yeast deleted for wild-type (WT) Pdr5p, and then screened in *F. graminearum* culture filtrate to identify those mutants enabling increased yeast resistance to the culture filtrate when compared to WT Pdr5p. The culture filtrate used in this study was composed of all compounds produced and secreted by a 15A-DON-producing strain of *F. graminearum* grown in culture. Compounds found in the culture filtrate included mainly 15A-DON as well as the FK506-like inhibitor. Unfortunately, none of the mutants tested enabled increased yeast resistance to the culture filtrate, suggesting that none of the mutants conferred insensitivity to the FK506-like inhibitor produced by *F. graminearum*. The vast majority of Pdr5p mutants were, however, able to maintain the ability to export both DON and 15A-DON while certain mutants conferred insensitivity to the Pdr5p-specific inhibitors FK506 and/or enniatin B.

4.1 ABC transporters and mycotoxin export

Pdr5p is the major ABC transporter in exponentially growing *S. cerevisiae* cells (Ghaemmaghami et al., 2003) and has the ability to export over one hundred toxic compounds out of the cell (Kolaczkowski et al., 1998). These compounds include the trichothecene mycotoxins DON and 15A-DON produced by *F. graminearum*, and the trichothecene mycotoxin 4,15-diacetoxyscirpenol (DAS) produced by *F. poae* and *F. equiseti* (Muhitch et al., 2000; Mitterbauer & Adam, 2002; Suzuki & Iwahashi, 2012). While substrate specificity of Pdr5p for trichothecene mycotoxins has been clearly established, the potential involvement of additional ABC transporters has remained unknown. Since Pdr5p is a member of the PDR network of

ABC transporters, it was concluded that any other transporter with substrate specificity for trichothecene mycotoxins would most likely be found within this network. All 11 known or putative transporters from the PDR network were therefore selected for this study to determine their ability to export the *F. graminearum* mycotoxins DON and 15A-DON (Table 3.1). Among these 11 transporters, Pdr5p and its functional homologues Snq2p and Yor1p have been well-studied. While these three transporters are responsible for exporting distinct substrates, they also have overlapping substrate specificity. With Pdr5p already identified as an important exporter of DON and 15A-DON, Snq2p and Yor1p were considered as candidate exporters for these mycotoxins. Growth inhibitory assays performed using the haploid yeast knockout (YKO) strains corresponding to each of the 11 transporters clearly determined the involvement of each transporter in exporting DON and 15A-DON from yeast cells.

4.2 Phenotypic analyses of haploid YKO strains

The haploid YKO collection contains single-gene knockouts of genes coding for non-essential proteins (Winzeler et al., 1999). Phenotypic analyses of single-gene knockouts can therefore be conducted using YKO strains from this collection. An important advantage of YKO strains is that they can be validated by PCR. Each strain has two sets of strain-specific primers, either of which can be used to verify that the desired gene has been knocked out of the corresponding YKO strain. The identity of each of the 11 YKO strains used in this study was validated with either one or both sets of strain-specific primers (Figure 3.1); therefore, phenotypic variations observed in the YKO strains when they were grown in the presence of mycotoxins produced by *F. graminearum* were caused by the absence of their single knocked-out gene.

By using strains from the haploid YKO collection, it is possible to observe the phenotypic effects caused by the complete lack of expression of a gene of interest in the presence of a cytotoxic compound. This can, however, only be conducted if the gene of interest is non-essential. Despite their known or putative involvement in mediating toxin export, none of the genes encoding the ABC transporters selected for this study are essential. It was therefore possible to use the haploid YKO strains corresponding to each of these transporters for phenotypic analyses in the presence of trichothecene mycotoxins produced by *F. graminearum*.

4.3 Growth inhibitory assays of *S. cerevisiae* in liquid culture

As demonstrated in this study, growth inhibitory assays of *S. cerevisiae* can be used to functionally characterize ABC transporters in the presence of a toxin of interest. Performing such assays either on agar plates or in liquid culture is a simple, straightforward approach to determining the involvement of individual transporters in exporting specific cytotoxic compounds (Ernst et al., 2008). Yeast growth assays in liquid culture have been shown to be more accurate than assays on agar plates in detecting small toxin sensitivity variations among different yeast strains (Tutulan-Cunita et al., 2005). All growth inhibitory assays performed during this thesis were conducted in liquid culture. Yeast growth was easily determined according to optical density values obtained over a determined period of time of 20 hours. This approach was efficient in quantifying the phenotypic variation of the yeast strains grown in the presence of *F. graminearum* mycotoxins and/or Pdr5p-specific inhibitors. Additionally, at least three biological replicates ($n \geq 3$), each with two or three technical replicates, were completed for every yeast strain in each growth treatment, which strongly supports the validity of the results presented in this thesis.

4.4 Pdr5p is the major exporter of DON and 15A-DON

For the purpose of this study, concentrations of 125 μg/mL DON and 25 μg/mL 15A-DON were selected. During a screen of the WT strain BY4741 grown in liquid culture in a range of DON and 15A-DON concentrations, these were the maximum concentrations that did not visibly affect growth of the WT strain. The use of DON and 15A-DON at these concentrations ensured that any growth inhibitory effects would be noticeable in the YKO strains corresponding to the transporters involved in exporting either of these mycotoxins. It is interesting to note that a concentration of DON five times greater than that of 15A-DON was required to observe similar growth inhibitory effects in the WT strain. This is in agreement with previous studies that recognized 15A-DON as demonstrating higher toxicity in eukaryotic cells when compared to DON (Doyle et al., 2009; Suzuki & Iwahashi, 2012).

Since Pdr5p had previously been identified as an exporter of *F. graminearum* trichothecenes, it was not surprising that the Δ*pdr5* YKO strain showed significant growth inhibition in the presence of either DON or 15A-DON (Figure 3.2). Furthermore, growth inhibition of Δ*pdr5* was significantly greater in 15A-DON than in DON. This could be interpreted that in addition to Pdr5p, another transporter was exhibiting substrate specificity towards DON. A more probable explanation is that compared to DON, the more toxic mycotoxin 15A-DON was exerting a greater inhibitory effect on Δ*pdr5* cells. Aside from Δ*pdr5*, the other ten YKO strains, each missing a single transporter, grew at a similar rate compared to the WT in the presence of DON or 15A-DON. These results strongly indicate that Pdr5p is the only transporter responsible for exporting either *F. graminearum* mycotoxin. The presumed expression of Pdr5p by the WT strain and the YKO strains, apart from Δ*pdr5*, likely prevented the intracellular accumulation of either DON or 15A-DON, which would have prevented the

mycotoxins from exerting their numerous inhibitory effects, notably protein biosynthesis inhibition, on yeast cells.

To verify that the Δ*pdr5* YKO strain was not expressing the cognate transporter Pdr5p, Western blot analysis was performed following protein separation. In the WT strain BY4741, which was used as a positive control for Pdr5p expression, a single band was detected at ~150 kDa (Figure 3.4). Similarly, for all other Western blot analyses of Pdr5p conducted during this thesis, a single band was visible at ~150 kDa, rather than at the expected size of ~160 kDa. Furthermore, Western blot analyses of Pdr5p performed by Rutledge et al. (2011) or Kueppers et al. (2013) also detected a band at a position slightly lower than 160 kDa. These observations are, however, not uncommon for proteins separated by SDS-PAGE. In fact, most helical transmembrane proteins have been shown to migrate to positions on the gel that are unpredictably larger or smaller than their actual size (reviewed in Rath et al., 2013). Pdr5p consists of two transmembrane domains (TMDs), which are each formed of six α-helix bundles known as transmembrane helices (TMHs). It was therefore not surprising that a band was detected 10 kDa lower than expected. Furthermore, antibodies directed against a peptide mapping at the N-terminus (Figure 3.4A) or C-terminus (Figure 3.4B) of Pdr5p detected an identical single band at ~150 kDa; therefore, this band likely corresponded to Pdr5p. Since no bands were detected in Δ*pdr5*, it was concluded that Pdr5p was absolutely missing from this strain; therefore, the growth inhibitory effects observed with DON and 15A-DON were caused by the complete lack of Pdr5p expression.

The results described above strongly indicate that *S. cerevisiae* contains just one ABC transporter with substrate specificity for DON and 15A-DON, and that the absence of this transporter leads to growth inhibition in the presence of either of these mycotoxins. As

determined by growing selected haploid YKO strains in liquid culture, Pdr5p appears to be the main exporter of both DON and 15A-DON. While growth of the Δ*pdr5* YKO strain was significantly inhibited by both mycotoxins, growth of the remaining ten YKO strains analyzed remained unaffected when compared to the WT strain.

4.5 Pdr5p does not mediate yeast resistance to *F. graminearum* culture filtrate

Yeast grown in the presence of *F. graminearum* culture filtrate can be used as a small-scale model to replicate crop infection by this fungal pathogen. Most *F. graminearum* isolates that contaminate crops in North America are producers of 3-acetyl-deoxynivalenol (3A-DON) or 15A-DON (Gilbert et al., 2010). As mentioned previously, the culture filtrates used for this thesis were obtained from a 15A-DON-producing strain of *F. graminearum* grown under conditions conducive to 15A-DON production. These filtrates therefore contained high levels of 15A-DON in addition to all other compounds produced and secreted by *F. graminearum*, including the FK506-like inhibitor. It is important to note that the exact composition of the culture filtrates was unknown; however, the concentration of 15A-DON was quantified by high-performance liquid chromatography (HPLC). Diluted culture filtrate containing 100 μg/mL 15A-DON was selected for growth inhibitory assays with the YKO strains since it was shown to have a slight inhibitory effect on growth of the WT. By using a concentration of culture filtrate that had a slight inhibitory effect on growth of the WT, this ensured that any growth inhibitory effects would be noticeable in the YKO strains for transporters involved in exporting 15A-DON, the predominant cytotoxic compound found in the culture filtrate. Growth of the Δ*pdr5* YKO strain was nearly completely inhibited in culture filtrate, while growth of the other ten YKO strains was only slightly inhibited; in a similar manner to the WT strain (Figure 3.3).

The FK506-like inhibitor produced by *F. graminearum* has yet to be identified or completely characterized; therefore, it cannot currently be quantified in the culture filtrate. There was consequently no possible way of knowing the quantity of FK506-like inhibitor found in the diluted culture filtrate that was added to the yeast cells. It is therefore currently impossible to determine definitively whether the FK506-like inhibitor produced by *F. graminearum* specifically blocks Pdr5p. This will only be possible to verify once the inhibitor has been identified and isolated from the culture filtrate. Despite the limitations associated with the use of *F. graminearum* culture filtrate, from results presented above, it was clear that to prevent contamination by DON or 15A-DON, the ABC transporter Pdr5p was the best candidate to study. An apparent solution to mediating resistance against *F. graminearum* would be to overexpress Pdr5p. Theoretically, increasing the quantity of Pdr5p at the plasma membrane should lead to greater transport efficiency of trichothecene mycotoxins. In the presence of a Pdr5p-specific inhibitor produced by *F. graminearum*, overexpressed WT Pdr5p transporters would nonetheless remain as targets for inhibition. This would have repercussions on cell viability in the presence of cytotoxic compounds such as DON and 15A-DON, normally transported by Pdr5p. The following analogy can be used to explain this problem: In a flooding basement, pumps are used as a first line of defense to evacuate water entering the basement, just as Pdr5p is used as a first line of defense by *S. cerevisiae* to transport DON and 15A-DON out of the cell. In the event of a power failure, no matter the quantity of pumps, it would be impossible for them to evacuate water entering the basement. In a similar manner, in the presence of a Pdr5p-specific inhibitor, Pdr5p transporters overexpressed at the plasma membrane would be blocked in a concentration-dependant manner; therefore, DON or 15A-DON would not be efficiently transported out of the cell, leading to their intracellular accumulation. A more practical solution to mediate resistance against *F. graminearum* would be

to engineer a Pdr5p transporter that could maintain the export of mycotoxins while in the presence of a Pdr5p-speficic inhibitor.

4.6 Modifying substrate specificity and inhibitor sensitivity of Pdr5p

Pdr5p consists of two nucleotide binding domains (NBDs), which bind and hydrolyze ATP, and two TMDs, each composed of six TMHs, which ensure substrate transport across biological membranes. Despite ongoing effort, the mechanism by which the TMDs of Pdr5p recognise and transport such a wide range of structurally and functionally unrelated substrates is not well understood. Although the crystal structure of Pdr5p has not yet been resolved, this transporter has been computationally modeled, based on the crystal structures of the ABC transporters P-glycoprotein (P-gp) of mouse, Sav1866 of *Staphylococcus aureus*, and Haemolysin B (HlyB) of *Escherichia coli* (Rutledge et. al., 2011). According to this model, the TMDs of Pdr5p form a large substrate-binding pocket. An important objective towards understanding the mechanism by which Pdr5p transports such a wide range of compounds is to identify and analyze individual amino acid residues lining the substrate-binding pocket that affect substrate recognition, binding, and transport, as well as inhibitor susceptibility. Residues S1360 and T1364 were the first residues identified as modulators of Pdr5p toxin resistance and inhibitor insensitivity (Egner et al., 1998; 2000). Both residues are predicted to be localized on the hydrophilic face of the substrate-binding pocket of Pdr5p (Rutledge et al., 2011; Kueppers et al., 2013). Mutational analyses revealed that single amino acid substitutions at either residue cause insensitivity of Pdr5p to inhibitory compounds, notably FK506 and enniatin B. For this project, Pdr5p mutants containing a single amino acid substitution at residue S1360 or T1364 were generated and analyzed to determine their potential to modulate resistance to *F. graminearum*. An overview of the localization of the mutations as well as the substrates and inhibitors used to

analyze the mutants that were generated for this project is shown in Figure 3.38. To my knowledge, aside from the S1360A/F/T and T1364A/F/S mutants described by Egner et al. (1998; 2000), no analyses of these mutants have previously been published.

4.7 Analysis of Pdr5p mutants at residue S1360

4.7.1 Pdr5p expression

Under control conditions, none of the S1360 Pdr5p mutants affected yeast growth. Certain amino acid substitutions at residue S1360 had pronounced negative impacts on Pdr5p expression levels when compared to that of WT Pdr5p (Figure 3.14A). Since Pdr5p was identified as the main exporter of DON and 15A-DON, it was predicted that the Pdr5p mutants demonstrating reduced protein expression levels would be unable to maintain adequate mycotoxin export, thereby causing growth inhibitory effects on the yeast strains expressing any of these mutants. The mutants S1360A/F/T were expressed at levels similar to or slightly greater than that of WT Pdr5p which is in accordance with previous results (Egner et al., 2000).

4.7.2 DON and 15A-DON transport

An essential component of *F. graminearum* resistance involves the ability to effectively export the trichothecene mycotoxins produced by this fungal pathogen. During crop infection by a 15A-DON-producing strain of *F. graminearum* for example, both DON and 15A-DON typically accumulate within contaminated grain (Gilbert et al., 2010; Alexander et al., 2011). To be considered as candidates for mediating yeast resistance against a 15A-DON-producing *F. graminearum* strain such as the one used in this study, Pdr5p mutants were required to maintain efficient export of both DON and 15A-DON, comparable to that of WT Pdr5p. While none of the Pdr5p S1360 mutants were more effective than WT Pdr5p at exporting either DON or

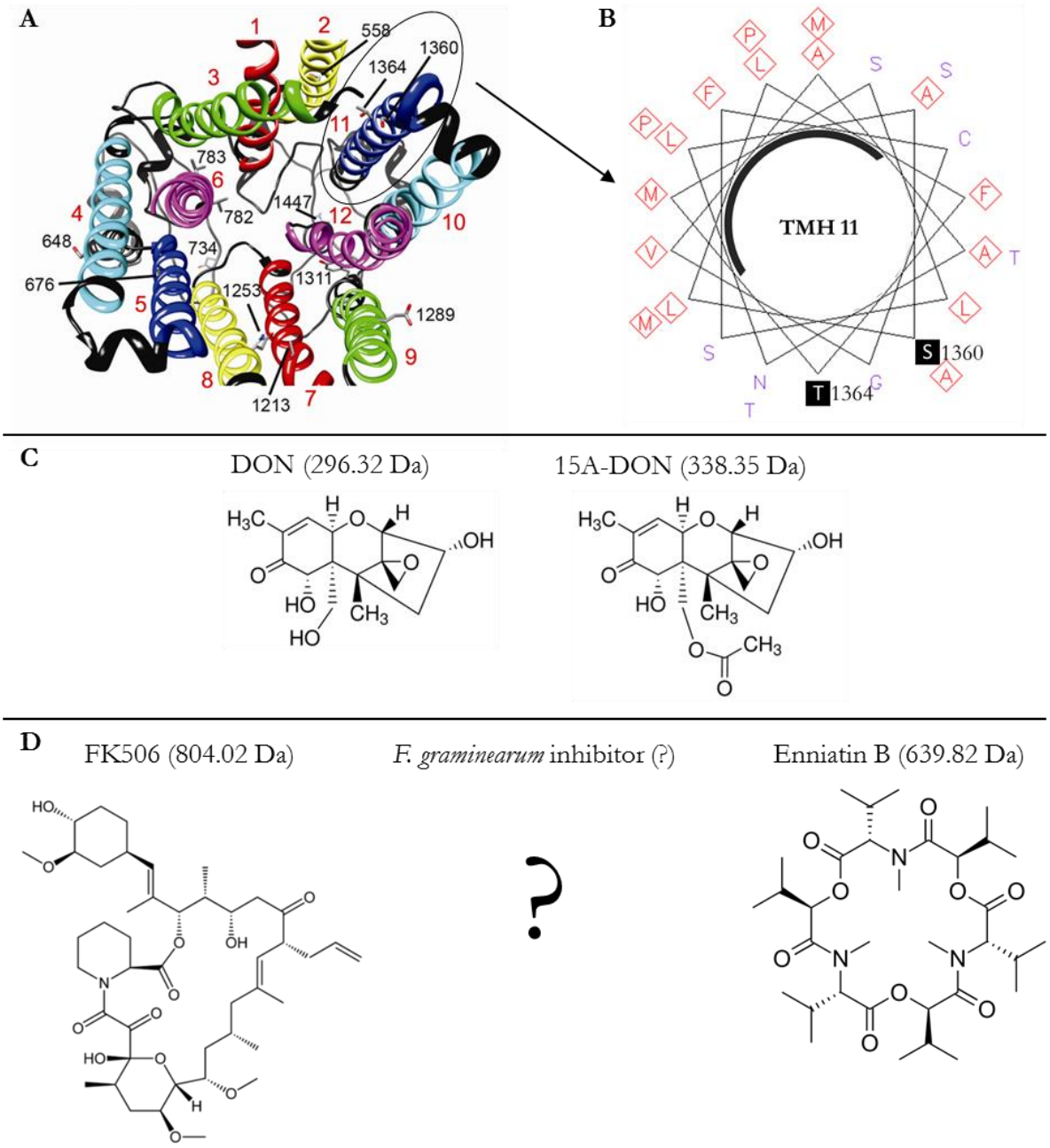

Figure 3.38 Overview of the localization of the S1360 and T1364 mutations within Pdr5p, as well as the mycotoxins and inhibitors used for analyses with the Pdr5p mutants that were generated. (**A**) Bottom view of the 12 TMHs of Pdr5p, arranged to form the substrate-binding pocket. Residues S1360 and T1364 are localized in TMH 11 (circled in black), and face the substrate-binding pocket (modified from Rutledge et al., 2011). (**B**) Helical wheel projection of TMH 11 [generated using the EMBOSS pepwheel program (Rice et al., 2000)]. The hydrophobic face of this helix is shown by the dark grey curve. Residues S1360 and T1364, which are localized on the hydrophilic face of this helix, are highlighted in black. (**C**) F. *graminearum* trichothecene mycotoxins DON and 15A-DON. (**D**) Pdr5p-specific inhibitors FK506 and enniatin B, and an unknown inhibitor (?) produced by *F. graminearum*.

15A-DON, all except for two were capable of maintaining a high level of export of both mycotoxins (Figure 3.16). The amino acid substitutions associated with each of these mutants therefore enabled Pdr5p to maintain affinity for its substrates DON and 15A-DON. Previous studies have shown that the S1360 residue is moderately conserved in other fungal ABC transporters related to Pdr5p (Saini et al., 2005; Kueppers et al., 2013), which could explain why Pdr5p can support such a wide variety of amino acids at this residue. Furthermore, despite the reduced protein expression levels of certain Pdr5p mutants, they all demonstrated a high level of DON and 15A-DON export. Pdr5p expression levels were not verified in yeast cells grown in the presence DON or 15A-DON; therefore, it is possible that their expression was induced or reduced by either mycotoxin. Egner et al. (2000) determined, however, that this was not the case for the WT or the S1360A/F/T mutants, which were expressed similarly in the absence or presence of the Pdr5p substrates that were tested.

It has previously been shown that the S1360A and S1360T mutants were capable of maintaining drug export at a level comparable to that of WT Pdr5p, while drug export efficiency of S1360F was negatively affected (Egner et al., 2000). In agreement, in this present study, S1360A and S1360T, but not S1360F, maintained a high level of DON and 15A-DON export. While the S1360F substitution had a significant negative effect on the ability of Pdr5p to transport both mycotoxins, this effect was not equal: the S1360F mutant retained a significantly higher ability to export 15A-DON, which was surprising since 15A-DON (~340 Da) is a slightly larger molecule than DON (~300 Da) (Figure 3.8). Increasing the size of a side chain within the substrate-binding pocket would, theoretically, cause greater obstruction to the passage of larger substrates. At residue S1360, the relatively small side chain of serine (S) was replaced by the much larger aromatic side chain of phenylalanine (F); therefore, DON, being the smaller molecule, should have been transported more easily than 15A-DON by the S1360F

mutant, assuming that the substitution had no impact on the conformation of the substrate-binding pocket. It has been proposed that substituting the hydrophilic amino acid S with the hydrophobic amino acid F at residue S1360, which is located on the hydrophilic side of the substrate-binding pocket, influences its hydrophobic-hydrophilic balance (Egner et al., 1998; Kueppers et al., 2013). In this present study, modification of this balance in the substrate-binding pocket possibly caused a significant decrease in the affinity of Pdr5p to DON. Additionally, the S1360W substitution caused a significant reduction of Pdr5p transport efficiency of both DON and 15A-DON. Like F, tryptophan (W) has a large hydrophobic aromatic side chain, which was likely obstructing the export of both mycotoxins. Furthermore, 15A-DON was transported less efficiently than DON by the S1360W mutant, which could be due to its slightly larger molecular size. Since protein expression levels of the S1360F and S1360W mutants were greater than that of WT Pdr5p, growth reduction of the yeast strains expressing each of these mutants in either mycotoxin was not likely the result of decreased protein expression. Interestingly, the S1360Y mutation did not have a drastic effect on the DON or 15A-DON transport efficiency of Pdr5p. Like F and W, tyrosine (Y) has a large hydrophobic aromatic side chain. Furthermore, the protein expression level of the S1360Y mutant was similar to that of WT Pdr5p.

4.7.3 DON and 15A-DON transport in the presence of FK506

As explained above, it was not possible to determine the level of insensitivity of the Pdr5p mutants to the FK506-like inhibitory compound produced by *F. graminearum* since it has yet to be identified and isolated. For this study, the Pdr5p-specific inhibitor FK506 was therefore used as the closest known substitute. On its own, FK506 (20 μg/mL, 24.8 μM) was non-toxic to yeast cells since it did not have a significant impact on yeast growth (Figure 3.19A).

Growth inhibitory effects observed in yeast, when either DON or 15A-DON was combined with FK506, were therefore a result of FK506-induced inhibition of mycotoxin transport. In agreement with results presented by Egner et al. (2000), S1360A and WT Pdr5p were hypersensitive to FK506 when it was combined with DON or 15A-DON, while S1360F and S1360T demonstrated insensitivity, by maintaining an intermediate level of export of either mycotoxin in its presence (Figure 3.20). The reason for the intermediate rather than high level of mycotoxin export in the presence of FK506 was different for both mutants: The mutant S1360T maintained DON and 15A-DON export as efficiently as WT Pdr5p; however, its ability to maintain this level of export was negatively affected by FK506. This was in contrast to S1360F, which was insensitive to FK506, but was unable to maintain mycotoxin export as efficiently as WT Pdr5p. Furthermore, relative to the growth inhibitory effects caused by DON or 15A-DON alone, the combination of DON and FK506 had slightly smaller growth inhibitory effects than the combination of 15A-DON and FK506 on yeast cells expressing S1360F (Figure 3.8). This was likely the result of the higher level of toxicity of 15A-DON on eukaryotic cells. In addition, FK506 was previously shown to have no effect on the expression of WT Pdr5p or the S1360A/F/S mutants (Egner et al. 2000). In total, six S1360 mutants demonstrated insensitivity to FK506 by maintaining a high level of DON and 15A-DON export in its presence. These mutants appear to have lost affinity for FK506 as a substrate. At a much higher concentration of 15A-DON, three of the six mutants, S1360H/N/Q, impressively prevented complete yeast growth inhibition in the presence of FK506 (Figure 3.21C). These mutants were therefore considered to be promising candidates for *F. graminearum* resistance.

4.7.4 Resistance to *F. graminearum* culture filtrate

Following yeast growth in *F. graminearum* culture filtrate (Figures 3.26 & 3.27), none of the S1360 mutants appeared to be candidates for *F. graminearum* resistance since they were unable to provide increased yeast resistance to the culture filtrate when compared to WT Pdr5p. This was particularly noticeable when S was substituted for amino acids with large hydrophobic side chains (S1360F/W/Y), as these substitutions had significantly negative effects on yeast resistance to the filtrate. The following elements must, however, be considered when interpreting these results: the exact composition of either culture filtrate was unknown and the *F. graminearum* FK506-like inhibitor has not yet been identified; therefore, it cannot be quantified, making it impossible to determine the concentration of inhibitor in the culture filtrate that was added to the yeast cells. Until this FK506-like inhibitor has been identified and fully characterized, its inhibitory mechanism cannot be fully understood.

4.7.5 DON and 15A-DON transport in the presence of enniatin B

Enniatin B is among the type A and type B enniatins produced by *F. avenaceum*, a *Fusarium* species associated with Fusarium head blight (FHB) of cereal grains in the Western Canadian Prairie provinces (Logrieco et al., 2002; Gräfenhan et al., 2013). In the context of this study, this fungal secondary metabolite was a biologically relevant Pdr5p-specific inhibitor. Mutants demonstrating insensitivity towards enniatin B could therefore be considered as potential candidates for *F. avenaceum* resistance. On its own, enniatin B (20 μg/mL, 31.3 μM) was non-toxic to yeast cells since it did not have a significant impact on yeast growth (Figure 3.31A). Like with FK506, growth inhibitory effects observed in yeast when either DON or 15A-DON was combined with enniatin B were therefore the result of mycotoxin transport inhibition caused by enniatin B. Compared to FK506, which completely inhibited DON and

15A-DON transport by WT Pdr5p, enniatin B was not as potent (Figure 3.32). This was not surprising, since the molecular structure and size of both inhibitors are substantially different (Figure 1.6). This was, however, contrary to results presented by Hiraga et al. (2005), which showed that enniatin B was a more potent inhibitor compared to FK506. It must be taken into consideration that the concentrations of FK506 and enniatin B used in the present study were about 5 times greater than the concentrations used by Hiraga et al. (2005), and the effects of these two inhibitory compounds on mycotoxin (DON and 15A-DON) transport, rather than drug (cerulenin and cycloheximide) transport was analyzed. In agreement with further results presented by Hiraga et al. (2005), compared to WT Pdr5p, S1360A was slightly more sensitive to enniatin B when it was combined with DON or 15A-DON, while S1360F was insensitive. Furthermore, at a much higher concentration of 15A-DON, mutants S1360D and S1360E were capable of preventing compete yeast growth inhibition in the presence of enniatin B (Figure 3.33C). Substitution of S with aspartic acid (D) or glutamic acid (E) at residue S1360 appears to cause the loss of Pdr5p affinity for enniatin B as a substrate. The S1360D and S1360E mutants were therefore considered to be promising candidates for *F. avenaceum* resistance.

4.7.6 Preliminary assays in *F. avenaceum* culture filtrate

Under natural conditions, cereal grains are rarely contaminated by a single *Fusarium* species (Wagacha et al., 2012). In fact, grain sample analysis regularly detects multiple mycotoxins, including DON, fumonisins, moniliformin (MON), nivalenol, and zearalenone, produced by different *Fusarium* species (Roscoe et al., 2008; Gräfenhan et al., 2013; Tittlemier et al., 2013). In the case of a coinfection by *F. graminearum* and *F. avenaceum*, two species that commonly infect cereal grains in the Canadian prairies, crops would be contaminated by toxins produced by both fungal pathogens. In a preliminary assay, yeast strains expressing the S1360D

and S1360E Pdr5p mutants were grown to determine the ability of either mutant to maintain 15A-DON export in the presence of *F. avenaceum* culture filtrate (Figure 3.37). The two culture filtrates used for these assays contained all compounds, including enniatins, produced and secreted by two *F. avenaceum* species grown individually in culture. Preliminary results are encouraging since both mutants enabled yeast growth in the presence of 15A-DON and *F. avenaceum* filtrate. Furthermore, protein expression levels of both mutants was lower than that of WT Pdr5p; therefore, these results were not caused by the expression of a greater number of transporters, assuming that protein expression was not induced by any of these compounds.

In summary, most single amino acid substitutions at residue S1360 did not drastically affect the ability of Pdr5p to export DON and 15A-DON. Although none of the S1360 mutants could be identified as candidates for resistance to *F. graminearum*, two mutants were identified as promising candidates for resistance to *F. avenaceum*. The ability of T1364 mutants to provide resistance yeast resistance to *F. graminearum* was also analyzed.

4.8 Analysis of Pdr5p mutants at residue T1364

4.8.1 Pdr5p expression

Under control conditions, none of the Pdr5p T1364 mutants affected yeast growth. Half of the amino acid substitutions at residue T1364, however, had pronounced negative impacts on Pdr5p expression levels when compared to that of WT Pdr5p (Figure 3.14B). The mutants T1364A/F/S were expressed at levels similar to or slightly greater than that of WT Pdr5p, which is in accordance with previous results (Egner et al., 2000).

4.8.2 DON and 15A-DON transport

Despite the fact that none of the Pdr5p T1364 mutants were more resistant than WT Pdr5p to either DON or 15A-DON, all but one maintained a high level of export of both mycotoxins (Figure 3.18). The amino acid substitutions associated with each of these mutants therefore enabled Pdr5p to maintain affinity for both DON and 15A-DON. Previous studies have shown that the T1364 residue is moderately conserved in other fungal ABC transporters related to Pdr5p (Saini et al., 2005; Kueppers et al., 2013), which could explain why Pdr5p can support such a large variety of amino acids at this residue. Apart from mutant T1364D, all other mutants at residue T1364 with reduced protein expression levels demonstrated a high level of DON and 15A-DON export.

The T1364D substitution had a significant negative effect on Pdr5p transport efficiency of both DON and 15A-DON. Furthermore, protein expression levels of the T1364D mutant were exceptionally low. Misfolded Pdr5p mutants have been shown to be retained in the endoplasmic reticulum (ER) for degradation, preventing their normal localization at the plasma membrane (PM). Yeast strains expressing Pdr5p mutants either with a C1427Y substitution or a L183P substitution were completely inhibited in the presence of all Pdr5p-specific cytotoxic compounds tested, including azole antifungals (Egner et al., 1998; de Thozée et al., 2007). Since Pdr5p was localized to the ER rather than to the PM in these mutants, they were incapable of exporting these toxins, which therefore inhibited yeast growth. All S1360 and T1364 mutants analyzed in this present study, however, maintained either an intermediate or high level of export of DON and 15A-DON, which highly suggests that they all localized to the PM of yeast cells, although this was not verified experimentally. The mislocalization of any of these mutants would have gone unnoticed in this study, since whole-cell preparations, rather than membrane

preparations were used for Western blot analysis of Pdr5p. In the case of T1364, the reason for intermediate rather than high level of mycotoxin export was possibly due to reduced affinity for both mycotoxins. A more likely explanation is that this mutation had a negative impact on Pdr5p expression and, as a result, the yeast strain expressing this mutant had an insufficient quantity of expressed Pdr5p to maintain a suitable level of DON or 15A-DON export to prevent yeast growth inhibition. The level of export remained the same for both mycotoxins, suggesting that the side chain of aspartic acid (D) did not obstruct the passage of either compound. Furthermore, as opposed to the results at residue S1360, the substitution of threonine (T) at residue T1364 for amino acids with large hydrophobic side chains (T1364F/W/Y) did not negatively affect the ability of Pdr5p to transport either DON or 15A-DON. This suggests that another factor, aside from amino acid size or shape, is important in determining substrate specificity by either S1360 or T1364. Single amino acid substitutions might be affecting the overall conformation of the substrate-binding pocket.

4.8.3 DON and 15A-DON transport in the presence of FK506

When the Pdr5p-specific inhibitor FK506 was combined with DON or 15A-DON, mycotoxin export by WT Pdr5p was inhibited; however, all T1364 mutants mediated insensitivity to FK506 (Figure 3.23). In agreement with results presented by Egner et al. (2000), the mutants T1364A/F/S demonstrated insensitivity towards FK506 by maintaining an intermediate level of export of DON or 15A-DON in its presence. Furthermore, similarly to S1360F, the mutant T1364D was insensitive to FK506 despite its lack of mycotoxin transport efficiency. These mutants were, however, not among the most insensitive. In fact, 10 of the T1364 mutants, of which six demonstrated reduced protein expression levels, maintained a high level of DON and 15A-DON export in the presence of FK506. These mutants appear to have

lost affinity for FK506 as a substrate. Remarkably, at a much higher concentration of 15A-DON, four of the ten mutants, T1364C/E/N/P, prevented complete yeast growth inhibition in the presence of FK506 (Figure 3.24). These mutants were therefore considered as potential candidates for *F. graminearum* resistance.

4.8.4 Resistance to *F. graminearum* culture filtrate

Similar to what was observed at residue S1360, none of the T1364 mutants appeared to be candidates for *F. graminearum* resistance since they were unable to provide increased yeast resistance to the culture filtrate when compared to WT (Figures 3.29 & 3.30). Additionally, substitution of threonine (T) at residue T1364 for amino acids with large hydrophobic side chains (T1364F/W/Y) had a negative effect on Pdr5p resistance to *F. graminearum* culture filtrate; however, this effect was not as pronounced when compared to the results observed at residue S1360.

4.8.5 DON and 15A-DON transport in the presence of enniatin B

When FK506 was combined with DON or 15A-DON, all T1364 mutants were insensitive when compared to WT Pdr5p. Despite this, most mutants demonstrated a level of enniatin B insensitivity similar to or less than WT Pdr5p when it was combined with either DON or 15A-DON (Figure 3.35). For those demonstrating a level of insensitivity greater than WT Pdr5p, they exhibited considerable yeast growth inhibition at a much higher concentration of 15A-DON (Figure 3.36C). This was in contrast to the mutants S1360D and S1360E, which were capable of preventing compete yeast growth inhibition under these conditions. None of the T1364 mutants were therefore considered as potential candidates for *F. avenaceum* resistance.

In summary, most single amino acid substitutions at residue T1364 did not drastically affect the ability of Pdr5p to export DON and 15A-DON. None of the T1364 mutants could be identified, however, as candidates for resistance to *F. graminearum* or *F. avenaceum*.

4.9 Conclusions and future directions

Using yeast as a model organism, this study has shown that the ABC transporter Pdr5p is the main exporter of the *F. graminearum* mycotoxin DON and its acetylated derivative 15A-DON. This study has also demonstrated that the majority of single amino acid substitutions at residue S1360 or T1364 of Pdr5p are capable of maintaining DON and 15A-DON export at a level similar to that of WT Pdr5p. Furthermore, certain of these mutants have the ability to mediate insensitivity to the Pdr5p-specific inhibitors FK506 and enniatin B while maintaining substrate specificity for DON and 15A-DON. Although none of the mutants could be identified as candidates for resistance to *F. graminearum*, preliminary studies have identified mutants S1360D and S1360E as candidates for resistance to *F. avenaceum*. While assays with these two mutants will need to be repeated, this is a promising area for future research.

Aside from T1364D, all other Pdr5p mutants that demonstrated reduced protein expression levels were capable of maintaining a level of DON and 15A-DON export similar to that of WT Pdr5p. By increasing the expression of any of these mutants, it might be possible to improve their mycotoxin export efficiency. The yeast strains AD1-3, AD1-7, AD1-8, and R-1 all contain a *PDR1-3* mutation, which causes the overexpression of genes controlled by the pleiotropic drug resistance gene *PDR1* (Sauna et al., 2008; reviewed in Lis et al., 2012). The *PDR5* gene, which is controlled by *PDR1*, is knocked-out from these four strains, therefore, the *PDR5* gene variants corresponding to the Pdr5p mutants with reduced protein expression levels could be individually overexpressed in any of these strains to determine whether DON and

15A-DON export could be increased to a level greater than that allowed by WT Pdr5p. This would be particularly interesting to perform with T1364D. While this was the only mutant that demonstrated both reduced protein expression and decreased DON and 15A-DON export, it showed complete insensitivity to FK506 and enniatin B.

Once the inhibitory compound produced by *F. graminearum* has been identified, fully characterized, and isolated, it will then be possible to verify whether any of the mutants analyzed in this study are insensitive to known concentrations of this inhibitor. In addition to residues S1360 and T1364, molecular modeling and mutagenesis studies suggest that TMD2 of Pdr5p contains at least five other residues involved in substrate recognition. If all the mutants from both residues analyzed in this study are unable to mediate insensitivity to the *F. graminearum* inhibitor, any of the other five residues could then also be mutagenized to analyze their ability to mediate inhibitor insensitivity and DON and 15A-DON export.

Since crop infections are rarely caused by a single *Fusarium* species, it would be useful to identify Pdr5p mutants that could be considered as candidates for resistance to other *Fusarium* species. Furthermore, it might be possible to generate a Pdr5p mutant with substitutions at multiple key residues, enabling resistance to multiple species of *Fusarium*. In this study, preliminary results demonstrated that the S1360D and S1360E mutants were capable of mediating yeast resistance to *F. avenaceum* culture filtrates. While *F. avenaceum* does not produce DON or 15A-DON, it produces the mycotoxin MON (Gräfenhan et al., 2013). The mutants S1360D and S1360E will therefore need to be analyzed to determine their ability to export MON, compared to WT Pdr5p. Additionally, it would be of interest to verify whether Pdr5p expression of either of these mutants is induced or reduced in the presence of toxins or inhibitory compounds.

Ultimately, knowledge gained through the use of yeast could then be extended to plants, in an attempt to improve their ability to export mycotoxins, while mediating insensitivity to inhibitory compounds produced by *Fusarium* species. Muhitch et al. (2000) demonstrated that transgenic tobacco seedlings expressing *S. cerevisiae* Pdr5p displayed a significant increase in resistance to the trichothecene mycotoxin DAS. A similar approach could be used with interesting Pdr5p mutants, by expressing them in the model plant *Arabidopsis thaliana* and determining whether they can mediate plant resistance to *F. graminearum* or other *Fusarium* species of interest.

Another possibility would be to analyze Pdr5p-like plasma membrane transporters found in plants. Since these transporters have not yet been extensively studied, it is uncertain whether any of them are involved in the export of mycotoxins. In *A. thaliana* and *Zea mays* respectively, 15 and 17 Pdr5p-like proteins have been identified (van den Brûle & Smart, 2002; Pang et al., 2013). An important point worth noting is that to ensure effective plant resistance against *Fusarium* species, Pdr5p mutants would need to be expressed in plant tissues that are targets for infection. In *Z. mays*, one of these Pdr5p-like transporters is mainly localized in the cob, while another is mainly localized in the silks, two locations that are targeted during the infection of this crop plant by *F. graminearum*.

Considering the economic repercussions and health risks associated with the contamination of cereal grains by DON and its acetylated derivatives, it is vital to identify effective resistance mechanisms against them. The findings of this study strongly suggest that the transporter Pdr5p could be engineered to mediate yeast resistance to *F. graminearum* as well as other *Fusarium* species. If this knowledge could then be applied to crop plants, it could have important implications in ensuring the safety of the food and feed supply chains.

REFERENCES

Alexander NJ, Proctor RH, McCormick SP. 2009. Genes, gene clusters, and biosynthesis of trichothecenes and fumonisins in *Fusarium*. Toxin Reviews 28:198-215.

Alexander NJ, McCormick SP, Waalwijk C, van der Lee T, Proctor H. 2011. The genetic basis for 3-ADON and 15-ADON trichothecene chemotypes in *Fusarium*. Fungal Genetics and Biology 48:485-495.

Aller S.G., Yu J., Ward A., Weng Y., Chittaboina S., Zhuo R, Harrell P.M., Trinh Y.T., Zhang Q., Urbatsch I.L., Chang G. 2009. Structure of P-glycoprotein reveals a molecular basis for poly-specific drug binding. Science 323:1718-1722.

Amberg D.C., Burke D.J., Strathern J.N. 2005. High-efficiency transformation of yeast in: *Methods in Yeast Genetics: A Cold Spring Harbor Laboratory Course Manual*. Cold Spring Harbor Laboratory Press, Cold Spring Harbor, NY.

Ananthaswamy N., Rutledge R., Sauna Z.E., Ambudkar S.V., Dine E., Nelson E., Xia D., Golin J. 2010. The signaling interface of the yeast multidrug transporter Pdr5 adopts a cis conformation, and there are functional overlap and equivalence of the deviant and canonical Q-loop residues. Biochemistry 49:4440-4449.

Arunachalam C., Doohan F.M. 2013. Trichothecene toxicity in eukaryotes: cellular and molecular mechanisms in plants and animals. Toxicology Letters 217:149-158.

Balzi E., Wang M., Leterme S., Van Dyck L., Goffeau A. 1994. PDR5, a novel yeast multidrug resistance conferring transporter controlled by the transcription regulator PDR1. The Journal of Biological Chemistry 269:2206-2214.

Bartosiewicz D., Krasowska A. 2009. Inhibitors of ABC transporters and biophysical methods to study their activity. Zeitschrift fur Naturforschung - Section C Journal of Biosciences 64:454-458.

Bauer B.E., Wolfger H., Kuchler K. 1999. Inventory and function of yeast ABC proteins: about sex, stress, pleiotropic drug and heavy metal resistance. Biochimica et Biophysica Acta 1461:217-236.

Beyer M., Verreet J.-A., Ragab W.S.M. 2005. Effect of relative humidity on germination of ascospores and macroconidia of *Gibberella zeae* and deoxynivalenol production. International Journal of Food Microbiology 98:233-240.

Biemans-Oldehinkel E., Doeven M.K., Poolman B. 2006. ABC transporter architecture and regulatory roles of accessory domains. FEBS Letters 580:1023-1035.

Brown D.W., Dyer R.B., McCormick S.P., Kendra D.F., Plattner R.D. 2004. Functional demarcation of the *Fusarium* core trichothecene gene cluster. Fungal Genetics and Biology 41:454-462.

Bullerman L.B., Bianchini A. 2007. Stability of mycotoxins during food processing. International Journal of Food Microbiology 119:140-146.

Cannon R.D., Lamping E., Holmes A.R., Niimi K., Baret P.V., Keniya M.V., Tanabe K., Niimi M., Goffeau A., Monk B.C. 2009. Efflux-mediated antifungal drug resistance. Clinical Microbiology Reviews 22:291-321.

Coppock R.W., Jacobsen B.J. 2009. Mycotoxins in animal and human patients. Toxicology and Industrial Health 25:637-655.

Cordon-Cardo C., O'Brien J.P., Boccia J., Casals D., Bertino J.R., Melamed M.R. 1990. Expression of the multidrug resistance gene product (*P*-glycoprotein) in human normal and tumor tissues. The Journal of Histochemistry and Cytochemistry 38:1277-1287.

Davidson A.L., Dassa E., Orelle C., Chen J. 2008. Structure, function, and evolution of bacterial ATP-binding cassette systems. Microbiology and Molecular Biology Reviews 72:317-364.

Dawson R.J.P. Locher K.P. 2006. Structure of a bacterial multidrug ABC transporter. Nature 443:180-185.

Dean M., Rzhetsky A., Allikmets R. 2001. The human ATP-binding cassette (ABC) transporter superfamily. Genome Research 11:1156-1166.

de Thozée C.P., Cronin S., Goj A., Golin J., Ghislain M. 2007. Subcellular trafficking of the yeast plasma membrane ABC transporter, Pdr5, is impaired by a mutation in the N-terminal nucleotide-binding fold. Molecular Microbiology 63:811-825.

Dolghih E., Bryant C., Renslo A.R., Jacobson M.P. 2011. Predicting binding to P-glycoprotein by flexible receptor docking. PLoS Computational Biology 7:e1002083.

Downes M.T., Mehla J., Ananthaswamy N., Wakschlag A., Lamonde M., Dine E., Ambudkar S.V., Golin J. 2013. The transmission interface of the *Saccharomyces cerevisiae* multidrug transporter Pdr5: Val-656 located in intracellular loop 2 plays a major role in drug resistance. Antimicrobial Agents and Chemotherapy 57:1025-1034.

Doyle P.J., Saeed H., Hermans A., Gleddie S.C., Hussack G., Arbabi-Ghahroudi M., Seguin C., Savard M.E., MacKenzie C.R., Hall J.C. 2009. Intracellular expression of a single domain antibody reduces cytotoxicity of 15-acetyldeoxynivalenol in yeast. The Journal of Biological Chemistry 284:35029-35039.

Dreyer I., Horeau C., Lemaillet G., Zimmermann S., Bush D.R., Rodríguez-Navarro A., Schachtman D.P., Spalding E.P., Sentenac H., and Gaber R.F. 1999. Identification and characterization of plant transporters using heterologous expression systems. Journal of Experimental Botany 50:1073-1087.

Egner R., Rosenthal F.E., Kralli A., Sanglard D., and Kuchler K. 1998. Genetic separation of FK506 susceptibility and drug transport in the yeast Pdr5 ATP-binding cassette multidrug resistance transporter. Molecular Biology of the Cell 9:523-543.

Egner R., Bauer B., Kuchler K. 2000. The transmembrane domain 10 of the yeast Pdr5p ABC antifungal efflux pump determines both substrate specificity and inhibitor susceptibility. Molecular Microbiology 35:1255-1263.

Eitinger T., Rodionov D.A., Grote M., Schneider E. 2011. Canonical and ECF-type ATP-binding cassette importers in prokaryotes: diversity in modular organization and cellular functions. FEMS Microbiology Reviews 35:3-67.

Ernst R., Kueppers P., Klein C.M., Schwarzmueller T., Kuchler K., Schmitt L. 2008. A mutation of the H-loop selectively affects rhodamine transport by the yeast multidrug ABC transporter Pdr5. Proceedings of the National Academy of Sciences 105 5069-5074.

Fromm M.F. 2004. Importance of P-glycoprotein at blood–tissue barriers. Trends in Pharmacological Sciences 25:423-429.

Geisler M., Blakeslee J.J., Bouchard R., Lee O.R., Vincenzetti V., Bandyopadhyay A., Titapiwatanakun B., Peer W.A., Bailly A., Richards E.L., Ejendal K.F.L., Smith A.P., Baroux C., Grossniklaus U., Müller A., Hrycyna C.A., Dudler R., Murphy A.S., Martinoia E. 2005. Cellular efflux of auxin catalyzed by the Arabidopsis MDR/PGP transporter AtPGP1. The Plant Journal 44:179-194.

George A.M., Jones P.M. 2012. Perspectives on the structure-function of ABC transporters: the switch and constant contact models. Progress in Biophysics and Molecular Biology 109 95-107.

George A.M., Jones P.M. 2013. An asymmetric post-hydrolysis state of the ABC transporter ATPase dimer. PLoS One 6:e59854.

Ghaemmaghami S., Huh W.-K., Bower K., Howson R.W., Belle A., Dephoure N., O'Shea E.K., and Weissman J.S. 2003. Global analysis of protein expression in yeast. Nature 425:737-741.

Giaever G., Chu A.M., Ni L., Connelly C., Riles L., Véronneau S., Dow S., Lucau-Danila A., Anderson K., André B., Arkin A.P., Astromoff A., El Bakkoury M., Bangham R., Benito R., Brachat S., Campanaro S., Curtiss M., Davis K., Deutschbauer A., Entian K.-D., Flaherty P., Foury F., Garfinkel D.J., Gerstein M., Gotte D., Güldener U., Hegemann J.H., Hempel S., Herman Z., Jaramillo D.F., Kelly D.E., Kelly S.L., Kötter P., LaBonte D., Lamb D.C., Lan N., Liang H., Liao H., Liu L., Luo C., Lussier M., Mao R., Menard P., Ooi S.L., Revuelta J.R., Roberts C.J., Rose M., Ross-Macdonald P., Scherens B., Schimmack G., Shafer B., Shoemaker D.D., Sookhai-Mahadeo S., Storms R.K., Strathern J.N., Valle G., Voet M., Volckaert G., Wang C.-y., Ward T.R., Wilhelmy J., Winzeler E.A., Yang Y., Yen G., Youngman E., Yu K., Bussey H., Boeke J.D., Snyder M., Philippsen P., Davis R.W., Johnston M. 2002. Functional profiling of the *Saccharomyces cerevisiae* genome. Nature 418:387-391.

Gilbert J., Clear R.M., Ward T.J., Gaba D., Tekauz A., Turkington T.K., Woods S.M., Nowicki T., O'Donnell K. 2010. Relative aggressiveness and production of 3- or 15-acetyl deoxynivalenol and deoxynivalenol by *Fusarium graminearum* in spring wheat. Canadian Journal of Plant Pathology 32:146-152.

Gilbert J., Haber S. 2013. Overview of some recent research developments in Fusarium head blight of wheat. Canadian Journal of Plant Pathology 35:149-174.

Gillet J.P., Efferth T., Remacle J. 2007. Chemotherapy-induced resistance by ATP-binding cassette transporter genes. Biochimica et Biophysica Acta 1775:237-262.

Goffeau A., Barrell B.G., Bussey H., Davis R.W., Dujon B., Feldmann H., Galibert F., Hoheisel J.D., Jacq C., Johnston M., Louis E.J., Mewes H.W., Murakami Y., Philippsen P., Tettelin H., Oliver S.G. 1996. Life with 6000 genes. Science 274:546-567.

Goswami R.S., Kistler H.C. 2004. Heading for disaster: *Fusarium graminearum* on cereal crops. Molecular Plant Pathology 5:515-525.

Gottesman M.M., Fojo T., Bates S.E. 2002. Multidrug resistance in cancer: role of ATP-dependant transporters. Nature Reviews Cancer 2:48-58.

Gottschling Lab. High Efficiency Yeast Plasmid Rescue [online]. http://labs.fhcrc.org /gottschling/Yeast%20Protocols/yplas.html [accessed March 1, 2013].

Gräfenhan T., Patrick S.K., Roscoe M., Trelka R., Gaba D., Chan J.M., McKendry T., Clear R.M., Tittlemier S.A. 2013. *Fusarium* damage in cereal grains from Western Canada. 1. Phylogenetic analysis of moniliformin-producing Fusarium species and their natural occurrence in mycotoxin-contaminated wheat, oats, and rye. Journal of Agricultural and Food Chemistry 61:5425-5437.

Gupta R.P., Kueppers P., Schmitt L., Ernst R. 2011. The multidrug transporter Pdr5: a molecular diode? Biological Chemistry 393:53-60.

Harris L.J. 1999. Possible role of trichothecene mycotoxins in virulence of *Fusarium graminearum* on maize. Plant Disease 83:954-960.

Hawkey P.M., Jones A.M. 2009. The changing epidemiology of disease. Journal of Antimicrobial Chemotherapy. 64:i3-i10.

Higgins C.F. 1992. ABC transporters: from microorganisms to man. Annual Review of Cell Biology 8:67-113.

Higgins C.F. 2001. ABC transporters: physiology, structure and mechanism – an overview. Research in Microbiology 152:205-210.

Higgins C.F. 2007. Multiple molecular mechanisms for multidrug resistance transporters. Nature 446:749-757.

Hiraga K., Yamamoto S., Fukuda H., Hamanaka N., Oda K. 2005. Enniatin has a new function as an inhibitor of Pdr5p, one of the ABC transporters in *Saccharomyces cerevisiae*. Biochemical and Biophysical Research Communications 328:1119-1125.

Hohl M., Briand C., Grütter M.G., Seeger M.A. 2012. Crystal structure of a heterodimeric ABC transporter in its inward-facing conformation. Nature Structural & Molecular Biology 19:395-402.

Hollenstein K., Dawson R.J.P., Locher K.P. 2007. Structure and mechanism of ABC transporter proteins. Current Opinion in Structural Biology 17:412-418.

Hyde S.C., Emsley P., Hartshorn M.J., Mimmack M.M., Gileadi U., Pearce S.R., Gallagher M.P., Gill D.R., Hubbard R.E., Higgins C.F. 1990. Structural model of ATP-binding proteins associated with cystic fibrosis, multidrug resistance and bacterial transport.346:362-365.

Ilgen P., Hadeler B., Maier F.J., Schäfer W. 2009. Developing kernel and rachis node induce the trichothecene pathway of *Fusarium graminearum* during wheat head infection. Molecular Plant-Microbe Interactions 22:899-908.

Jansen C., von Wettstein D., Schäfer W., Kogel K.-H., Felk., Maier F.J. 2005. Infection patterns in barley and wheat spikes inoculated with wild-type and trichodiene synthase gene disrupted *Fusarium graminearum*. Proceedings of the National Academy of Sciences 102:16892-16897.

Jardetzky O. 1966. Simple allosteric model for membrane pumps. Nature 211:969-970.

Kartner N., Riordan J.R., Ling V. 1983. Cell surface P-glycoprotein associated with multidrug resistance in mammalian cell lines. Science 221:1285-1288.

Kimura M., Tokai T., Takahashi-Ando N., Ohsato S., Fujimura M. 2007. Molecular and genetic studies of *Fusarium* trichothecene biosynthesis: pathways, genes, and evolution. Bioscience, Biotechnology, and Biochemistry 71:2105-2123.

Knazek R.A., Rizzo W.B., Schulman J.D., Dave J.R. 1983. Membrane microviscosity is increased in the erythrocytes of patients with adrenoleukodystrophy and adrenomyeloneuropathy. The Journal of Clinical Investigation: 72:245-248.

Knöller A.S., Murphy A.S. 2011. ABC transporters and their function at the plasma membrane. The Plant Plasma Membrane, Plant Cell Monographs 19:353-377.

Kolaczkowska A., Goffeau A. 1999. Regulation of pleiotropic drug resistance in yeast. Drug Resistance Updates 2:403-414

Kolaczkowska A., Kolaczkowski M., Goffeau A., Moye-Rowley W.S. 2008. Compensatory activation of the multidrug transporters Pdr5p, Snq2p, and Yor1p by Pdr1p in *Saccharomyces cerevisiae*. FEBS Letters 582:977-983.

Kolaczkowski M., van der Rest M., Cybularz-Kolaczkowska A., Soumillion J.P., Konings W.N., Goffeau A. 1996. Anticancer drugs, ionophoric peptides, and steroids as substrates of the yeast multidrug transporter Pdr5p. The Journal of Biological Chemistry 271:31543-31548.

Kolaczkowski M., Kolaczkowska A., Luczynski J., Witek S., Goffeau A. 1998. *In vivo* characterization of the drug resistance profile of the major ABC transporters and other components of the yeast pleiotropic drug resistance network. Microbial Drug Resistance 4:143-158.

Kovalchuk A., Driessen A.J.M. 2010. Phylogenetic analysis of fungal ABC transporters. BMC Genomics 11:177.

Kueppers P., Gupta R.P., Stindt J., Smits S.H.J., Schmitt L. 2013. Functional impact of a single mutation within the transmembrane domain of the multidrug ABC transporter Pdr5. Biochemistry 52:2184-2195.

Leslie E.M., Deeley R.G., Cole S.P.C. 2005. Multidrug resistance proteins: role of P-glycoprotein, MRP1, MRP2, and BCRP (ABCG2) in tissue defense. Toxicology and Applied Pharmacology 204:216-237.

Licht A., Schneider E. 2011. ATP binding cassette systems: structures, mechanisms, and functions. Central European Journal of Biology 6:785-801.

Lis P., Zarzycki M., Ko Y.H., Casal M., Pedersen P.L., Goffeau A., Ulaszewski S. 2012. Transport and cytotoxicity of the anticancer drug 3-bromopyruvate in the yeast *Saccharomyces cerevisiae*. Journal of Bioenergetics and Biomembranes 44:155-161.

Logrieco A., Rizzo A., Ferracane R., Ritieni A. 2002. Occurrence of beauvericin and enniatins in wheat affected by *Fusarium avenaceum* head blight. Applied and Environmental Microbiology 68:82-85.

Longley D.B., Johnston P.G. 2005. Molecular mechanisms of drug resistance. Journal of Pathology 205:275-292.

Loo T.W., Bartlett C., Clarke D.M. 2002. The"LSGGQ" motif in each nucleotide-binding domain of human P-glycoprotein is adjacent to the opposing Walker A sequence. The Journal of Biological Chemistry 277:41303-41306.

Lõoke M., Kristjuhan K., Kristjuhan A. 2011. Extraction of genomic DNA from yeasts for PCR-based applications. BioTechniques 50:325-328.

Mamnum Y.M., Schüller C., Kuchler K. 2004. Expression regulation of the yeast *PDR5* ATP-binding cassette (ABC) transporter suggests a role in cellular detoxification during the exponential growth phase. FEBS Letters 559:111-117.

Marcil M., Brooks-Wilson A., Clee S.M., Roomp K., Zhang L.-H., Yu L., Collins J.A., van Dam M., Molhuizen H.O.F., Loubster O., Ouellette B.F.F., Sensen C.W., Fichter K., Mott S., Denis M., Boucher B., Pimstone S., Genest Jr. J., Kastelein J.J.P., Hayden M.R. 1999. Mutations in the *ABC1* gene in familial HDL deficiency with defective cholesterol efflux. The Lancet 354:1341-1346.

McMullen M., Jones R., Gallenberg D. 1997. Scab of wheat and barley: a re-emerging disease of devastating impact. Plant Disease 81:1340-1348.

Mesterházy Á., Lemmens M., Reid L.M. 2012. Breeding for resistance to ear rots caused by *Fusarium* spp. in maize – A review. Plant Breeding 131:1-19.

Mitterbauer R., Adam G. 2002. *Saccharomyces cerevisiae* and *Arabidopsis thaliana*: useful model systems for the identification of molecular mechanisms involved in resistance of plants to toxins. European Journal of Plant Pathology 108:699-703.

Morschhäuser J. 2010. Regulation of multidrug resistance in pathogenic fungi. Fungal Genetics and Biology 47:94-106.

Muhitch M.J., McCormick S.P., Alexander N.J., Hohn T.M. 2000. Transgenic expression of the *TRI*101 or *PDR*5 gene increases resistance of tobacco to the phytotoxic effects of the trichothecene 4,15-diacetoxyscirpenol. Plant Science 157:201-207.

Multani D.S., Briggs S.P., Chamberlin M.A, Blakeslee J.J., Murphy A.S., Johal G.S. 2003. Loss of an MDR transporter in compact stalks of maize *br2* and sorghum *dw3* mutants. Science 302:81-84.

Munkvold G.P. 2003. Epidemiology of *Fusarium* diseases and their mycotoxins in maize ears. European Journal of Plant Pathology 109:705-713.

Nagy P.D. 2008. Yeast as a model host to explore plant virus-host interactions. Annual Review of Phytopathology 46:217-242.

Niu W., Li Z., Zhan W., Iyer V.R., Marcotte E.M. 2008. Mechanisms of cell cycle control revealed by a systematic and quantitative overexpression screen in *S. cerevisiae*. PLoS Genetics 4:e1000120.

Ouellette M., Légaré D., Papadopoulou B. 2001. Multidrug resistance and ABC transporters in parasitic protozoa. Journal of Molecular Microbiology and Biotechnology 3:201-206.

Pang K., Li Y., Liu M., Meng Z., Yu Y. 2013. Inventory and general analysis of the ATP-binding cassette (ABC) gene superfamily in maize (*Zea mays* L.). Gene 526:411-428.

Pestka J.J., Smolinski A.T. 2005. Deoxynivalenol: toxicity and potential effects on humans. Journal of Toxicology and Environmental Health 8:39-69.

Pronk M.E.J., Schothorst R.C., and van Egmond H.P. 2002. Toxicology and occurrence of nivalenol, fusarenon X, diacetoxyscirpenol, neosolaniol and 3- and 15-acetyldeoxynivalenol: a review of six trichothecenes [online]. RIVM Report 388802024/2002 [accessed November 6, 2011].

Quinton P.M. 1999. Physiological basis of cystic fibrosis: a historical perspective. Physiological Reviews 79:S3-S22.

Rath A., Cunningham F., Deber C.M. 2013. Acrylamide concentration determines the direction and magnitude of helical membrane protein gel shifts. Proceedings of the National Academy of Sciences 110:15668-15673.

Rea P.A. 1999. MRP subfamily ABC transporters from plants and yeast. Journal of Experimental Botany 50:895-913.

Rees D.C., Johnson E., Lewinson O. 2009. ABC transporters: the power to change. Nature Reviews 10:218-227.

Reid L.M., Mather D.E., Hamilton R.I. 1996. Distribution of deoxynivalenol in *Fusarium graminearum*-infected maize ears. Phytopathology 86:110-114.

Reid L.M., Sinha R.C. 1998. Maize maturity and the development of gibberella ear rot symptoms and deoxynivalenol after inoculation. European Journal of Plant Pathology 104:147-154.

Rice P., Longden I., Bleasby A. 2000. EMBOSS: The European Molecular Biology Open Software Suite. Trends in Genetics 16: 276-277.

Roscoe V., Lombaert G.A., Huzel V., Neumann G., Melietio J., Kitchen D., Kotello S., Krakalovich T., Trelka R., Scott P.M. 2008. Mycotoxins in breakfast cereals from the Canadian retail market: a 3-year survey. Food Additives and Contaminants 25:347-355.

Rutledge R.M., Esser L., Ma J., Xia D. 2011. Toward understanding the mechanism of action of the yeast multidrug resistance transporter Pdr5p: a molecular modeling study. Journal of Structural Biology 173:333-344.

Saccharomyces Genome Database (SGD). Saccharomyces Genome Database. [online]. http://www.yeastgenome.org/. [accessed February 15, 2012].

Saini P., Prasad T., Gaur N.A., Shukla S., Jha S., Komath S.S., Khan L.A., Haq Q.M.R., Prasad R. 2005. Alanine scanning of transmembrane helix 11 of Cdr1p ABC antifungal efflux pump of *Candida albicans*: identification of amino acid residues critical for drug efflux. Journal of Antimicrobial Chemotherapy 56:77-86.

Sauna Z.E., Bohn S.S., Rutledge R., Dougherty M.P., Cronin S., May L., Xia D., Ambudkar S.V., Golin J. 2008. Mutations define cross-talk between the N-terminal nucleotide-binding domain and transmembrane helix-2 of the yeast multidrug transporter Pdr5. Journal of Biological Chemistry 283:35010-35022.

Schaafsma A.W. 1999. 1996 epidemic in winter wheat – aftermath. pp. 31-32 in: Proceedings of the 1999 Canadian Workshop on Fusarium Head Blight.

Schaafsma A.W., Hooker D.C., Baute T.S., Illincic-Tamburic L. 2002. Effect of *Bt*-corn hybrids on deoxynivalenol content in grain at harvest. Plant Disease 86:1123-1126.

Scheffer G.L., Pijnenborg A.C.L.M. Smit E.F., Müller M., Postma D.S., Timens W., van der Valk P., de Vries E.G.E., Scheper R.J. 2002. Multidrug resistance related molecules in human and murine lung. Journal of Clinical Pathology 55:332-339.

Schmitt L., Benabdelhak H., Blight M.A., Holland I.B., Stubbs M.T. 2003. Crystal structure of the nucleotide-binding domain of the ABC-transporter haemolysin B: identification of a variable region within ABC helical domains. Journal of Molecular Biology 330:333-342.

Smith P.C., Karpowich N., Millen L., Moody J.E., Rosen J., Thomas P.J., Hunt J.F. 2002. ATP binding to the motor domain from an ABC transporter drives formation of a nucleotide sandwich dimer. Molecular Cell 10:139-149.

Sobrova P., Adam V., Vasatkova A., Beklova M., Zeman L., Kizek R. 2010. Deoxynivalenol and its toxicity. Interdisciplinary toxicology 3:94-99.

Sun H., Molday R.S., Nathans J. 1999. Retinal stimulates ATP hydrolysis by purified and reconstituted ABCR, the photoreceptor-specific ATP-binding cassette transporter responsible for Stargardt disease. The Journal of Biological Chemistry 274:8269-8281.

Suter B., Auerbach D., Stagljar I. 2006. Yeast-based functional genomics and proteomics technologies: the first 15 years and beyond. BioTechniques 40:625-644.

Suzuki T., Iwahashi Y. 2012. Comprehensive gene expression analysis of type B trichothecenes. Journal of Agricultural and Food Chemistry 60:9519-9527.

Szewczak A., Ziomkiewickz I., Jasiński M. 2011. Hiring cell gatekeepers – ABC transporters in plant biotechnology. BioTechnologica 92:132-139.

Taglicht D., Michaelis S. 1998. *Saccharomyces cerevisiae* ABC proteins and their relevance to human health and disease. Methods in Enzymology 292:130-162.

Thiebault F., Tsuruo T., Hamada H., Gottesman M.M., Pastan I., Willingham M.C. 1987. Cellular localization of the multidrug-resistance gene product P-glycoprotein in normal human tissues. Proceedings of the National Academy of Sciences 84:7735-7738.

Tittlemier S.A., Gaba D., Chan J.M. 2013. Monitoring of *Fusarium* trichothecenes in Canadian cereal grain shipments from 2010 to 2012. Journal of Agricultural and Food Chemistry 61:7412-7418.

Trail F. 2009. For blighted waves of grain: *Fusarium graminearum* in the postgenomics era. Plant Physiology 149:103-110.

Tutulan-Cunita A.C., Mikoshi M., Mizunuma M., Hirata D., Miyakawa T. 2005. Mutational analysis of the yeast multidrug resistance ABC transporter Pdr5p with altered drug specificity. Genes to Cells 10:409-420.

UniProt. Protein Knowledgebase (UniProtKB). [online]. http://www.uniprot.org/uniprot/. [accessed February 15, 2012].

van den Brûle S., Smart C.C. 2002. The plant PDR family of ABC transporters. Planta 216:95-106.

Vasiliou V., Vasiliou K., Nebert D.W. 2009. Human ATP-binding cassette (ABC) transporter family. Human Genomics 3:281-290.

Verrier P.J., Bird D., Burla B., Dassa E., Forestier C., Geisler M., Klein M., Kolukiasoglu Ü., Lee Y., Martinoia E., Murphy A., Rea P.A., Samuels L., Schulz B., Spalding E.P., Yazaki K., Theodoulou F.L. 2008. Plant ABC proteins – A unified nomenclature and updated inventory. Trends in Plant Science 13:151-159.

Videmann B., Tep J., Cavret S., Lecoeur S. 2007. Epithelial transport of deoxynivalenol: involvement of human P-glycoprotein (ABCB1) and multidrug resistance-associated protein 2 (ABCC2). Food and Chemical Toxicology 45:1938-1947.

von der Haar T. 2007. Optimized protein extraction for quantitative proteomics of yeasts. PLoS One 2:e1078.

Wagacha J.M., Oerke E.C., Dehne H.W., Steiner U. 2012. Interactions of Fusarium species during prepenetration development. Fungal Biology 116:836-847.

Ward A., Reyes C.L., Yu J., Roth C.B., Chang G. 2007. Flexibility in the ABC transporter MsbA: alternating access with a twist. Proceedings of the National Academy of Sciences 104:19005-19010.

Windsor B., Roux S.J., Lloyd A. 2003. Multiherbicide tolerance conferred by AtPgp1 and apyrase overexpression in *Arabidopsis thaliana*. Nature Biotechnology 21:428-433.

Winzeler E.A., Shoemaker D.D., Astromoff A., Liang H., Anderson K., Andre B., Bangham R., Benito R., Boeke J.D., Bussey H., Chu A.M., Connelly C., Davis K., Dietrich F., Whelen Dow S., El Bakkoury M., Foury F., Friend S.H., Gentalen E., Giaever G., Hegemann J.H., Jones T., Laub M., Liao H., Liebundguth N., Lockhart D.J., Lucau-Danila A., Lussier M., M'Rabet N., Menard P., Mittmann M., Pai C., Rebischung C., Revuelta J.L., Riles L., Roberts C.J., Ross-MacDonald P., Scherens B., Snyder M., Sookhai-Mahadeo S., Storms R.K., Véronneau S., Voet M., Volckaert G., Ward T.R., Wysocki R., Yen G.S., Yu K., Zimmermann K., Philippsen P., Johnston M., Davis R.W. 1999. Functional characterization of the *S. cerevisiae* genome by gene deletion and parallel analysis. Science 285:901-906.

Xie X., Cheng T., Wang G., Duan J., Niu W., Xia Q. 2012. Genome-wide analysis of the ATP-binding cassette (ABC) transporter gene family in the silkworm, *Bombyx mori*. Molecular Biology Reports 39:7281-7291.

Yazaki K., Shitan N., Sugiyama A., Takanashi K.. 2009. Cell and molecular biology of ATP-binding cassette proteins in plants. International Review of Cell and Molecular Biology 276:263-299.

Yesilirmak F., Sayers Z. 2009. Heterologous expression of plant genes. International Journal of Plant Genomics 2009:296482.